

PHOTOLUMINESCENCE AS A DIAGNOSTIC OF SEMICONDUCTORS

P. J. Dean

Royal Signals and Radar Establishment,
St. Andrews Road, Gt. Malvern, Worcs, U.K.

(Submitted 20th February 1981)

ABSTRACT

Photoluminescence provides a non-destructive technique for the analysis of semiconductors. The method provides information both on intrinsic and extrinsic semiconductor properties. This article reviews application to extrinsic effects induced by impurities or lattice defects. The method is shown to be particularly suitable for the centres responsible for the shallow donor and acceptor species by which the electrical properties are usually controlled, as well as all forms of explicit luminescence activator. It can also be applied to certain deep states, provided that carrier exchange with these centres does not involve so much local lattice relaxation that the associated transitions become entirely non-radiative. Even when this is so, transition metals may still be detected through internal electronic relaxations within a given charge state, at least the final step of which is frequently radiative. In all cases, measurements at low cryogenic temperatures are required to obtain the fullest spectroscopic information usually necessary to characterise a given type of transition and to discriminate between species within a given class. The donor and acceptor-related recombinations may be of bound exciton, donor acceptor pair or free to bound type, and equivalent processes may be seen for other types of centre. These topics are treated in separate sections of the review, following an introduction which includes general remarks about equipment and application of the technique. Examples are taken from the most technologically important semiconductor systems. Compared with the usual elementary techniques of electrical characterisation, photoluminescence has advantages of generally easy discrimination between species and can provide simultaneous information on many types of centre. However, it is comparatively less well suited to the determination of impurity concentration, particularly for the electrical majority species. Techniques whereby concentration information may

be obtained for various types of species are briefly described. The review ends with a subsection devoted to topographic techniques involving photoluminescence, or the closely-related cathodoluminescence and junction electroluminescence, which can reveal information on totally non-radiative extended defects as well as on spatial distributions of radiative species.

1. INTRODUCTION

(i) General Remarks

Photoluminescence spectroscopy is capable of providing a great deal of information about electronic processes in semiconductors. Indeed, the majority of our best founded knowledge of these properties has been obtained through optical characterisation, and photoluminescence measurements have played an important role. Optical measurements provide information both about the host semiconductors, involving so-called *intrinsic* optical processes and about the wide variety of impurities or defects which are endemic in practical semiconductor materials, involving *extrinsic* optical processes. Photoluminescence is one from a range of optical techniques, which includes optical absorption, various types of light scattering, photoemission, photoconductivity, photocapacitance, recombination processes under various alternative excitation mechanisms as in cathodoluminescence as well as techniques involving extensions to other frequency domains, as in the wide variety of X-ray techniques. These techniques have the general advantage of being non-destructive, and several can be readily adapted to measurements directly on device structures as well as bulk semiconducting material. However, some may require a modest degree of special sample preparation, as in optical absorption (appropriate specimen thickness) or light scattering (high quality external surfaces to minimise Rayleigh scattering). It is usually advantageous to employ more than one optical technique upon a given problem. In particular, a comparison of photoluminescence with optical absorption or photoluminescence excitation spectroscopy (Fig. 1a) often provides vital evidence required for the identification of spectral processes and their exploitation to yield the maximum of diagnostic information on the properties of a semiconductor.

(ii) Techniques

Photoluminescence is a generally convenient technique, requiring in the simplest form a suitable source of optical excitation, a spectrograph or spectrometer and a suitable detector for the emitted light (Fig. 1a). Additional refinements (Table 1) are usually necessary for all but the most routine, elementary investigations. In particular, basic assessment of a semiconductor usually requires measurements at low temperatures, so the sample must be placed in a suitable cryostat with a strain-

SCHEMATIC APPARATUS FOR ABSORPTION AND LUMINESCENCE STUDIES

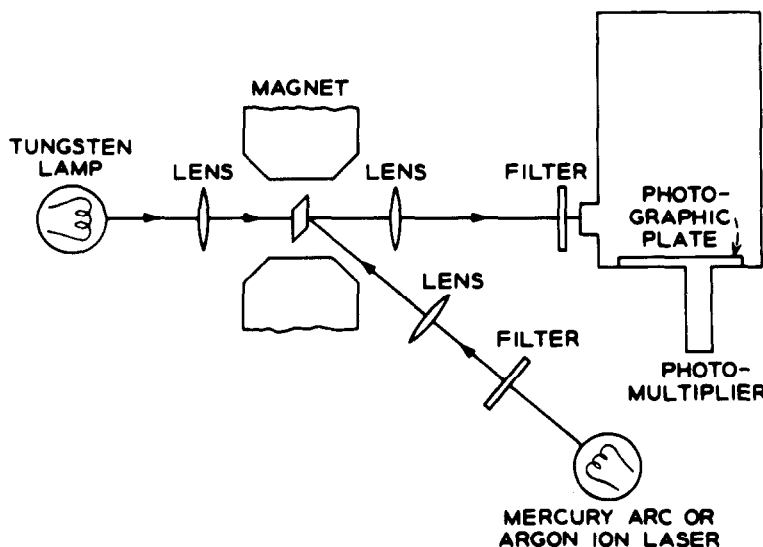


Fig. 1a. Schematic apparatus for absorption and luminescence studies. The sample at the centre of the magnet gap is placed in a cryostat, most conveniently immersed directly in liquid refrigerant for good sample cooling without introduction of mechanical strain. The sample temperature may be varied over some convenient ranges by pumping on the refrigerant vapour, $\sim 1.5 + 4.2$ K for liquid He. A variety of optical sources, spectrometers (right hand box) and detectors are required to cover the total energy range of interest for photoluminescence (Table 1).

free mounting technique (Fig. 1b). There are two principal reasons for this need. First, specific information about the centres which promote electrical conductivity, the donors and acceptors, can be obtained only when the electronic particles are frozen out in these centres. Once the electronic particles are thermally liberated, necessarily by 300 K in a semiconductor of practical device interest, the impurities or defects which released them only reveal their presence through some inhibition of carrier mobility. This inhibition is slight at 300 K for the most common semiconductors used in devices, which generally have Debye temperatures $\lesssim 500^{\circ}\text{K}$, and at doping densities $\lesssim 10^{17}\text{ cm}^{-3}$. Under these circumstances, the 300 K mobilities are dominated by lattice scattering.^{1,2} Impurity scattering is also relatively insensitive to the nature of the donor or acceptor and mobility measurements are quite unsuitable for their distinction. The second strong advantage of low temperature measurements is

TABLE I. Typical equipment for photoluminescence studies in different spectral regions

Energy Region	Source	Spectrometer (all grating)	Detector
$\sim 0.22 \rightarrow \sim 1$ eV	Neernst filament, W lamp, Tunable F-centre Laser	$\frac{1}{4}$ m, f/4 \rightarrow $\frac{1}{4}$ m f/7	77 K InSb photovoltaic (transient) or photoconductive
$\sim 0.35 \rightarrow \sim 1$ eV	W lamp, Nd laser	$\frac{1}{4}$ m, f/4 \rightarrow $\frac{1}{4}$ m f/7	200 K PbS photoconductive
$\sim 0.7 \rightarrow \sim 1.5$ eV	W lamp, GaAs laser, He-Ne laser, Kr ⁺ laser	$\frac{1}{4}$ m, f/7 \rightarrow 1m f/9	77 K Ge photodiode plus cooled pre-amplifier
$\sim 1.0 \rightarrow \sim 1.5$ eV	As above, plus CW tunable dye laser	1m f/9*	200 K Si-response photomultiplier
$\sim 1.05 \rightarrow \sim 3$ eV (~ 7 eV) ⁺	As above, plus Ar ⁺ laser	1m f/9*	77 K quaternary III-V photomultiplier
$\sim 1.4 \rightarrow \sim 3$ eV ^X	As above	1m f/9*	250 K GaAs photomultiplier
	W-lamp \rightarrow Xe lamp, He-Cd laser, Kr ⁺ or Ar ⁺ laser, N ₂ laser (kinetics), frequency multiplied VAG or ruby lasers, CW or pulsed tunable dye laser		300 K quartz window S20-response photomultiplier
$\sim 1.5 \rightarrow \sim 6.5$ eV	D ₂ lamp or e beam for high energy excitation	1m f/9	As above

* Double monochromator essential for excitation spectroscopy close to excitation energy for all but brightest luminescent materials.

+ Limit near 6.5 eV due to atmospheric absorption, detector available with quartz window but not optimum choice for measurements primarily in the UV.

X Detector limit due to boro-silicate glass window.

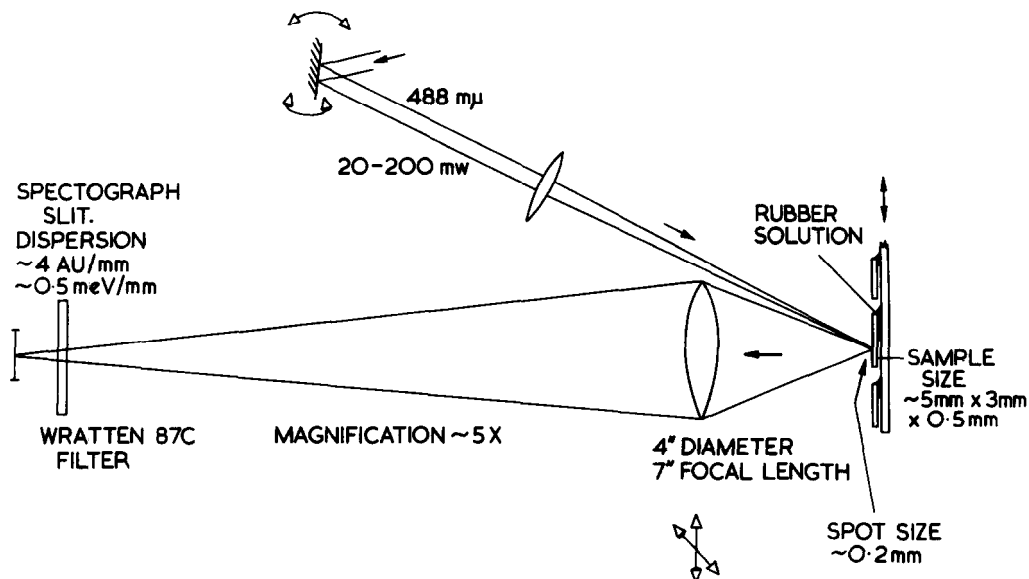


Fig. 1b. Apparatus used in the author's laboratory for the study of luminescence from GaAs and InP (a He-Ne or Kr⁺ laser provides a better match to E_g) and for GaP and several II-VI semiconductors (the spectrograph contains an alternative grating with dispersion $\sim 2 \text{ \AA/mm}$ preferable for high resolution studies in the visible). Many samples may be mounted on both sides of the sample stick, which also contains slots for optical transmission measurements as in Fig. 1a. Freely suspended, strain-free sample mounting techniques are essential for most detailed studies. The large magnification of the luminescing crystal and ability to focus and manipulate the exciting light, readily enables detection of the spatial variations of sample properties caused by built-in stresses etc.

the dramatic reduction of spectral broadening due to vibronic processes (Figs. 2 and 3), as the possibility of anti-Stokes processes is removed through the reduction of the thermal equilibrium value of the occupation number $n_{\delta}(\underline{k})$ of a mode of given type, wave-vector \underline{k} and branch δ of the lattice normal mode spectrum according to

$$n_{\delta}(\underline{k}) = \frac{1}{[\exp(\hbar\omega_{\delta}(\underline{k})/kT) - 1]} \quad (1)$$

Localised as well as lattice normal mode phonons are generally important in coupling to the electronic states between which photoluminescence transitions occur.³ However, the occupation numbers of these non-propagating modes also conform to eqn. (1), resulting in similar advantages for low temperature

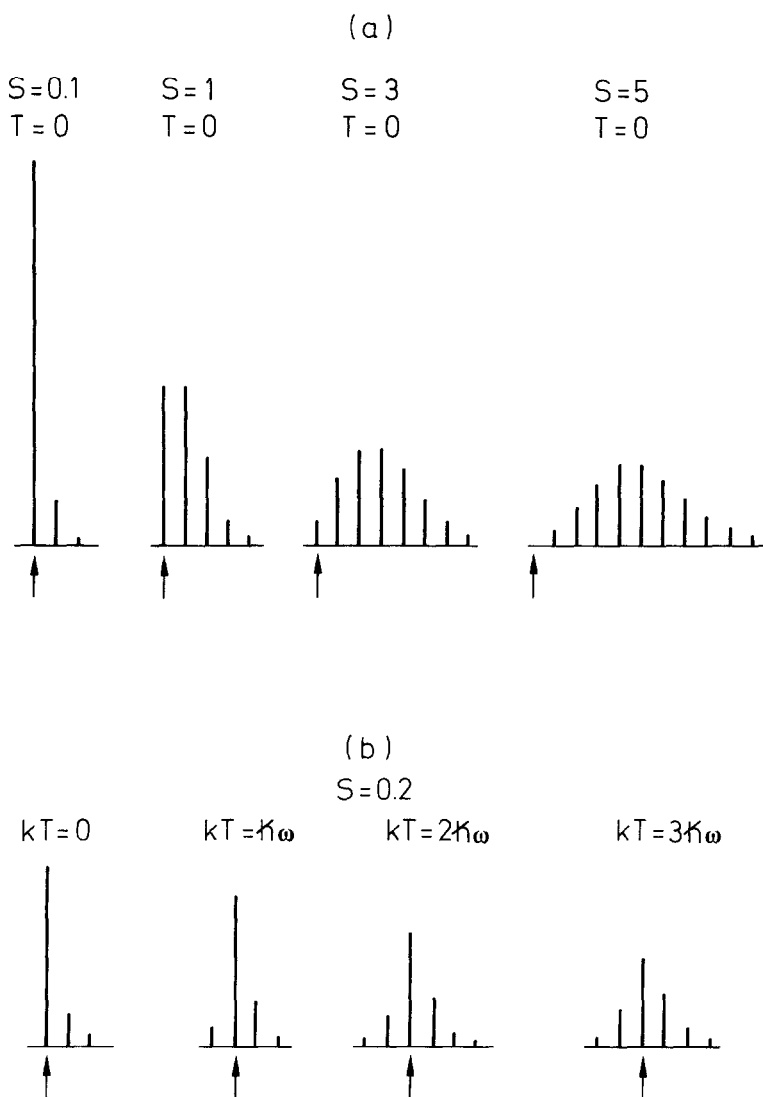


Fig. 2. Schematic representations of spectral distributions in luminescence involving the indicated values of the Huang-Rhys phonon coupling parameter S , the average number of emitted phonons. Data are presented (a) for various values of S at 0 K and (b) for various temperatures and $S = 0.2$. The temperatures are indicated in units of the energy $\hbar\omega$ of the single phonon assumed predominant in the vibronic coupling. No-phonon transitions are indicated by vertical arrows. The diagrams represent optical absorption (luminescence) if the transition energy increases to the right (left). The approximation to the electron-phonon coupling consistent with those simple spectra also results in a mirror symmetry between absorption and luminescence about the no-phonon lines.³

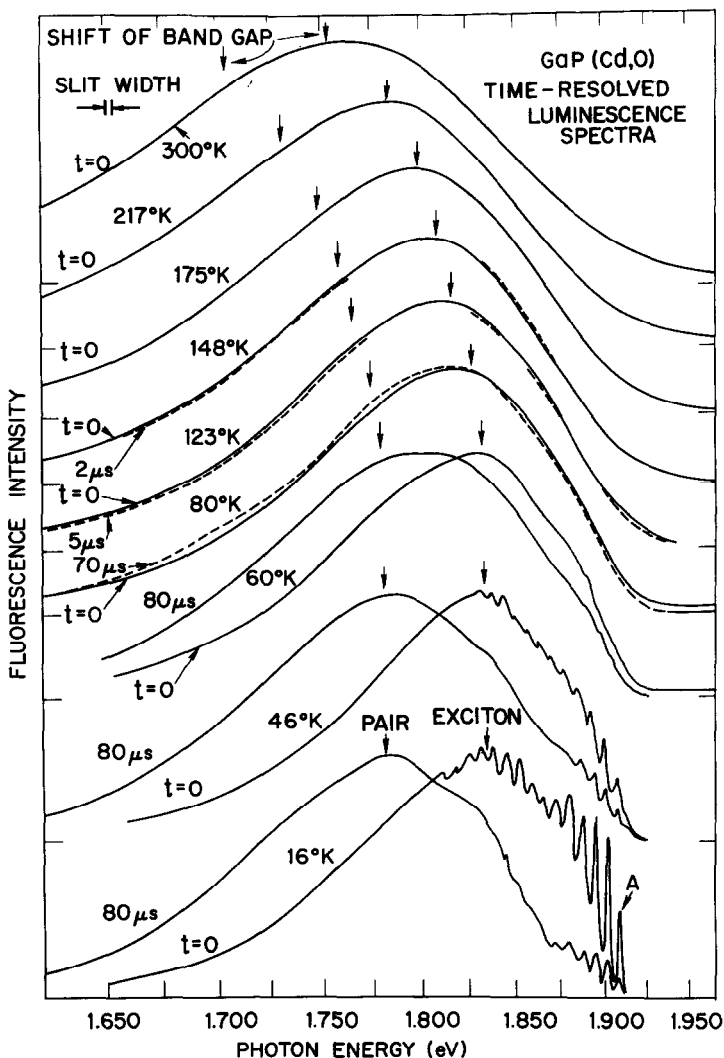


Fig. 3. Illustrative luminescence spectra for the Cd-O molecular isoelectronic associate in GaP, showing the strong spectral broadening of the vibronic structure associated with the bound exciton no-phonon transition A with increasing sample temperature. These spectra also show the predominance of exciton over distant (Cd-O)-Cd pair luminescence in spectra taken at short times after pulse excitation at low temperatures, and the thermal quenching of the long-lived distant pair luminescence in favour of the much faster bound exciton recombinations as the temperature is increased.¹³⁸

measurements.

(iii) Temperature Dependence - Comparison with Electrical Data

Temperature may also be as useful a variable in photoluminescence spectroscopy as

it is in electrical characterisation. Besides the opportunity of measuring characteristic activation energies of the system through thermal quenching or enhancement processes, the appearance of additional types of recombination processes can frequently help to identify the basic mechanisms involved and may be directly useful in the estimation of impurity state energies.⁴ The interpretation of activation energies derived from such thermal quenching studies, or from ancillary techniques such as thermoluminescence,⁵ is no more nor less problematical than for the electrical measurements. The heats of reaction so derived from the usual Arrhenius plot of $\ln I$ vs T^{-1} , where I is the intensity of some spectral component, are the changes in enthalpy, ΔH , provided that the $\ln I$ term properly expresses the temperature dependence of capture cross-sections, degeneracy factors, band density of states and carrier thermal velocities which may be required, as discussed below. Degeneracy factors g appear in the detailed balance equation relating the electron thermal emission rate from a localised state e_n and the corresponding capture cross section σ_n

$$e_n = \frac{\sigma_n \langle v_n \rangle N_c}{g} \exp(-\Delta G/kT) \quad (2)$$

where g is the degeneracy of the bound state, N_c is the effective density of states at the conduction band edge (which also subsumes a degeneracy factor), $\langle v_n \rangle$ is the average thermal velocity of the electrons and ΔG is the change in Gibbs free energy in the reaction.

An Arrhenius plot of $\ln(g\sigma_n \langle v_n \rangle N_c)$ vs $1/T$ has a local slope of $-\Delta H$, the change in enthalpy in the electron ionisation process. The temperature dependence of σ_n and g are frequently ignored in such analyses, but then the Arrhenius plot does not strictly yield ΔH . The free energy is to be compared with optical energies.⁶ When the wave function for a given extrinsic level is dominated by states derived from an adjacent band edge, then $\Delta S = 0$ and $\Delta G = \Delta H$. The extrinsic level may be said to be pinned to that band edge. However, this cannot simultaneously be true for both complementary transitions from the opposite band edges of the forbidden gap of a semiconductor. The entropy change ΔS must be recognised to accurate comparisons between thermal and optical activation energies, particularly for measurements on deep states.⁶ Such entropy changes are also important in thermal excitation processes between localised states of a given centre, for example between substates of a bound exciton due to the electron-hole exchange splitting where large differences in state degeneracy usually occur.³ It can be shown that the activation energy obtained from an Arrhenius plot using eqn. (2) is always equal to the free energy obtained by a linear extrapolation to 0 K of the temperature-dependent free energy derived from the different measurements at finite tempera-

atures. More serious problems arise in the basic identification of the enthalpy change measured from thermal activation with the electronic states of the impurity level system. The change in thermal activation energy factor in a Hall measurement from $E_{D/2}$ to E_D with increase in electrical compensation of a system containing a single donor level depth E_D is well known.⁷ Thus, the interpretation of the experimental data is very model-dependent. It may be difficult to discover which is the most appropriate model for analysis of data on a single sample without some additional, independent experimental data, such as an appropriate value of effective mass against which the density of states factor derived from the analysis may be checked. The directly measured thermal activation energy can be related to the optical measurement of ΔG only with the aid of such a soundly based analytical model. Large effects may be contributed from the strong temperature dependence of the Fermi level for very close compensation, which seems to occur all too frequently. An additional uncertainty in luminescence quenching studies is whether the thermal de-excitation is controlled by rate limiting or thermal equilibrium kinetics. Frequently, detailed analysis is possible only for the latter case, which is usually encountered at the higher temperatures.⁹ Thermal quenching of extrinsic luminescence processes is usually best studied under extrinsic, localised optical excitation.⁴ Equilibrium electrical measurements can provide information on the degree of compensation only in special circumstances, when a calibration exists for the limitations of low temperature mobility imposed by ionised impurity scattering.⁸ However, electrical measurements never give information on the nature of the compensating centres and not even on the energy position of their states. It has been argued recently that it is essentially impossible to derive from such thermal activation data an explicit energy level system for a semi-conductor containing a more complex type of deep centre which can adopt more than one charge state, typified by a transition metal, in the usual situation where the Fermi level is defined by the combined effect of these deep states and states from shallow donors and acceptors¹⁰ (Fig. 4). Further severe problems for the interpretation of thermal activation data result from effects of finite concentrations of donor or acceptor-like centres, because of conductivity processes between the shallow excited states which derive from the long-range part of the Coulomb potential present for all centres with charged cores. The measured value of ΔH for any thermal activation process in such a system then becomes a sensitive function of its concentration¹¹ (Fig. 5). This provides another reason, of very general applicability, why it may be difficult to relate ΔH measured for a particular sample to a particular centre. Detailed dependences as in Fig. 5 have not yet been obtained for many systems. Even where they do exist, it is clearly difficult to be sure that a particular measured ΔH relates to centre A, concentration

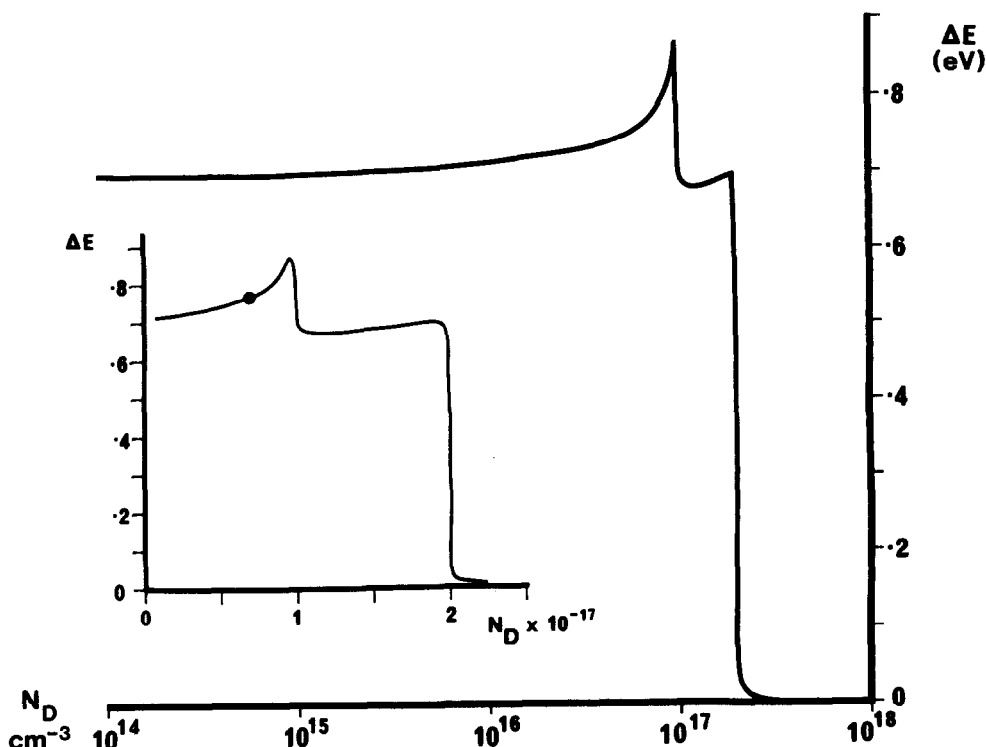


Fig. 4. Calculated apparent conduction activation energy ΔE (eV) at 300 K as a function of donor concentration in GaAs containing 10^{17} cm^{-3} Cr, assuming that the Cr levels are pinned to the valence band and zero compensation by shallow acceptors such as Zn. The Cr is assumed distributed between charge states Cr^{3+} , Cr^{2+} and Cr^+ . More recent studies favour Cr^{4+} instead of Cr^+ ,^{185,186} but the general principles illustrated in this figure remain valid. The donor scale is given in \log_{10} units in the main plot, but is linear in the inset. The point of maximum resistivity marked in the inset does not coincide exactly with the maximum in ΔE .

N_A rather than to centre 8 present at concentration N_B appropriately different as required to produce the same ΔH .

A self-consistent description of the influence of excited states on the analysis of Hall effect data on donor and acceptor-like centres, which inherently possess such states, is also frequently neglected. The existence of these states can be accounted for by a temperature-dependent degeneracy factor in the statistical mechanics of donor ionisation.²¹¹ This factor is divergent unless contributions from higher excited states are truncated. In practice, the natural point for truncation involves the highest excited state which is still well localised at the

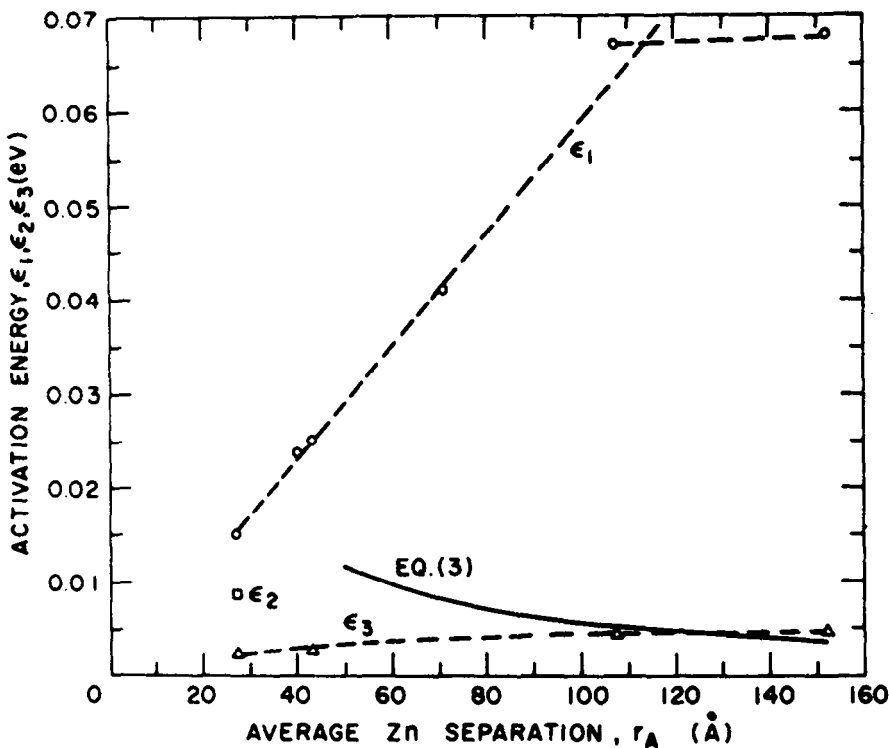


Fig. 5a. Variation of the activation energies ϵ_1 , ϵ_2 and ϵ_3 as a function of the average separation of Zn acceptors in GaP, $r_A = (3/4\pi N_{Zn})^{1/3}$, where N_{Zn} is the concentration of Zn acceptors. The terms ϵ_n are the activation energies in the usual three-term expression for the electrical properties of a system at finite concentration of mutually-interacting species. ϵ_1 is equivalent to the acceptor ionization energy E_A for measurements extrapolated to infinite dilution. ϵ_2 is observed in the 'intermediate-concentration' range and represents hole activation from acceptor ground states to a band involving interacting, positively charged acceptors. ϵ_3 involves phonon-assisted hopping of holes between ionized acceptors. The measured thermal value approaches the optical E_A when $r_A \sim 10a$, where a is the hydrogenic ground state acceptor radius. The solid line represents a theoretical form for ϵ_3 .

impurity concentration in question, according to criteria such as those discussed in Section 2 (IV). Fortunately, the degeneracy factor appears in the Fermi function in such a way as to be of greatest importance when the Fermi level is near the impurity ground state, for example below 200 K for shallow donors in Si.²¹² Then, only the deeper excited states are significant. The significance of all excited states becomes less for equilibrium thermal ionisation processes of strongly non-effective mass-like centres, since only the ground state is strongly

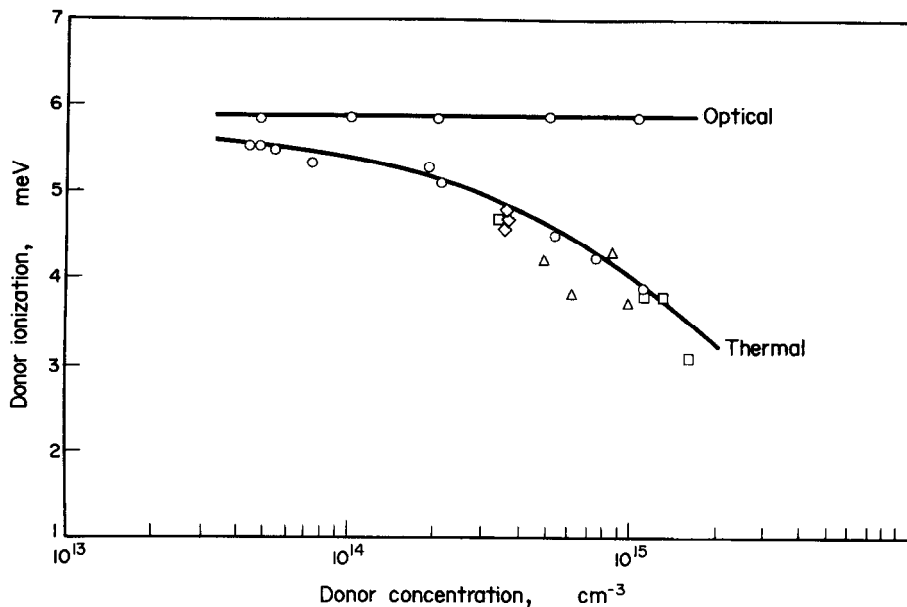


Fig. 5b. Dependence of the donor optical ionization energy determined from far-infrared photoconductivity measurements, and the thermal value obtained from Hall measurements, on the donor concentration in n-type VPE GaAs, including electrical data from a variety of sources.⁴³

deepened by the impurity central cell potential. However, the existence of shallow excited states can be very important in rate-limiting carrier capture processes for deep centres at low temperatures.²¹³

(iv) Emphasis of this Review

The present review will emphasise the basic uses of photoluminescence in semiconductor assessment through the form of the low temperature spectra and the evolution with temperature of the spectral components towards the forms which may be used directly in activated luminescence in room temperature devices. We shall see that these optical spectra are also perturbed by effects of finite concentrations. However, certain types of spectra are inherently relatively insensitive to these effects. Opportunities also exist to reduce the broadening effects for the more sensitive types, generally those involving states of particularly low binding energy, through the use of selective optical excitation.

(v) Limitations of Photoluminescence

The over-riding limitation of photoluminescence is obvious. Only those centres which introduce strongly or partly radiative recombination processes can be studied directly! Fortunately, this limitation is not very stringent, even in first order. Not only explicit luminescence activators (Section 3) but also the donor and acceptor species which are introduced to control the electrical conductivity

in virtually all types of semiconductor device, can produce characteristic radiative recombination processes (Section 2), particularly at low temperatures where their electronic particles become thermally stable at least in the ground states. Indeed, because of the general increase in phonon coupling with energy depth of the centre,¹² it is just the shallow centres needed to promote good electrical conductivity near 300 K which can also produce spectrally narrow, readily detected luminescence at \approx 20 K. Some of the recombination processes, particularly some of the bound exciton type (Section 2A), may not have high radiative efficiencies, because of the non-radiative Auger processes always possible when more than two electronic particles are involved.³ Fortunately, such systems frequently involve particularly low coupling to general phonons. The resulting weak but sharp luminescence lines may still be detected. Their study has provided much information about non-radiative as well as radiative recombination processes.³

(vi) Non-radiative Processes

Photoluminescence, or equivalent studies in electroluminescence or cathodoluminescence may also provide information on such non-radiative processes in second order, through their effect on transition rates for BE and other types of radiative process (Section 3) and through their influence for extended defects on topographic distributions of luminescence intensity (Section 4). Such techniques have provided information on dislocations and their aggregates, which has been important in the understanding of processes related to the rapid degradation of injection lasers and high radiance light emitting diodes.¹³

(vii) Study of Deep States; Alternative Techniques

The inherent limitations of photoluminescence for the study of recombination processes at very deep microscopic centres, where any radiative transitions typically give very broad spectra due to strong phonon coupling and may also be very inefficient for the same¹⁴ or other reasons, and where topographic studies cannot be made at the required spatial resolution, have encouraged the development of a family of alternative spectroscopic assessment techniques. Some, such as double source differential photocapacitance,¹⁵ still rely partially on optical processes, since optically filled deep levels in the depletion layer of a pn junction or Schottky barrier are probed optically. Clearly, this technique relies on suitable cross-sections for optical absorption. The complementary, widely used technique, deep level transient spectroscopy,¹⁶ uses free carrier capture and thermal release processes for electronic particles at deep traps. The spectroscopic parameter is then the temperature according to eqn. (2), with rate limiting statistics (no recapture) appropriate for measurements in a depletion layer. Such

techniques are also complementary to photoluminescence, since they are inherently limited to centres with binding energies large compared with those which directly promote electrical activity in the semiconductor and, for photocapacitance, to those whose threshold photon energies are convenient for the optical probe, usually for $h\nu \gtrsim 0.3$ eV. There is a significant margin of overlap between the capacitance and optical techniques. A few very deep centres, such as O in GaP,^{17,18} are very well treated by both.

The capacitance techniques have the general advantage compared with photoluminescence that accurate estimates of centre concentration are more readily obtained, and other important parameters such as capture cross-sections can be measured.^{16,18} We shall see that photoluminescence provides an approximate estimate of concentration, both absolutely from spatial linewidths and energy shifts and relatively from intensity ratios between spectral components involving different species. These estimates are not as quantitatively precise as those from the capacitance results for deep levels or from transport data for the shallow centres which promote electrical conductivity. However, it should always be remembered that the analysis of the electrical data is very model-dependent and that illusory results may appear for semiconductors of practical quality. These difficulties generally arise from the strong spatial inhomogeneities in doping level and compensation which occur all too frequently in all but the best-controlled semiconductors, namely Si, Ge and, less surely GaAs. In the remaining semiconductors, particularly, it is essential to combine as many different analytical techniques as possible to bear upon a given specimen, in order to have the very best chance of revealing such spurious and complex situations.

The purely optical techniques, optical absorption, photoluminescence and photoconductivity, remain the most successful for the *identification* of electronically active species, present both deliberately and inadvertently. This success has arisen partly because of the relative ease of doping control for the shallower species, and partly because the low temperature optical spectra contain so much information against which to test the expectations for a given species. Many deep centres have been detected by the capacitance technique in several semiconductors, particularly for radiation damaged Si¹⁹ and GaAs,²⁰ though rather few have yet been identified with high confidence. The problem is that, on the one hand, the generic properties of deep centres are not yet well-understood theoretically, and on the other, that these experimental techniques give most readily overall properties such as concentration, energy depth and capture cross-sections^{16,18} rather than more specific information such as degeneracy, local symmetry etc. usually provided through the luminescence spectra.³ However, excellent progress has recently been made in GaAs and GaAlAs by combining information from optical

absorption, DLTS and attenuation of ballistic phonon transport²¹ for an interesting type of defect, the DX centre, whose strong phonon coupling leads to persistant low temperature photoconductivity.²² The combination of all of these techniques has provided rather strong support for the assignment of this totally non-radiative centre to a V_{AS-D} associate, where the donor may be on a Ga or an As site. Such detailed understanding is at present very exceptional for deep, non-radiative centres in semiconductors. However, considerable progress has also been made recently in the theoretical and experimental description of V_{Si} in Si, which exhibits some very interesting effects of strong lattice relaxation which deny the stability of an intermediate V^- charge state.²³

(viii) Scope of Review

We now consider examples of photoluminescence in semiconductors, selected to exemplify the different types of recombination process which are particularly useful in the identification of impurity and other defect species and illustrated by application to particularly important semiconductors. Information about non-radiative as well as radiative centres will be considered, and the extent to which information can be obtained from purely optical spectra on centre concentrations and compensation ratios will also be discussed.

2. PHOTOLUMINESCENCE FROM SHALLOW DONORS AND ACCEPTORS

A. BOUND EXCITON SPECTRA

(i) Introduction of Concept

Recombination of electrons and holes through bound exciton (BE) states are the first processes to appear in the near gap luminescence spectra as the donor or acceptor concentrations are increased from very low levels and particularly for slightly compensated material. Then, most of the donors (or acceptors in oppositely doped samples) will be neutral before photo-excitation. A prominent type of recombination process involves the annihilation of an exciton bound to either of these species in their *neutral* charge state. Minority species, necessarily ionized under dark equilibrium conditions, may also be photoneutralised for the typical case of photo-excitation above the semiconductor band gap (Fig. 6a) and can subsequently capture excitons to produce BE spectra intermingled with those of the majority species. These two types of BE species may be distinguished by different rates of dependence of their luminescence intensity upon the intensity of photoexcitation as well as by different properties of the BE states under stress and particularly under applied magnetic fields.³ The sensitivity of these sharp photoluminescence components to local strains in the sample may be exploited to reveal macroscopic built-in stress from any inadvertently present

DONOR AND ACCEPTOR-RELATED RADIATIVE RECOMBINATION

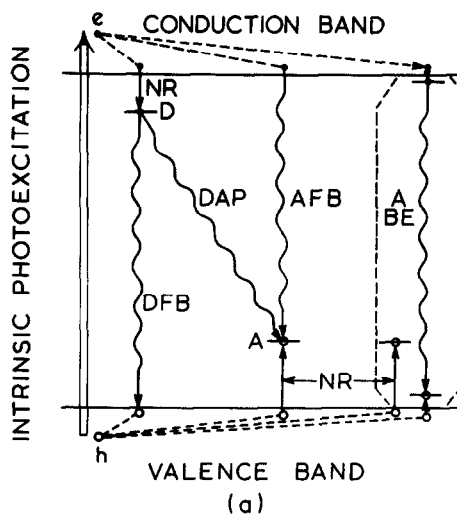


Fig. 6a. A schematic representation of a variety of radiative recombination processes induced by shallow donor and acceptor species in a semiconductor. Photo-excitation of free electrons and holes favour the DFB, AFB and distant DAP processes, whereas free exciton creation favours recombinations at more closely-spaced DAP and at the ABE neutral acceptor-bound exciton as well as the corresponding DBE process not illustrated.

line splittings.¹⁷ Microscopic stresses may be detected from their contributions to the spectral linewidth when these effects dominate in the broadening, rather than electric field processes which are frequently important in dilutely doped, compensated crystals.¹⁷⁸ Similar information is available from multiline DAP spectra whenever such lines can be detected (Section 2 B). These BE spectra were first recognised in Si,²⁴ where the doping control was sufficiently good even in 1960 that there was no doubt as to the nature of the chemical impurity involved, and therefore the type, donor or acceptor (Fig. 7). By contrast, the semiconductor wherein the detailed properties of these states were first extensively studied, CdS,²⁵ was not well controlled. Indeed, the identity of the donors and acceptors involved became established only after nearly a decade of additional work.^{26,27} Zeeman spectroscopy proved essential for the distinction between spectra involving donor and acceptor species in CdS. However, since $E_D \ll E_A$ there was a general expectation^{24,28} that the donor-related recombination lines should lie closer to the exciton gap, i.e. the exciton localisation energy E_{BX} for donors should be less than for acceptors, in direct proportion to the ratio E_D/E_A according to the data

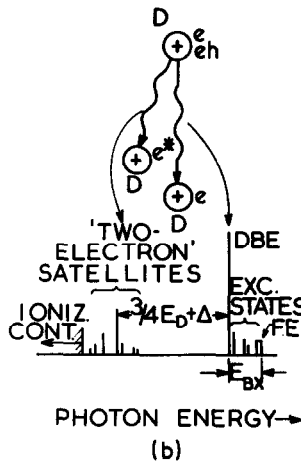


Fig. 6b. A schematic representation of bound exciton recombination at a neutral donor. The principal recombination lines are shown to the right, in which the neutral BE recombines from its ground and excited states leaving the donor in its ground state. The 'two-electron' satellites to the left involve transitions in which the donor is either left in one of a series of excited states or the electron is promoted to the bottom of the conduction band.

for Si (Fig. 7).

Hopfield²⁸ first discussed the binding of excitons in the various types of complex possible for donors and acceptors. He concluded that excitons could not bind to ionized acceptors if they formed bound states at ionized donors, already proved to occur for CdS.²⁵ Neither of these types of complex should be stable for a semiconductor like Si or GaP, where the electron to hole effective mass ratio $m_e^*/m_h^* \sim 1$.

(ii) Differentiation of Donors and Acceptors; Haynes' Rule

Hopfield also showed that exciton binding is always possible for neutral donors or acceptors, although the coefficient of proportionality in the Haynes' rule relationship between E_{BX} and E_D or E_A , discovered in Si (Fig. 7a), was sensitive to m_e^*/m_h^* for the host semiconductor. The generalised form of this relationship is²⁹

$$E_{BX} = a + b E_i \quad (3)$$

where $a \neq 0$ in general and b is dependent on the nature of the impurity of energy

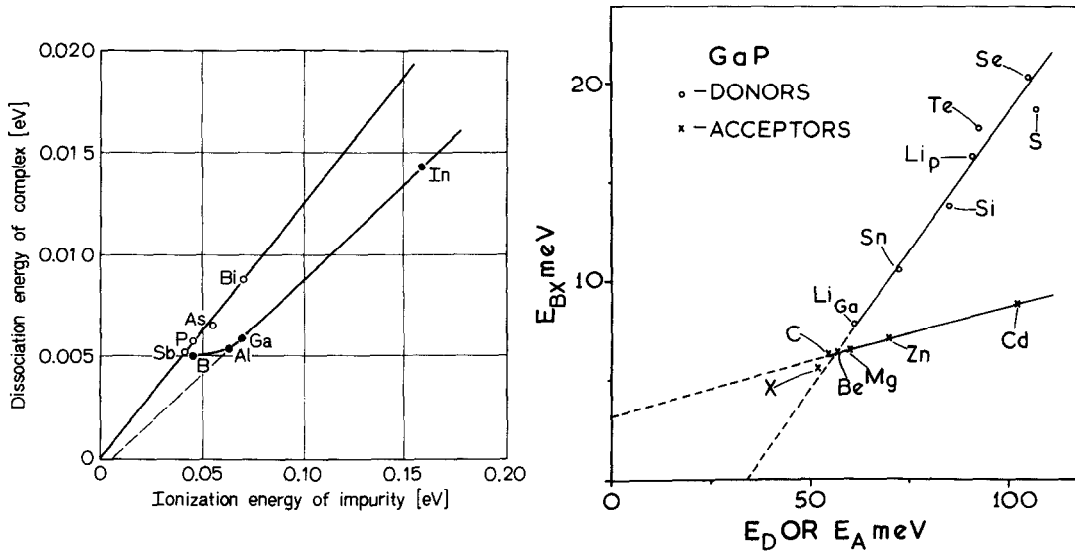


Fig. 7. (a) Variation of the exciton localisation energy E_{BX} with the binding energy of the neutral donor (\circ points) or acceptor (\bullet points) species to which the excitons are bound in Si.²⁴
 (b) Corresponding data for neutral donors and neutral acceptors in GaP, showing that the origin is not generally a point of particular significance in these dependences (revised from²⁹).

E_i , that is whether donors or acceptors are considered. By chance, both of these conditions are violated for the particular case of Si (Fig. 7a) but are not in GaP²⁹ (Fig. 7b). It should be noted that several BE states occur in general,³ due to J-J coupling between the electronic particles, excitations to orbital excited states of the bound exciton or within the bound exciton and pseudo spin-orbit (spin-valley) or valley-orbit splitting of the electron in the case of donor BE (DBE) in an indirect gap semiconductor. Equation (3) applies to the lowest energy of all these states, which is usually particularly sensitive to the central cell of the impurity to which the exciton is bound for reasons fully discussed elsewhere.³

The predictions made by Hopfield²⁸ have stood the test of time to date for many semiconductors, including GaAs and InP. However, it has been found that Haynes' rule, even in the generalised form of eqn. (3), does not apply for shallow acceptors in direct gap semiconductors. Indeed, non-monotonic behaviour within a

general insensitivity of E_{BX} to E_A has been observed for several semiconductors including CdS,²⁷ ZnTe³⁰ and GaAs.³¹ This violation of eqn. (3) strongly reduces the usefulness of the principal BE luminescence lines (Fig. 6b) for chemical identification in these cases.

(iii) Satellite Spectral; 'Two-electron' and 'Two-hole' Transitions

Associated BE recombination channels may be considered when the P BE states are inadequately resolved, in particular, the 'two-electron' or 'two-hole' transitions, also shown in Fig. 6b. These are displaced below the principal BE transition by energies which carry almost the entire chemical shift of the impurity ground state. These satellite transitions are as general as the neutral donor or acceptor BE (ABE) transitions themselves. They have now been utilised in many semiconductors to provide much detailed information on the donor and acceptor centres, including their basic binding energies derived from analysis of the relative energies of the several excited states which stand revealed in optimum cases.³⁰ A good example is ZnTe, where many acceptors have been distinguished using this technique.³² In addition the systematics of the 'two-hole' satellites (Fig. 8) have clearly shown³³ that the ~ 150 meV acceptor normally dominant in ZnTe cannot be due to a single hole bound to a V_{Zn} or to any other double acceptor, as suggested in the 'Classical' view of ZnTe and its relationship with other II-VI semiconductors. Careful doping experiments in recently available high quality single crystals have indicated that, instead this important acceptor is Cu_{Zn} with the Cu core in the $3d^{10}$ configuration.^{33,34}

(iv) Sensitivity Limits and Spectral Broadening

The sensitivity limits for detection and recognition of donor and acceptor species by these techniques depend upon the detector available (Table 1) and upon the semiconductor. The 'two-electron' and 'two-hole' BE satellites inevitably fall upon the high energy tail of the donor-acceptor pair (DAP) transitions, discussed in Section 2 B, and may be masked by them in significantly doped and compensated material (Fig. 9). However, the PBE states may still be seen in optical absorption up to the doping concentrations where they remain sufficiently well resolved, even when luminescence from them is quenched by energy migration to deeper states before recombination can occur. The limiting impurity concentration for the useful detection and recognition of donor bound excitons by absorption is in the mid 10^{17} cm^{-3} range in GaP. Corresponding limiting values for other types of bound excitons or for other semiconductors can be deduced from the relationship

$$N_i \approx \frac{3}{4\pi a^3 \tau_s^3} \quad (4)$$

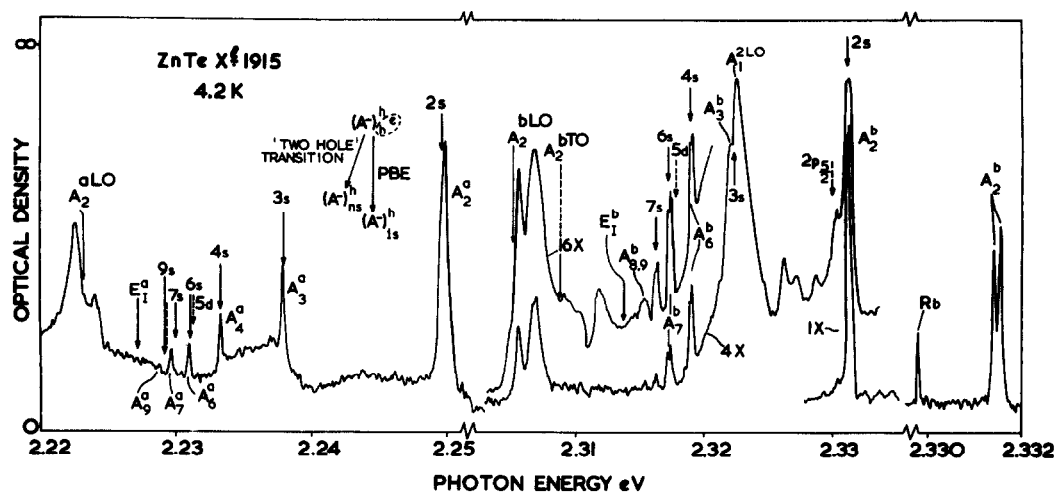


Fig. 8. 'Two-hole' bound exciton recombination satellites for the two acceptors normally dominant in the electrical properties of p-type ZnTe, recorded photographically. The b series involves the acceptor Li, $E_A = 61$ meV, whereas the a series involves the deeper acceptor Cu, $E_A = 149$ meV. Subscripts denote the orbital excited state of the hole remaining after BE recombination (inset). The b series is influenced by a small splitting in the BE for the Li acceptor. Vertical arrows denote theoretical estimates of transitions to the indicated acceptor excited states. The phonon replicas of the dominant transition to the 2s acceptor excited state are strongly distorted by a quantum-mechanical interference effect.^{30,32}

where a is the radius of the bound state and α_s is a critical parameter equal to 2.5 for a Mott transition in a system where the bound state involves the long-range Coulomb interaction.³⁵ This parameter may be larger for an electron-hole bound state, perhaps ~ 5 as for free excitons in CdS.³⁶ The radius of a bound exciton state may be derived from

$$a_{BX} = \frac{\hbar}{(2m^* E_{BX})^{\frac{1}{2}}} \quad (5)$$

where m^* is the sum of appropriately averaged electron and hole effective masses, respectively m_e^* and m_h^* .

Relations similar to eqn. (4) applied to the impurity excited states can also be used to show how the thermal activation energy ΔE_{th} measured from electrical

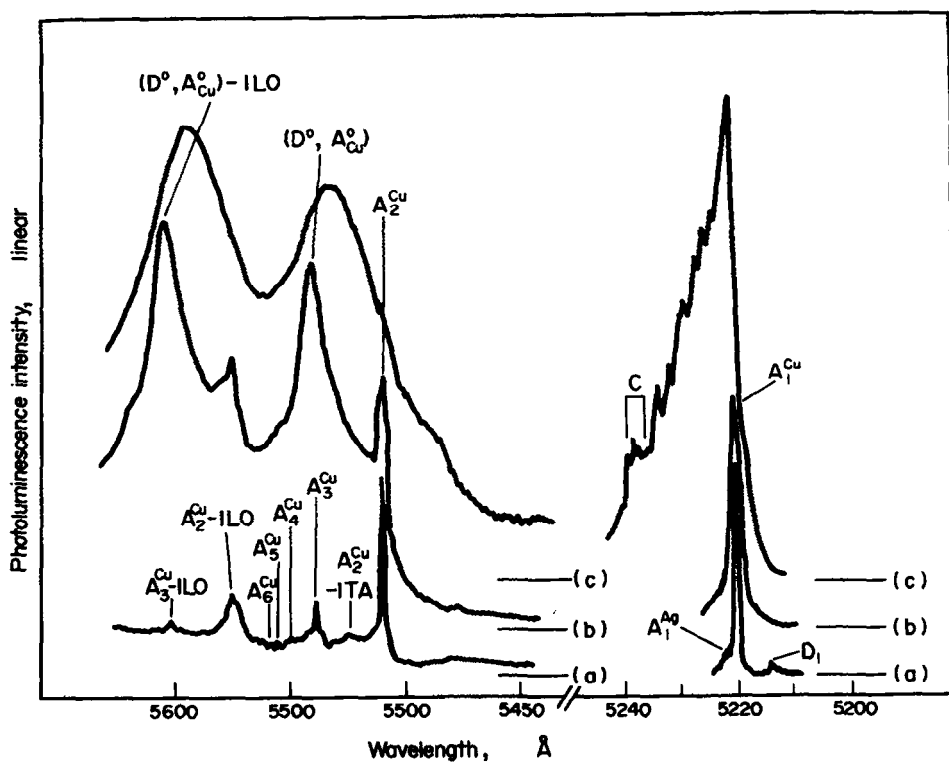


Fig. 9. Photoluminescence spectra of ZnTe recorded at 5 K. Spectrum (a) is for an ingot grown from a Te-rich melt with $N_A \sim 10^{15} \text{ cm}^{-3}$, while (b) and (c) are from Cu-diffused crystals containing $\sim 5 \times 10^{16} \text{ cm}^{-3}$ and $5 \times 10^{17} \text{ cm}^{-3}$ Cu acceptors. The evolution of the principal ABE line A, toward a broadened, asymmetric lineshape with superimposed structure is shown at the right. To the left, the 'two-hole' satellites A_i^{Cu} predominant in (a) are masked by the broad DAP band (D^0, A_{Cu}^0) as the Cu concentration is increased.¹⁸⁷

conductivity decreases with increasing impurity concentration (Fig. 5b). The effect sets in at very low concentrations for *n*-type GaAs, since m_e^* is only $\sim 0.067 m_0$ where m_0 is the free electron mass. For example, ΔE_{th} only approaches the optical value ΔE_{op} determined from 'two-electron' DBE satellites or from infra-red photoconductivity below $N_D - N_A \sim 10^{14} \text{ cm}^{-3}$ even in lightly compensated GaAs, and ΔE_{th} is reduced to $\sim 0.5 \Delta E_{op}$ at $N_D - N_A$ only $\sim 2 \times 10^{15} \text{ cm}^{-3}$,⁴³ (Fig. 5b).

(v) Dependence of Sensitivity on Type of Semiconductor

The detection sensitivity of these BE luminescence systems also depends upon the semiconductor, since their radiative efficiency is generally reduced to 0.1 + 1% for indirect gap semiconductors by Auger processes, the magnitude of the reduction depending upon the exact band structure and its influence upon recombinations

involving different species.^{37,38} The relatively weak luminescence from D and ABE may be masked by that from other, inherently efficient species, such as the isoelectronic trap luminescence activator N in GaP.³⁹ Assuming low concentrations of N, which require careful sample preparation, detection limits of mid 10^{13} cm^{-3} for P site donors and mid 10^{14} cm^{-3} for Ga site donors and acceptors which promote much weaker PBE lines can be attained in GaP. Detection limits are much lower in Si, where sensitivity down to 10^{11} cm^{-3} for B and P has been claimed in the absence of competition from other extrinsic recombination processes.⁴⁰ This is within an order of magnitude of the greater sensitivity limits demonstrated in Si for the photothermal photoconductivity process involving direct excitation of the neutral centres by far infra-red light.⁴¹ Similar limits should be readily achieved in direct gap semiconductors, assuming band gaps corresponding to detection by a sensitive Ge photodiode or by a photomultiplier (Table 1). Bound exciton recombination processes have 100% radiative efficiency in direct gap semiconductors, at least for the shallower species.⁴² These latter estimates cannot be fully tested, since all direct gap semiconductors are binary compounds and the control of shallow impurities in the best such materials stops not far below 10^{13} cm^{-3} , for GaAs.⁴³

(vi) 'Undulation' Spectra

At high impurity concentrations BE spectra provide evidence for localisation at neighbouring pairs of neutral acceptors⁴⁴ or donors,⁴⁵ through the asymmetric broadening to lower energies induced by this interaction at concentrations where the exciton begins to be delocalised from a given donor according to a relationship similar to eqn. (4). The asymmetry of the resulting luminescence line is reduced with increase in temperature as the tendency of BE to percolate to closer spaced impurity pairs with higher localisation energy is reduced by anti-Stokes phonon-assisted hopping processes (Figs. 9 and 10). This is the opposite of the temperature shift expected if the breadth arose from a homogeneous process within a set of localised but mutually isolated states lying just below the free exciton states, wherein those states with lowest E_{BX} would be expected to have a lower temperature onset of thermal quenching. There appears to be a fairly well-defined mobility edge below which energy percolation before recombination of the bound excitons no longer occurs.⁴⁴ Related broadening effects of BE in p-type Si have been analysed recently in terms of very similar inter-impurity interactions between neutral acceptors.¹⁸² In favourable cases, undulatory structure can be seen on the low energy tail. These have been interpreted in terms of fluctuations in the overall envelope of the distribution function of acceptor pair states allowed by the crystal structure,⁴⁴ similar to the effects reported for interactions between the isoelectronic trap N and neutral acceptors in GaP.⁴⁶

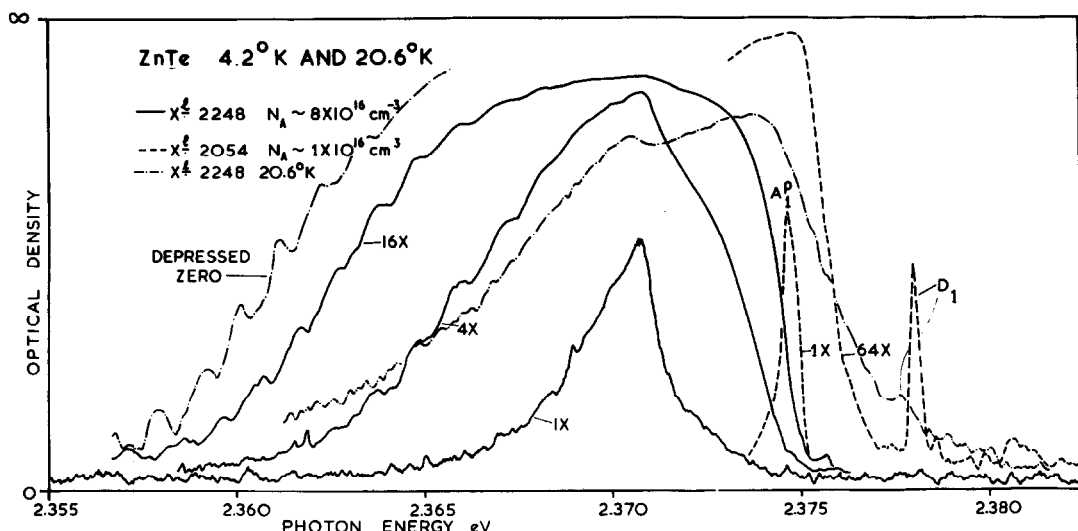


Fig. 10. Near gap photoluminescence spectra from ZnTe single crystals at the indicated temperatures and concentrations of doping by P acceptors. The crystals are only lightly compensated, and the principal DBE line D_1 is much less broadened than that involving the majority acceptor A_1^P . These spectra were recorded photographically, with the indicated relative exposures.⁴⁴

(vii) Relation Between Photoluminescence Intensity and Activator Concentration

The dependence of the intensity of the BE or other type of impurity-induced luminescence signal upon the impurity concentration is not as straightforward as in optical absorption. A linear increase in the integrated absorption is anticipated up to concentrations where the relevant electronic states become too heavily broadened through eqn. (4) for measurements to be possible. By contrast, the photoluminescence intensity must saturate once the concentration of a particular type of centre has increased to the point where the recombinations through it account for the available generation rate of free carriers by the absorbed primary light. As an example, interband optical excitation in a direct gap semiconductor may involve a 250 mW primary beam of diameter 0.5 mm, absorbed in a distance much less than the ambipolar diffusion length of say 1 μm at 4.2 K. Assuming an impurity-related recombination channel with life-time $\sim 1 \text{ nsec}$, quite plausible for recombination through weakly bound exciton states in a direct gap semiconductor,⁴² the excitation density can be balanced by recombination through only $\sim 3 \times 10^{15} \text{ cm}^{-3}$ centres. In addition, comparison of absolute intensities of luminescence obtained from measurements on different samples is notoriously difficult in the absence of integrating sphere techniques, technically very difficult to apply in photoluminescence at low temperatures. However, in the

presence of one or more additional recombination channels competing strongly with the extrinsic processes, it is found empirically that very good consistency with electrical estimates of carrier concentrations can be obtained when the *intensity ratio* of extrinsic to intrinsic luminescence components is recorded under carefully standardised conditions of photoexcitation and recording of the luminescence. Measurement of the intensity ratio minimises the influence of undesirable factors, potentially strongly variable between samples grown and prepared by different methods, such as the influence of surface recombination.⁴⁷

Tajima *et al.*^{40,48} have obtained such calibration curves for P donors and Al and B acceptors which are the main contaminants of floating zone-refined Si, using computer-assisted deconvolution of neighbouring spectral lines where necessary. The technique appears to work very well over a wide relevant concentration range when the donors are introduced into ultra-refined crystals (Fig. 11), and measurements are made at moderate excitation levels.⁴⁹ The exponent n in the relationship

$$I_{BE}/I_{FE} = N_I^n \quad (6)$$

is close to unity for all three impurities, according to the revised scale obtained with nuclear transmutation doping of this refined material, where well-

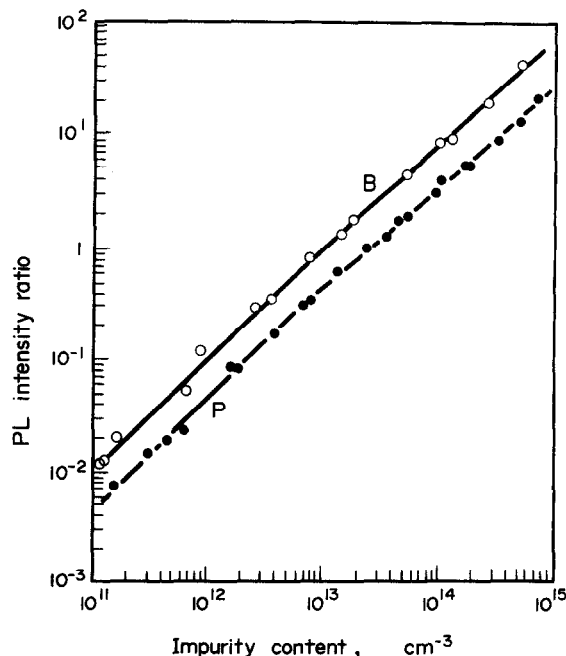


Fig. 11. Calibration curves for the P donor and B acceptor concentrations determined in Si from analysis of the BE and FE photoluminescence ratios $P_{T0}(\text{BE})/I_{T0}(\text{FE})$ and $B_{T0}(\text{BE})/I_{T0}(\text{FE})$.⁴⁸

resolved spectra were obtained and the P concentration was determined below $2 \times 10^{12} \text{ cm}^{-3}$ by nuclear conversion estimates.⁴⁸ A change to a slightly lower value of n near 10^{13} cm^{-3} is seen in Fig. 11. Relative to the free exciton (FE) luminescence, the luminescence intensities of BE due to As and β do not change in an n -irradiated and annealed crystal, while that of the P donor greatly increases due to a nuclear conversion from Si³⁰ (Fig. 12). Either the no-phonon or TO phonon-assisted BE

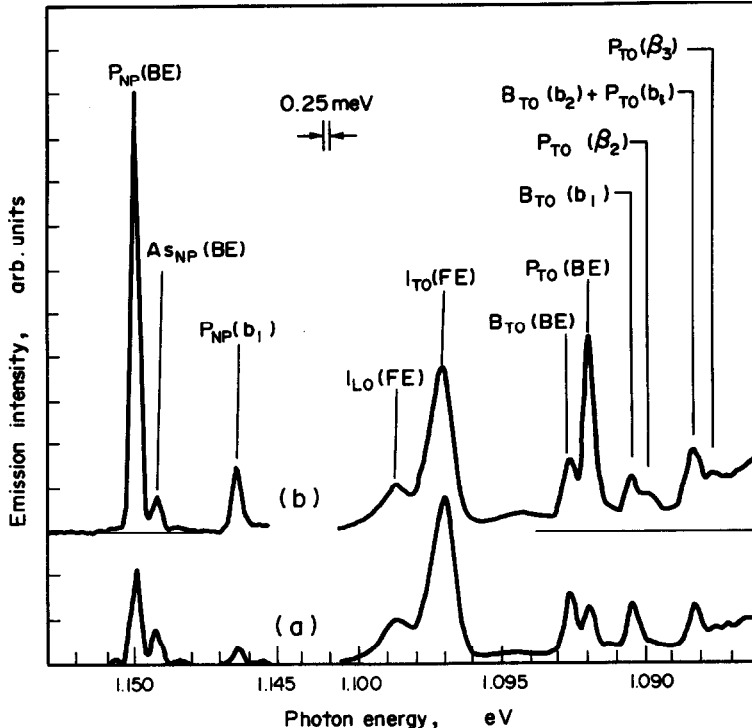


Fig. 12. Portions of the near gap photoluminescence of selected commercial bulk Si (a) before and (b) after increase of the concentration of P donors to $2.7 \times 10^{13} \text{ cm}^{-3}$ by nuclear transmutation of Si³⁰ with slow neutrons, and appropriate subsequent thermal annealing. There is a small concentration of residual As donors. Components labelled b_n and β_n are due to recombination of multiple bound excitons.⁴⁸

component and the TO phonon assisted FE component are used in eqn. (6), whichever has the more convenient strength. Calibration curves such as Fig. 11 are useful only for relatively uncompensated material.⁴⁹ The abscissa is proportional to N_p or N_A , since all donors and acceptors are photoneutralised under the excitation conditions prescribed by Tajima,⁴⁰ 150 mW in a 1 mm diameter spot. Thus, the experimental points are displaced to the left compared with Fig. 11 if the abscissa is derived from the electrical data of Irvin.⁵⁰ This analytical technique has proved very useful in identifying exactly how each separate impurity species is

distributed along a multiply passed zone-refined ingot, impossible to derive from the electrical analysis. The results agree with expectation from the known coefficients of segregation and evaporation for these impurities.⁵¹ The technique has also proved useful in the study of a variety of novel donors recently discussed in Si, related to O and introduced by thermal treatments.⁵² A complex evolution of form of the bound exciton photoluminescence spectrum occurs with increasing temperature of thermal anneal. Luminescence of the BE type also appears mainly at lower energies than shown in Fig. 12 for *n*-irradiated and otherwise damaged (ion implanted) and suitably annealed Si.⁵³ This luminescence is proving useful in the study of recovery of lattice perfection by laser annealing, since layer stripping experiments using anodisation techniques can reveal exactly where the residual damage-related centres congregate.⁵⁴ The detailed theoretical analysis of the calibration curves in Fig. 11, is difficult, since they were obtained at excitation intensities where effects due to electron-hole drops become significant, whose relatively broad luminescence is not included in Fig. 12. Nakayama *et al.*⁴⁹ have shown that ratios such as in eqn. (6) are independent of optical level only < 0.15 W cm⁻² and can then be used to estimate both the major dopant concentration and the composition ratio. This analysis is based upon rate equations, involving both free, bound and multiple bound excitons. Useful parameters such as the capture cross-sections of the neutral impurity species for FE may be derived from this analysis.⁴⁹

Similar types of investigation can prove useful in other semiconductors, although none have been made in such a quantitative manner as those just described for Si. Table 2 contains a strong qualitative trend for increase in the acceptor-related photoluminescence in VPE InP as the electrical properties change from good, relatively high mobility *n*-type, through material with lower mobility and higher freeze-out (ratio of carrier concentrations at 300 K and 77 K), through 'high resistivity' material for which no electrical assessment is readily possible, to *p*-type.⁵⁵ The photoluminescence data suggest that much of this trend can be associated with an increase in the concentration of shallow Zn acceptors⁵⁶ relative to donors which are yet unidentified but probably involve Si_{In}. The strength of the deeper DAP and free electron to bound hole (FB) bands also increases with increasing compensation of donors by shallow acceptors. Substantial increase in electrical freeze-out is expected with increase in the compensation ratio even for 8 meV donors in this temperature range,⁵⁷ but the electrical data yield no information on the nature of the compensating centres.

(viii) Selective Excitation of Photoluminescence and Photoluminescence Excitation Spectra

The intensities of BE spectra involving a particular species can be dramatically

TABLE 2. Correlation of electrical and photoluminescence data
in VPE InP

Electrical characteristic	D/A BE	A BE/FE	DAP
Good n-type			
$N_D - N_A \sim 10^{15} \text{ cm}^{-3}$, no freeze-out $\mu_{77} \gtrsim 25,000 \text{ cm}^2 \text{ V}^{-1} \text{ sec}^{-1}$	~ 20	~ 0.1	Very Weak, FE-L0 dominant
Moderate n-type			
$N_D - N_A \sim 3 \times 10^{13} \rightarrow 3 \times 10^{14} \text{ cm}^{-3}$ $\sim 3\text{-fold freeze-out}$ $\mu_{77} \sim 15,000 \text{ cm}^2 \text{ V}^{-1} \text{ sec}^{-1}$	$0.3 \rightarrow 1$	~ 3	Moderately Weak Zn DAP + FB, Zn 'two-hole'
High resistivity	$0.1 \rightarrow 0.5$	~ 10	Moderately Strong Zn DAP and FB, latter dominant
Good p-type			
$N_A - N_D \sim 5 \times 10^{15} \text{ cm}^{-3}$ $\mu_{77} \gtrsim 1500 \text{ cm}^2 \text{ V}^{-1} \text{ sec}^{-1}$	0.02	50	Strong Zn FB

increased by selective excitation within the no-phonon absorption lines associated with that species, readily possible with a tuneable dye laser. The effect is very useful for the enhancement of transitions associated with minority species, as exemplified recently for the study of donors in relatively lightly compensated p-type ZnTe,⁵⁸ where very little DBE luminescence appears under non-selective above band gap excitation.³⁰ As we have seen, the near gap luminescence lines tend to be inhomogeneously broadened by interactions between neighbouring species (Fig. 10) and by the effects of general strain. However, selective excitation with a very narrow laser line promotes satellite luminescence. This greatly facilitates the distinction of contributions from different chemical species due to the central cell shifts in the 'two-electron' spectra (Fig. 13), the derivation of magnetic properties of the donor states⁵⁸ and the study of excited states of the DBE which occur both just below the $n = 1$ FE state (excitations of the BE relative to the neutral donor) and below the $n = 2$ FE state (excitations of the electron within the BE). These different types of BE excited state can be seen in luminescence excitation spectra⁶⁰ (Fig. 14), and their symmetry properties can be derived from the ratios of satellite transitions to $2p$ and $2s$ excited states in selectively excited luminescence spectra^{58,59} (Fig. 15).

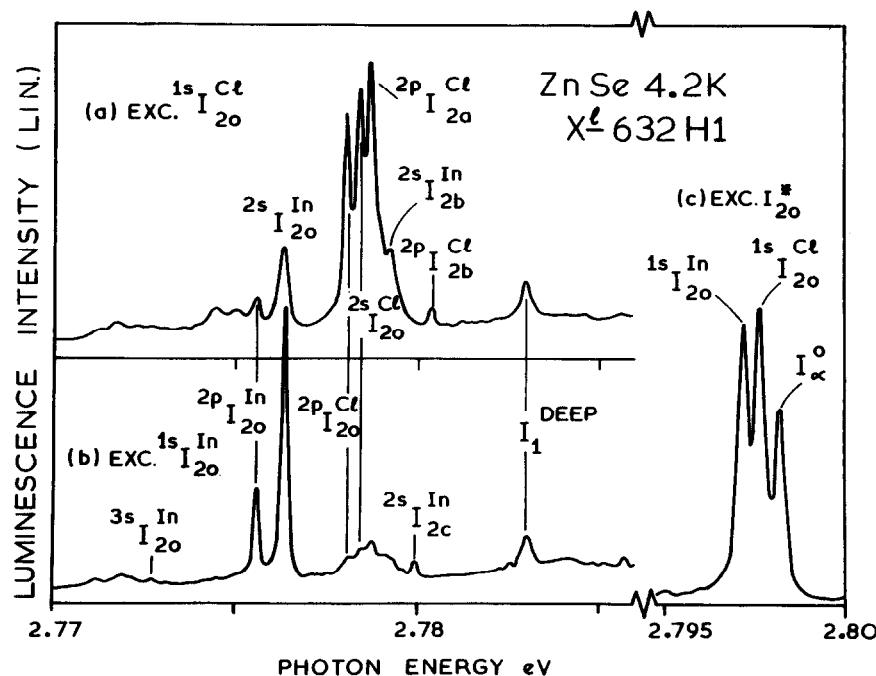


Fig. 13. Portions of the near-gap photoluminescence of an LPE ZnSe single crystal showing the effect on the relative intensities of 'two-electron' transitions involving the indicated donors of selective excitation into the principal BE components $1sI_{2o}Cl$ (spectrum (a)) and $1sI_{2o}In$ (spectrum (b)). The principal BE luminescence is shown in (c) for non donor-selective excitation. The orbital state of the donor left after BE recombination is indicated by the left-hand superscript, while the subscript denotes the BE state from which luminescence occurs.⁵⁹

The resonance process itself can be described as selectively excited DBE photoluminescence near the centre of the absorption line, where luminescence from relatively unperturbed species is selected. However, further from exact resonance, there is a competition between enhanced electronic Raman scattering⁶¹ and a background effect of selectively excited DAP luminescence⁶² which produces similar types of satellite spectra as described in Section 2 B. The reduction in linewidth compared with non-selective excitation can be very great, usually by a factor of ~ 10 to ~ 0.01 meV in the best quality crystals.⁵⁸ However, the effect persists to quite high doping levels. For example, DBE satellites of width 0.06 meV, adequate for species differentiation, can still be observed in acceptor doped ZnTe with $N_A - N_D \sim 4 \times 10^{16} \text{ cm}^{-3}$, where the ABE linewidth has broadened to over 1 meV through the effects described in Fig. 10. Similar selective excitation processes are used to advantage in impurity differentiation in laser excited far infra-red donor photoconductivity spectra using the photothermal technique.⁴¹

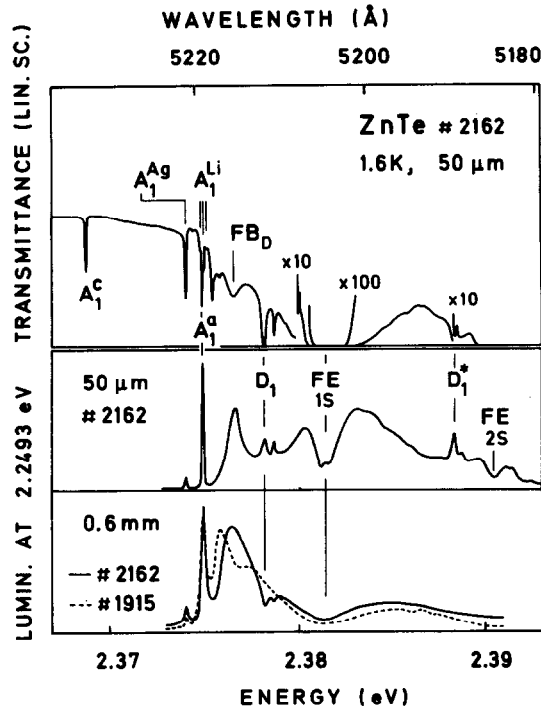


Fig. 14. Comparison of optical transmittance (upper) and excitation spectra for photoluminescence at the 2s component of 'two-hole' BE satellite luminescence for the Cu acceptor in high-purity ZnTe, recorded for thin (centre) and thick (lower) polished plates of single crystal. Principal ABE line A_1^a is due to Cu, A_1^c to an unidentified, complex acceptor.⁶⁰

Photoluminescence excitation (PLE) spectra provide very useful information about BE states, in addition to their beneficial application to DAP luminescence (Section 2 B), particularly when compared with absorption spectra (Fig. 14). Luminescence quenching by surface recombination usually produces negative PLE response for strongly absorbed light.⁴⁷ However, these can be returned to positive responses either by detection of the luminescence process intimately linked with a strong absorption feature, as for the ABE A_1^a (due to Cu_{Zn}) in Fig. 14, or by the use of an appropriately thinner specimen to avoid over-absorption, as for the DBE D_1 in Fig. 14. The excited DBE states D_1^* , connected with the $n = 2$ FE appear clearly in the PLE from the thin sample in Fig. 14, as well as the structure in the FE due to the longitudinal-transverse splitting of the $n = 1$ state of internal electron-hole binding.⁶⁰

Deviations may occur between the spectral forms of the impurity-induced BE absorption spectrum and the PLE spectrum of BE luminescence. The absorption

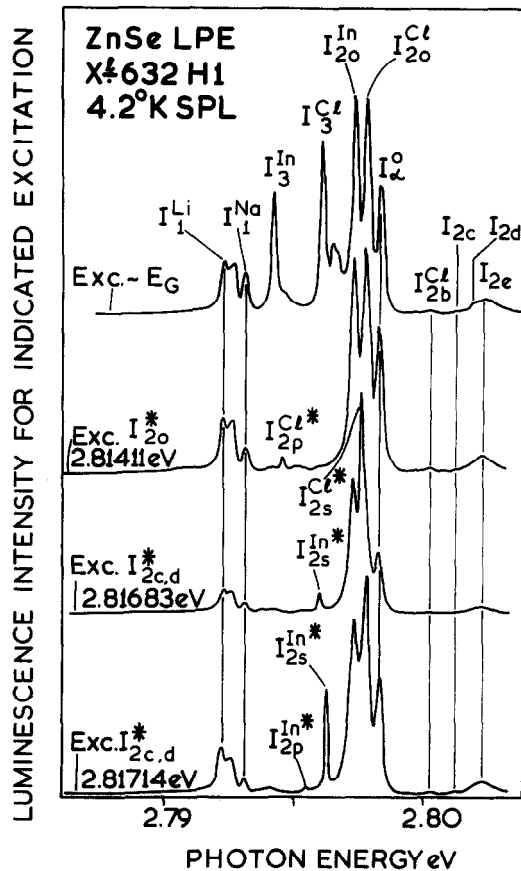


Fig. 15. Near-gap photoluminescence spectra of an LPE ZnSe single crystal recorded for excitation at the energies indicated at the left. The D⁺BE luminescence of the In and Cl⁻ donors dominant in this crystal are preferentially excited for laser energies just above E_G . Excitation into the DBE excited states I_{2o}^* and $I_{2c,d}^*$, which fall just below the $n - 2FE$, preferentially excites the DBE (non-resonantly) as well as the sharp 'two-electron' satellites of these high DBE excited states.⁵⁹

spectrum may either be measured directly¹⁹⁸ or through its contribution to the PLE of an independent luminescence system, as recently reported for DBE in GaP.¹⁹⁹ Such deviations may provide important information on the distinction between various features in the impurity-induced absorption, in this example between components due to excited states of the BE and FE transitions induced by the donor potential.¹⁹⁹

B. DONOR ACCEPTOR PAIR (DAP) SPECTRA

(i) Introduction of Concept

The recombination processes discussed in this section compete strongly with the BE processes when the compensation ratio is high and particularly when the concentration of donor and acceptor species is increased, (Fig. 16). The detailed properties of this recombination process have been reviewed elsewhere⁶³ and only the basic features will be discussed here. The electrostatic interaction within the ionized donor acceptor pair in the final state of the transition illustrated in Fig. 6a is responsible for the leading Coulomb interaction term - $e^2/\epsilon r$ in the expression for the dependence of the transition energy $\hbar\nu$ on the separation r

$$\hbar\nu = E_g - (E_A + E_D) + e^2/\epsilon r - E_{VdW} \quad (7)$$

where e is the electronic charge, ϵ the static dielectric constant and E_{VdW} is a polarization interaction term dominated by the inter-centre interaction in the initial state of the transition. To first order, the term $e^2/\epsilon r$ in eqn. (7) is responsible for the spectral dispersion into a very large number of discrete no-phonon lines. Each line is associated with a different discrete value of r allowed by the lattice structure which defines the relative positions of the donor and acceptor centres. Complications occur from several sources. The discrete line structure may be lost entirely if a large lattice relaxation accompanies the electronic transition, as is true for most DAP spectra involving recombinations through deep acceptors in II-VI compounds.⁶⁴ The DAP nature of the transitions may be established even in this case through some of the ancillary properties of DAP spectra mentioned below, particularly from their kinetic peculiarities.

The discrete DAP lines may also be lost if $E_A + E_D$ is so small that only recombinations at relatively distant DAP give bound states according to eqn. (7). Then, the energy dispersion term $\frac{d(\hbar\nu)}{dm}$ is small, where m is the shell number by which the DAP transitions are enumerated, $m = 1$ for closest pairs etc.⁶³ The energy separation between lines of adjacent m may then become smaller than the width of ~ 0.1 meV typical for non-selectively excited near gap luminescence in even well-refined semiconductor crystals, so that no fine structure can be resolved. Such a case occurs for DAP in both GaAs and InP, where E_A is modest and E_D very small. However, structure due to discrete DAP transitions can just be discerned in original photographic spectra for InP.⁵⁵ This structure cannot be convincingly reproduced either in a densitometer readout or in direct, photoelectrically recorded spectra, which do not benefit from the extreme sensitivity of the human eye to banded variations in density within a photographic stripe record of suitable height, some

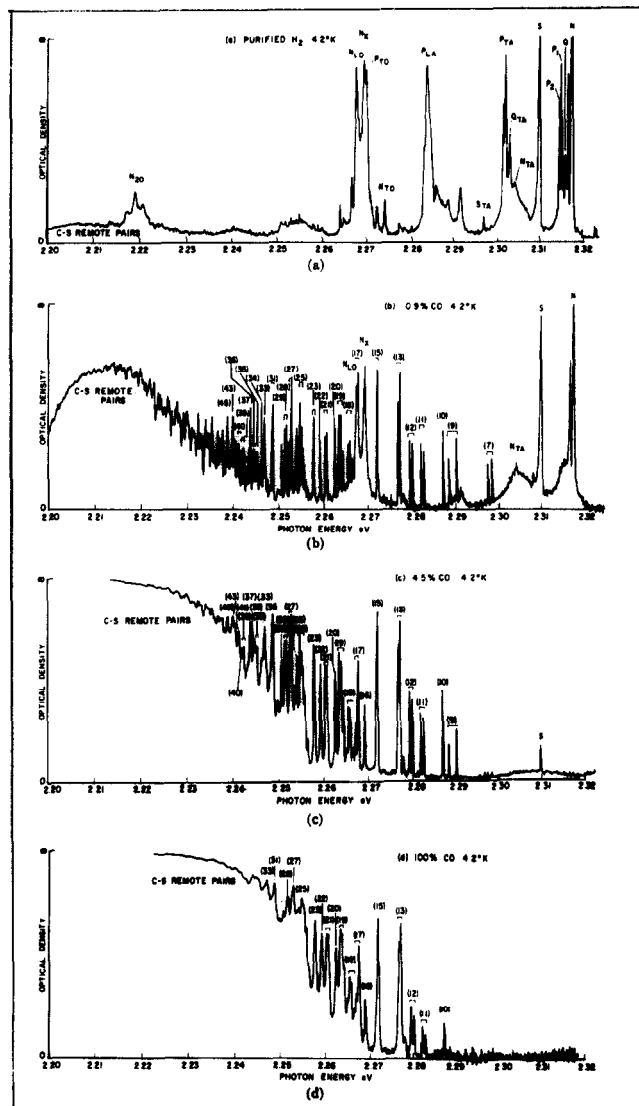


Fig. 16. The near-gap photoluminescence of GaP single crystals grown from Ga solution, doped with increasing concentrations of shallow C acceptors (spectra (a) + (d)) as well as S donors and N isoelectronic traps, recorded photographically. The concentration of S donors is low 10^{16} cm^{-3} in (a), with the C concentration somewhat lower, while the C concentration has increased to the high 10^{17} cm^{-3} by spectrum (d). The average compensation ratio probably remains near 0.3, though the crystals change from n to p-type with the addition of C acceptors. The bracketed numbers are the shell numbers m in the S-C DAP spectrum. The components P_1 , P_2 in (a) are now known to involve Si donors.⁶⁹

3-4 mm. A related problem is encountered for DAP in Si. Although the $E_A + E_D$ energy sums for typical shallow impurities are appreciably larger than in GaAs or InP, much of the advantage of this is lost because of the additional density of pair states in the lattice of an elemental semiconductor compared with a binary compound. Once again, no fine structure can be readily resolved.⁶⁵ The situation can be retrieved if at least one of E_D or E_A is large. In fact this provides a very good recipe by which such fine structure can be obtained. The appearance of the more easily resolved fine structure due to transitions at relatively close pairs (small m) is then ensured by the impurity of large ionisation energy, whereas the diffuse wave-function of the carrier bound to the shallow member ensures the good wave-function overlap over a large range of m with relatively similar intensities. Exactly this prescription has recently led to the first observation of resolved DAP structure in Si. Advantage is taken of the deep acceptor In, $E_A \sim 155$ meV and the shallow donor P, $E_D \sim 45.6$ meV in this work,⁶⁶ as well as the recent availability of a much better detector of luminescence just below the energy gap of Si (Table 1).

(ii) Demonstration of DAP Characteristics in GaP; Impurity Identification

Such considerations lead by the exact science of hindsight to the conclusion that a compound semiconductor in which E_A and E_D both lie in the range 50-100 meV would be ideal for the observation of multiline DAP spectra. Gallium phosphide fulfills this prescription very well and was available in the early 1960's with doping concentrations $\lesssim 10^{16} \text{ cm}^{-3}$, amply low enough to ensure sharp no-phonon lines for these relatively tightly bound states. Indeed one of the basic advantages of DAP spectra over BE spectra for analysis stems from the resistance of the impurity ground states to concentration broadening, consequent from eqn. (4) as a result of their relatively small effective radii a . Thus, it is no surprise that multiline DAP structure was firstly clearly recognised for GaP, in 1963⁶⁷ although the basic phonomenon had been suggested for ZnS as early as 1956⁶⁸ in consideration of spectra where no fine structure has ever been seen due to the strong lattice relaxation effects already mentioned. High quality DAP spectra such as in Fig. 17 can be reproduced for many D-A combinations in GaP, provided that sufficiently dominant doping by the impurities in question can be achieved without taking $N_A + N_D$ too far above 10^{17} cm^{-3} . The advantage of a spectrum involving transitions only between the ground states of these impurities, just mentioned, ensures that broadened but essentially unshifted and therefore readily classifiable lines can be recognised and identified up to $N_A + N_D$ approaching 10^{18} cm^{-3} in GaP⁶⁹ (Fig. 16). Following the original discovery, study of carefully purified and back-doped GaP led to the identification of the many shallow donors and acceptors shown in

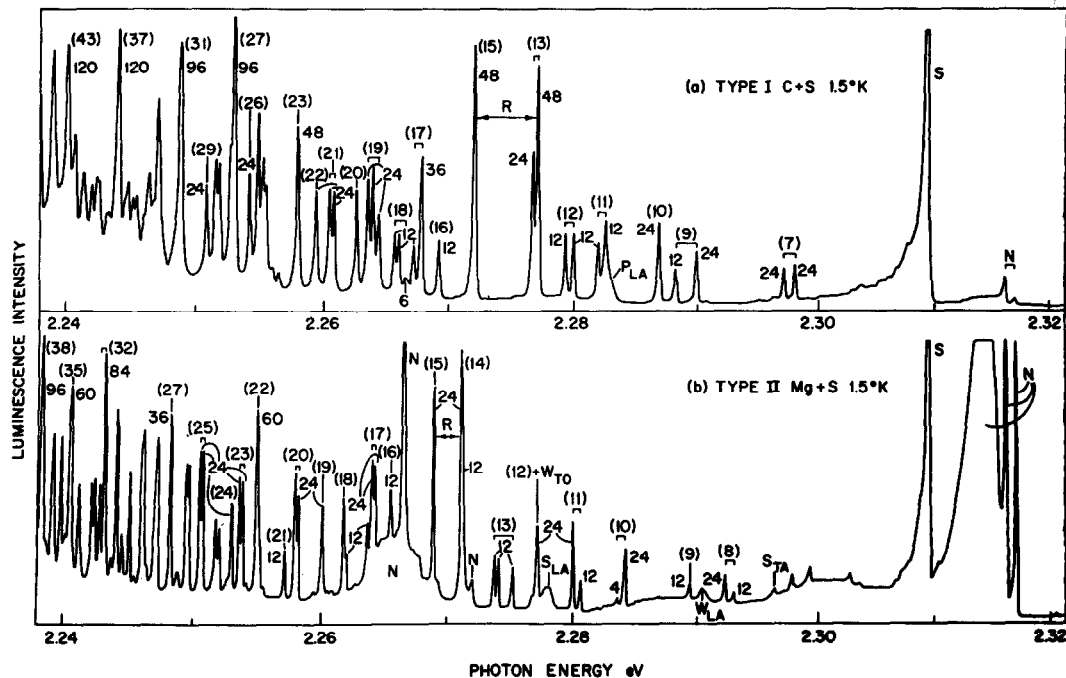


Fig. 17. A portion of the multiline luminescence of shallow DAP in GaP single crystals grown from Ga solution doped with S donors and C acceptors (a) and Mg acceptors (b). N and S BE luminescence occurs at the right. Type I indicates that both impurities fall on the same sublattice. The bracketed numbers are the DAP shell numbers m , while remaining numbers indicate the degeneracies of the DAP states. Enhancements of intensity occur near R due to resonance of an energy in the electronic capture process with that of an LO or TO lattice phonon.⁷¹

Fig. 18. Multiline DAP spectra have now been detected in a number of other semiconductors,⁶³ though in many cases definite chemical identifications are lacking because of inadequate control of the preparation techniques.

(ii) Secondary Characteristics of DAP Process

Gallium phosphide has also served as the main vehicle for the demonstration and detailed analysis of many of the most characteristic properties of DAP spectra, in particular their peculiar spectral shift and time decay⁷⁰ (Fig. 19), vagaries in the envelope of intensities of adjacent lines due to details of the mechanism of carrier capture⁷¹ and the role of multipole⁷² and piezoelectric⁷³ effects in the fine structure occurring for transitions at a given radius. These latter effects are responsible for splittings observed in the lowest temperature luminescence spectra, caused by interactions between the charged centres in the final state of the

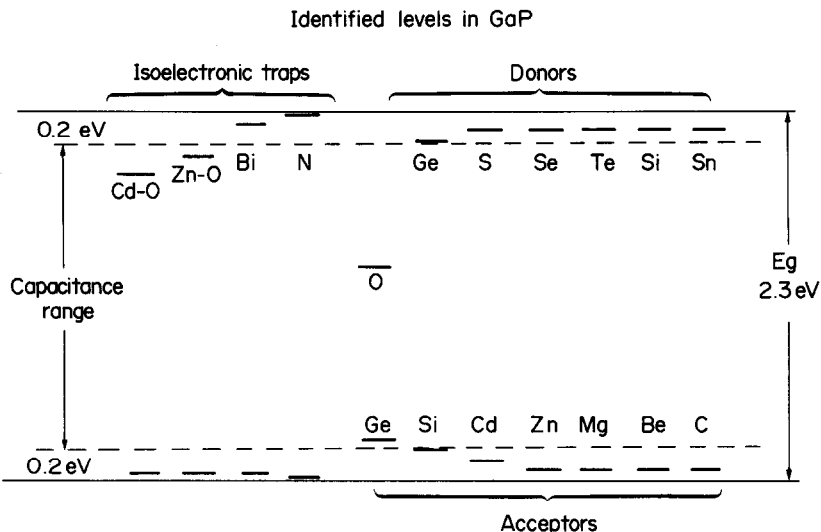


Fig. 18. A schematic indication of many of the shallow impurity species identified and measured by photoluminescence in GaP. Alternative, capacitance techniques are best suited to the indicated energy range, where the photoluminescence technique is less useful in general. Exceptions are deep centres which do not couple strongly to the lattice, such as O and certain electronic processes involving transition metals.¹⁸⁸

transition. Further structure appears in higher temperature spectra due to interactions between the neutral species in the initial state of the transition, attributed to strain splitting of the hole states in zincblende GaP.⁷⁴ It is clear that such detailed DAP spectra as are readily available in GaP can provide a very great deal of precise information on the properties of the impurities which produce them and their interactions with the host lattice. The degree of competition between the BE and DAP processes can be varied appreciably by changes in the excitation conditions. Direct creation of FE favours luminescence from D BE,¹⁷⁴ A BE⁵⁹ and relatively close DAP¹⁷⁴ while excitation near or above E_g favours luminescence from D^+BE^{59} (Fig. 15) or from distant DAP,¹⁷⁴ where the excitation process predominantly involves the sequential capture of free carriers rather than FE. Thus, excitation spectroscopy can provide revealing distinctions between luminescence bands involving different types of centre.^{173,174} Similar effects have been reported very recently in ZnS,¹⁸³ where it is also shown that the PLE spectrum of isoelectronic Mn_{Zn}^{2+} at $h\nu \gtrsim E_{GX}$ is suggestive of energy transfer through exciton states, as found for isoelectronic traps (Section 3) in GaP.¹⁷³ Such differences in PLE spectra may be used to differentiate types of recombination process contributing to strongly phonon-broadened luminescence bands, as for the UV-self activated and Te-activated luminescence in ZnS.¹⁸⁴

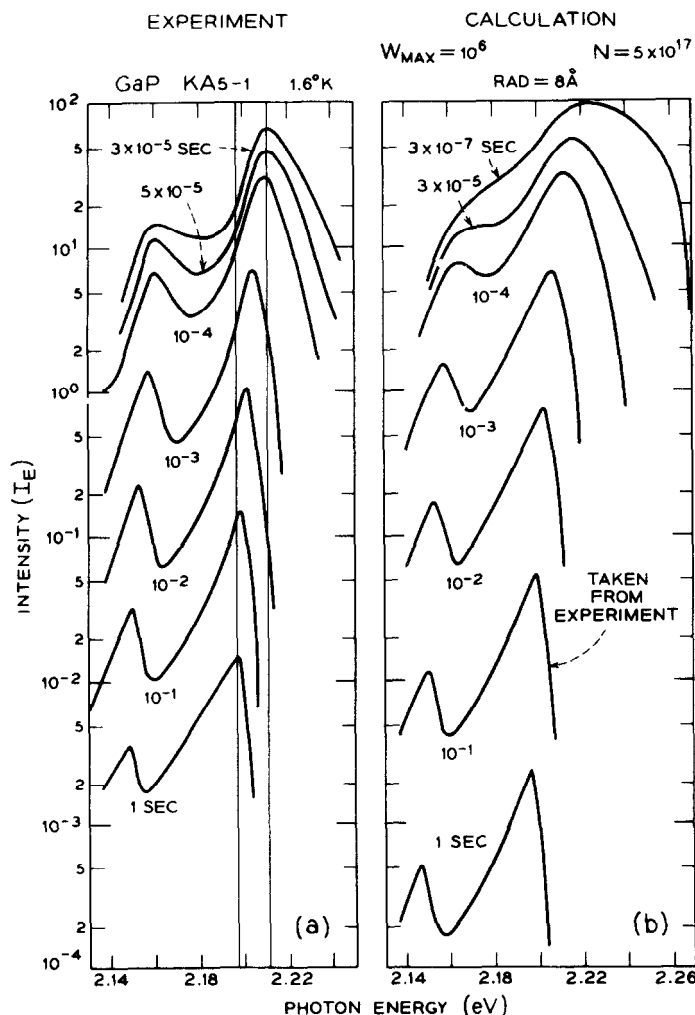


Fig. 19. Comparison between theory (right panel) and experiment for Sp-Cp DAP spectra from GaP single crystals grown from Ga solution, taken at the indicated time delays after flash photo-excitation. The theoretical curves were obtained from an equation similar to (11), using as basis the experimental curve for 0.1 sec delay to allow for the additional broadening from unresolved acoustic phonon-assisted recombinations. The additional broadening and peak shift to higher energies at short time delays, characteristics of the DAP process, are evident.²⁰¹

The fortunate circumstance that the shell substructure splittings, which are a function of the vector separation within the DAP, are generally less for a zinc-blende lattice than the inter-shell energy splittings, which are a function of their scalar separation, leads to the easy assignment of shell m values to the

observed lines (Fig. 17). Such assignments are made through a comparison of the theoretical degeneracy factors for the DAP states with the observed intensities.⁶³ Detailed line assignments have not proved possible for DAP spectra involving states of lower degeneracy than appropriate to point defect donors and acceptors in a zincblende semiconductor, for example spectra involving an unidentified (possibly $H_{Ga}-0p$) axial acceptor in GaP⁷⁵ (Fig. 20), and all shallow DAP spectra

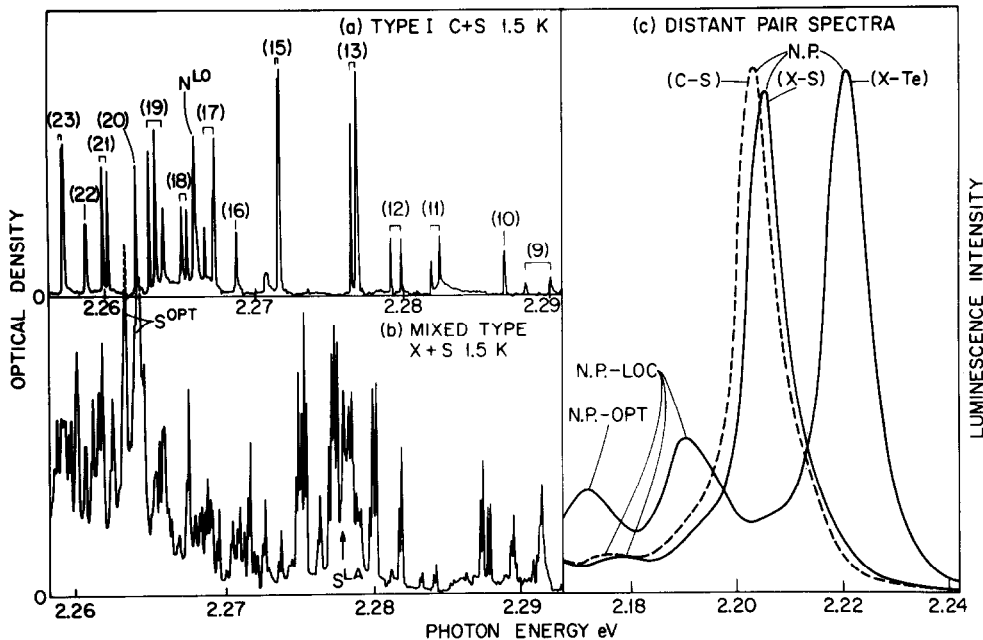


Fig. 20. Portions of DAP spectra from GaP single crystals grown in Ga solutions, recorded photographically for S donors and (a) C acceptors and (b) axial acceptors X, possibly $H_{Ga}-0p$. The energy scale of (a) is shifted 2 meV to the right to superpose transitions at given DAP separations. The numbers in (a) are the shell index number m . The spectra in (c) are recorded photoelectrically, with very low excitation intensities.⁷⁵

in wurtzite semiconductors such as CdS.⁷⁶ In the latter case, additional splittings appear in the acceptor states from the axial field of the host lattice. However, the spectrum is also complicated for wurtzite semiconductors since the static dielectric constant appropriate to eqn. (7) is significantly anisotropic relative to the c axis of the crystal.⁷⁶ Only the approximate value of m can be assigned in both these cases, from considerations of the energy density of discrete pair lines. Values of $E_A + E_D$ obtained in this way are accurate perhaps to $\sim \pm 1$ meV, instead of the $\sim \pm 0.1$ meV attainable from an accurate analysis of exactly assigned lines according to eqn. (7),⁷⁷ assuming E_g is known with appropriate accuracy.

The exact value of E_g has been difficult to establish in all indirect gap semiconductors so far examined in detail, including GaP. Only the exciton gap E_{GX} is readily obtained with reasonable accuracy from analysis of the intrinsic edge absorption⁷⁸ or luminescence⁷⁹ spectra. Relative values ΔE_D and ΔE_A have been available at high accuracy for many years from DAP spectra⁸⁰ and, for some donors, from 'two-electron' satellites.⁸¹ However, accurate independent values were held up by both uncertainties in $(E_A + E_D)$ due to absence of an accurate value of the internal binding energy of the FE, E_X and by the absence of an independently derived single value of either E_D or E_A . Severe problems existed for the analysis of available donor photoexcitation spectra obtained directly for shallow donors,⁸² via 'two-electron' satellites for P site donors⁸¹ or from luminescence excitation spectra for the deep O donor,⁸³ because of initial non-recognition of the 'camel's back' structure near the absolute minimum of the conduction band in GaP.⁸⁴ This problem has been clarified recently through the proper analysis of the donor spectra,^{85,86,200} the observation and proper analysis of acceptor photoexcitation spectra⁸⁷ and proper analysis of E_X taking account of the camel's back form.⁸⁸ This has resulted in a value of E_G close to 2.35 eV, some 12 meV larger than the initial estimate,⁷⁸ while $(E_D)_S$ is 107 meV, some 3 meV larger,⁶³ and $(E_A)_{Zn}$ is 70 meV, some 6 meV larger,⁶³ now in very good agreement with electrical data extrapolated to infinite dilution (Fig. 5a).

The alternative technique for evaluating $(E_A + E_D)$ in a new spectrum, also illustrated in Fig. 20, involves a comparison of the peak energy of the overall spectral envelope with that of a DAP spectrum for which E_A and E_D are both known. If the two spectra are chosen to have a common species, the difference in these peak energies leads directly to the energy of the species responsible for the unknown spectrum. This latter technique involves the opposite extreme excitation condition compared with any that depends on the observation of the multiline structure resolvable for pairs of moderate m . The lowest possible excitation intensity is required, so that the available excitation rate can be balanced by the very low probability recombinations through DAP of very large m and large κ (eqn. 7). In this way, the width of the band due to unresolved transitions at very distant DAP becomes as narrow as possible. Conversely, moderately high excitation rates are required to favour recombinations through DAP of moderately small m and κ . The significant residual width of the spectra recorded at low excitation rates in Figs. 19 and 20 is dominated by coupling to acoustic phonons. This width, and uncertainties in the appropriate limiting value of $e^2/\epsilon r$, limits the accuracy of absolute values of $(E_A + E_D)$ from analysis of these distant DAP envelopes to at least ± 2 meV in GaP. However, the intercomparison technique mentioned above gives E_D or E_A accurate to better than ± 1 meV.

(iv) Strong Phonon Coupling

We have already mentioned that the no-phonon transitions necessary for the DAP analyses just described become negligibly weak for pairs with large E_D and particularly, large E_A . Then, the envelope of the resulting very broad DAP spectra may be entirely dominated by phonon coupling. The spectral shifts as a function of excitation rate or delay time after pulse excitation, which are a hallmark of DAP spectra, may consequently be a minor feature of the overall bandwidth (Fig. 21). The degree of coupling to longitudinal optical (LO) phonons in a

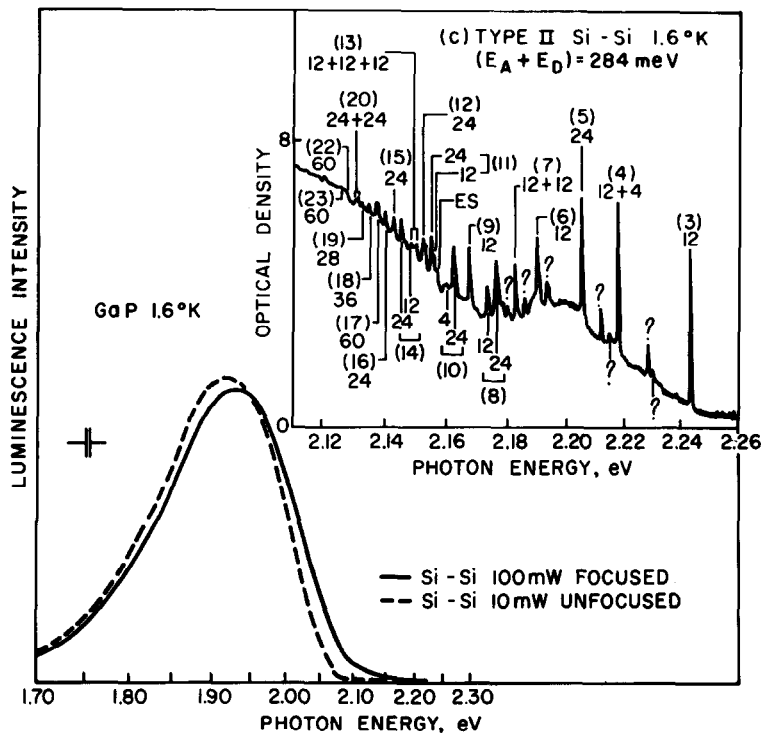


Fig. 21. The broad red photoluminescence spectrum characteristic of GaP:Si, due to $\text{Si}_\text{Ga}-\text{Si}_\text{p}$ DAP recombinations. The shift to high energies under large increase in excitation density is a characteristic of distant DAP transitions, but is small compared with the large bandwidth predominantly due to phonon-assisted recombinations arising from strong coupling at the deep Si acceptor. Weak but sharp lines due to no-phonon transitions at discrete DAP can still be detected in the high energy tail, as shown in the photographic spectrum in the inset. The notation follows Fig. 17. Several of the weak lines? are phonon replicas of discrete DAP lines.⁶³

polar lattice increases very rapidly with localisation,¹² particularly for the holes which generally have the larger mass and therefore larger Frohlich coupling constant α , according to

$$\alpha = \frac{e^2}{\hbar} \left(\frac{1}{\epsilon_\infty} - \frac{1}{\epsilon_0} \right) \sqrt{\frac{m^*}{2\hbar\omega}} \quad (8)$$

where ϵ_∞ and ϵ_0 are the high and low frequency dielectric constants and $\hbar\omega$ is the energy of the L0 phonon.

Comparable tendencies occur for coupling to phonons of intermediate energy from similar (for transverse acoustic (TA)) and other types of coupling mechanism.

Strong coupling to a wide range of modes is accentuated for a given total binding energy for localisation at a centre of lower symmetry. This is clearly exemplified by spectra observed in ZnTe:Cu^{30,34} and ZnTe:Al⁸⁹ which fall at similar energies dominated by a ~ 150 meV point defect acceptor in the former case and to an associate centre possibly involving both V_{Zn} and Al_{Zn} in the latter. The ZnTe:Cu spectrum shows well-resolved phonon structure (Fig. 9), whereas the spectrum involving the Al-related centre is nearly featureless. The general result is a rapid evolution towards the essentially structureless spectrum of Fig. 21 as E_A increases. This effect is abetted for Si_{Ga}-Sip DAP in GaP by a large reduction in oscillator strength for no-phonon transitions inherent for spectra involving Ga-site compared with P-site donors. This is an essential feature of the GaP band structure, as described elsewhere.³⁷ Weak no-phonon transitions are still detectable, with difficulty, for this particular DAP spectrum (Fig. 21). They are invaluable for the identification of the transition mechanism and the derivation of ($E_A + E_D$) through eqn. (7).

Many broad photoluminescence spectra occur for which no-phonon transitions are undetectably weak and other methods must be used for their assignment. This is true even in GaP, but to a much greater extent in the generally more polar II-VI semiconductors, where α is larger for a given hole mass (eqn. 8) and spectral broadening is consequently much greater for a given binding energy. Strong phonon coupling similar to that in DAP spectra is also inherent in the 'two-hole' satellites of ABE transitions (Fig. 22), since the phonon coupling of a localised electronic transition depends essentially upon the reaction of the lattice to the change in local charge ΔQ at the impurity site produce during the transition. The value of ΔQ is essentially the same for a 'two-hole' transition, in which the hole remaining after BE recombination ends up in the relatively diffuse $n = 2$ orbital state of the deep acceptor, as it is for the DAP transition, (Figs. 9 and 22), as a result of which the hole is essentially transferred to the distant donor. Many broad spectra with classical bell-shape and width ~ 0.4 eV, characteristic of very strong phonon coupling,⁶⁴ stand ready to be assigned in such semiconductors. Before describing techniques available for this task, we consider some methods for

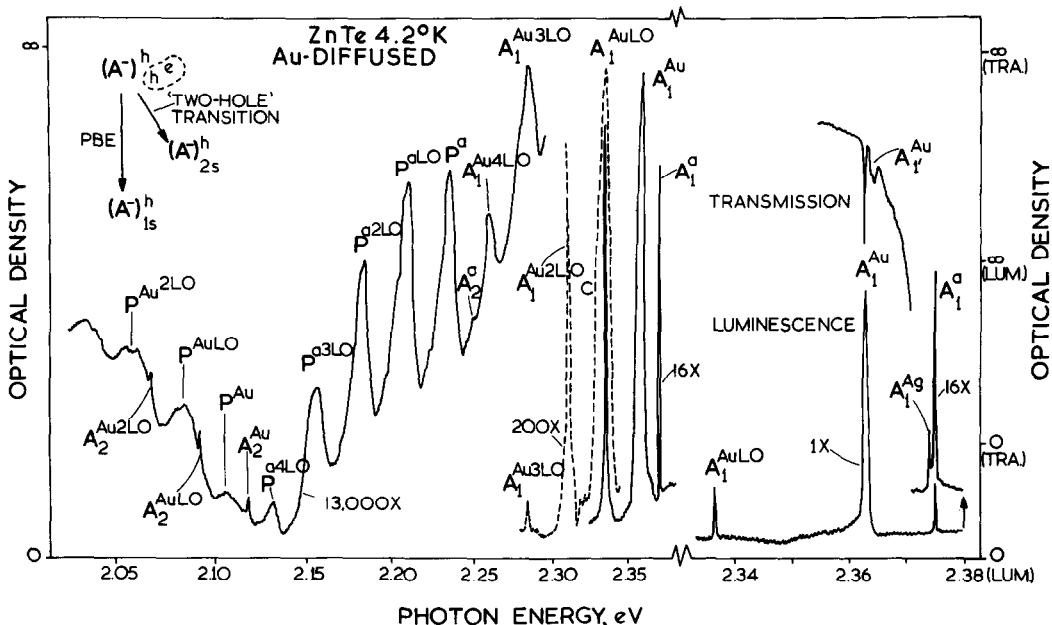


Fig. 22. The photoluminescence of Au-diffused ZnTe, recorded photographically. The detailed near-gap portion (right) contains principal ABE lines due to Cu (a), Ag and Au acceptors, the latter recorded also in optical transmission. The spectra at the left, recorded with the indicated relative photographic exposure times, show principal ABE phonon-assisted transitions and the DAP luminescence P due to Cu (a) and Au acceptors, as well as the 'two-hole' satellites of their BE transitions A_2^{Ag} and A_2^{Au} . Two-electron and DAP transitions involving the deep Au acceptor have weak intensities and are strongly phonon-coupled.¹¹⁴

obtaining structure from DAP spectra where the multiline transitions are hard to resolve for the reasons other than very low no-phonon oscillator strength which has just been described.

(v) Selective Excitation of DAP Photoluminescence and Photoluminescence Excitation Spectra

Donor acceptor pair spectra with no resolved multiline structure but reasonable strength of *no*-phonon transitions reveal detailed structure through two related techniques, either photoluminescence excitation (PLE) spectroscopy or selectively excited photoluminescence (SPL) already discussed for BE in Section 2 A. The key aspect in the former technique is the selection of luminescence from only a narrow range of λ (eqn. 7) by use of a high resolution detecting monochromator⁹⁰ while the latter technique depends upon the selective excitation of DAP within only a narrow range of λ .⁹¹ Both techniques are possible only through use of a tuneable dye laser. The high radiance from such a spectral source within the required narrow range of photon energy, compared with the standard broad band source and monochromator technique (Table 1), is vitally necessary to minimise the signal to noise problems otherwise consequent upon use of such a strictly limited portion

of the DAP spectrum.

The essential physics for the PLE process (Fig. 23) is closely related to that of

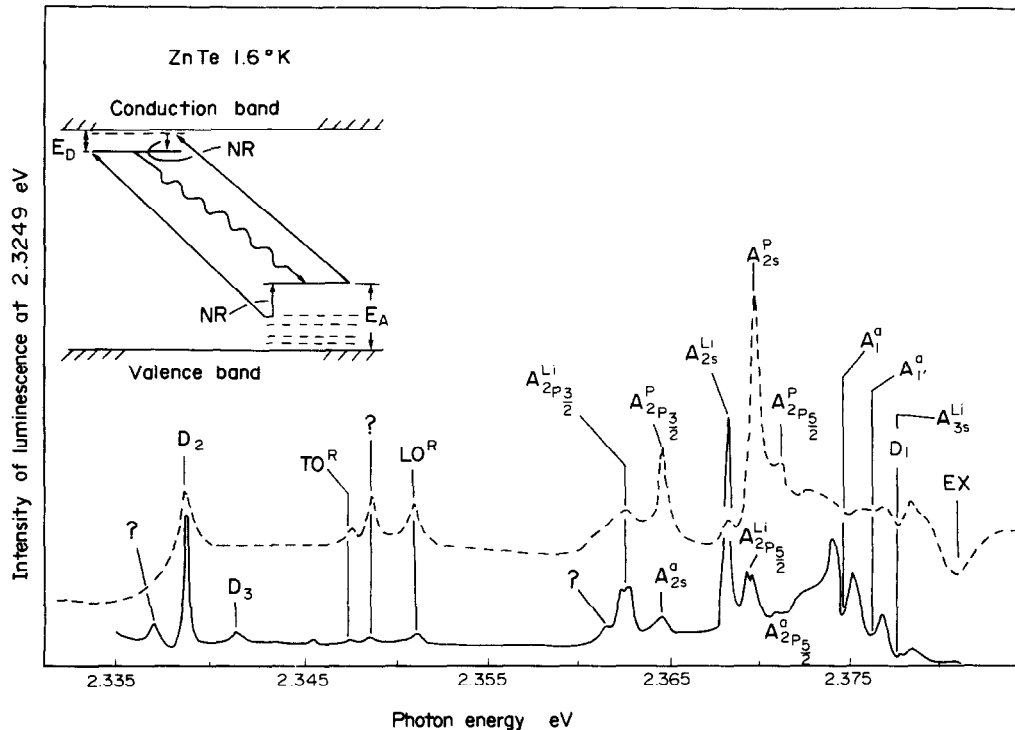


Fig. 23. Photoluminescence excitation spectra compared for undoped, refined p-type ZnTe grown from a Te-rich melt (solid curve) and an ingot back-doped with shallow P acceptors to give $N_A-N_D \sim 10^{16} \text{ cm}^{-3}$. The principle of the excitation technique of DAP luminescence recorded in a narrow energy range under excitation by a tuneable dye laser is shown in the inset. Structure appears involving excitations to excited states of an unknown donor D and of the P, Li and Cu (a) acceptors. Subscripts denote the orbital excited state involved in the excitation process. Creation of BE causes minima in the excitation of the distant DAP luminescence detected.¹⁸⁹

the SPL process. In these PLE spectra, photoluminescence from ground state to ground state recombinations for DAP lying within the narrow range of ν selected according to eqn. (7) is excited by absorption processes which leave either the donor or acceptor in a series of excited states. These include both s and p type orbital excited states, because the D-A interaction breaks the parity selection rule for transitions within an isolated centre. The excited to ground state de-excitations within the donor or acceptor occur very rapidly before radiative electron-hole recombination, since they are possible by emission of a single phonon

or pair of phonons for most shallow donor and acceptor centres. For the SPL process, the photon energy of the laser matches the excitation energy to different donor or acceptor excited states for DAP of different separations, with a similar subsequent non-radiative internal relaxation before luminescence. The overall effect is that excitation lines occur in the PLE at energies *above* that of the detected luminescence which are just the internal excitation energies of the D or A , while luminescence lines occur in the SPL displaced *below* the excitation energy by these same energies. The internal excitation energies so obtained are negligibly influenced by the DA interaction provided that data are taken at DA separations $r > a_D$ if the donor Bohr radius a_D dominates the DAP interaction, as is true for most direct gap semiconductors where $E_A > E_D$. This condition is readily fulfilled in a direct gap semiconductor, where the ~ 3 orders of magnitude increase in the scale of DAP transition rates readily allows excitation at $r/a_D \sim 2-3$.⁹² It is much less readily achieved in an indirect gap semiconductor such as GaP, where this type of PLE spectrum was first demonstrated.⁹⁰ Indeed, an interesting feature of the GaP work is that satisfactory spectra were obtained only for DAP involving P site donors and only contained excitation structure characteristic of acceptors,⁹⁰ in contrast to Fig. 23. The ~ 100 -fold reduction of DAP transition rates for spectra involving Ga site donors compared with P site donors⁹³ means that such PLE spectra are very difficult to obtain for Ga-site donors, even with a tuneable laser light source. Excitations to the $n = 2$ or higher orbital state of the P site donor for DAP spectra involving these species are of similarly low relative oscillator strength, since it is the binding of the electron in the ground state of the P site donor which provides the key feature of a high no-phonon oscillator strength in this indirect DAP transition. The relatively low oscillator strength of all shallow DAP transitions in GaP favours data from relatively small values of r . Then, the excitation energies are significantly dependent upon r , producing splittings as well as energy shifts as observed in InP⁹⁴ (Fig. 24) as well as in GaP.⁹⁵ The significant discrepancies between the values of E_A in GaP derived from DAP PLE spectra⁹⁰ and those obtained from direct infra-red absorption⁸⁷ presumably arise from the inadequately treated residual influence of this D-A interaction in the DAP spectra.

The SPL spectra contain contributions from non-selectively excited DAP as well as the sharp structures due to selectively excited species, since $h\nu$ generally lies above $E_G - E_A$ and so can produce the inverse of the FB recombination process described below. The resulting recombinations produce a narrow band characteristic of weakly but non-selectively excited DAP's, with the sharp structure superimposed^{91,94} (Fig. 25). The sharp components follow changes in the photoexcitation energy, whereas the energy of the broad distant pair peak remains constant.

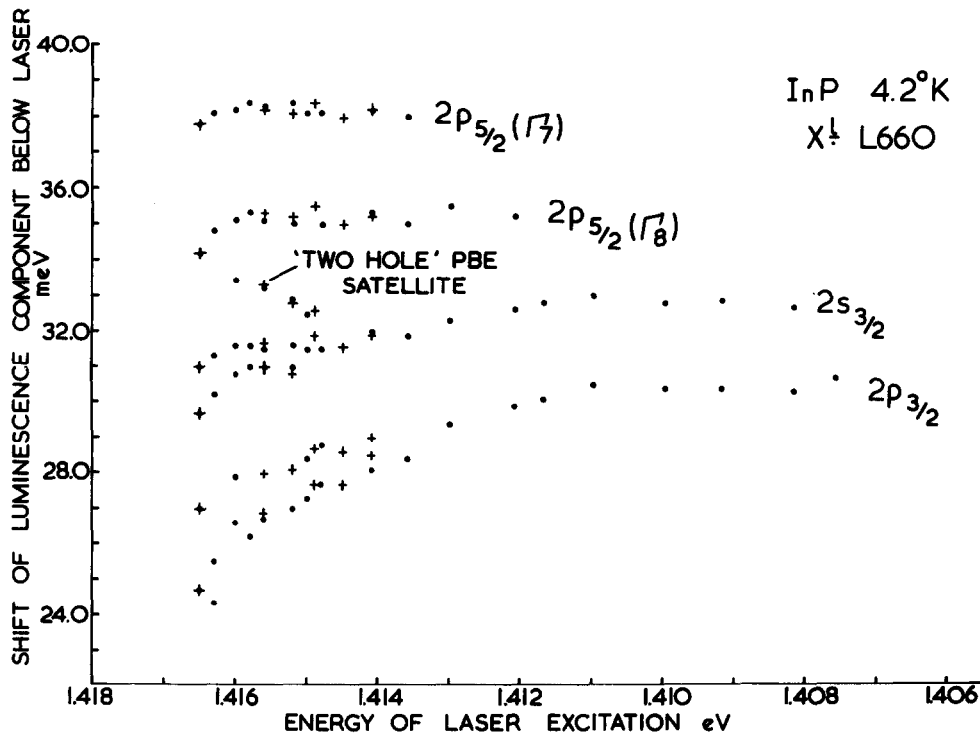


Fig. 24. The variation of the indicated excitation energies of the shallow Zn acceptor in InP, determined from SPL spectra as in Fig. 23 and also from PLE spectra of a refined crystal grown by the liquid encapsulated Czochralski (LEC) method. These energies decrease with increasing excitation energy, that is with decrease in the internal separation of the selectively-excited DAPs. Transitions involving Γ_8 -excited states also split when the DAP overlap becomes sufficiently strong.⁹⁴

Similarly, non-selectively excited luminescence causes a broad threshold to appear near $h\nu = E_G - E_A$ in the PLE spectra. Approximate values of E_A may be obtained from these thresholds,⁹⁶ as well as the more accurate estimates from analysis of the energies of transitions to shallow acceptor excited states.^{60,92} The values of E_A obtained from the broad thresholds in ZnTe⁹⁶ are systematically ~ 2 meV lower than those determined from the ABE.^{60,92} This is due to incorrect values of E_g used in the application of the former technique, rather than any large inherent inaccuracy in method. The DAP PLE technique has also recently been applied to ZnSe,⁹⁷ CdTe⁹⁸ and InP.⁹⁴

(vi) Kinetic and Other Analyses of Strongly Phonon Coupled DAP Spectra

Identification of strongly phonon - coupled DAP spectra containing negligible no-

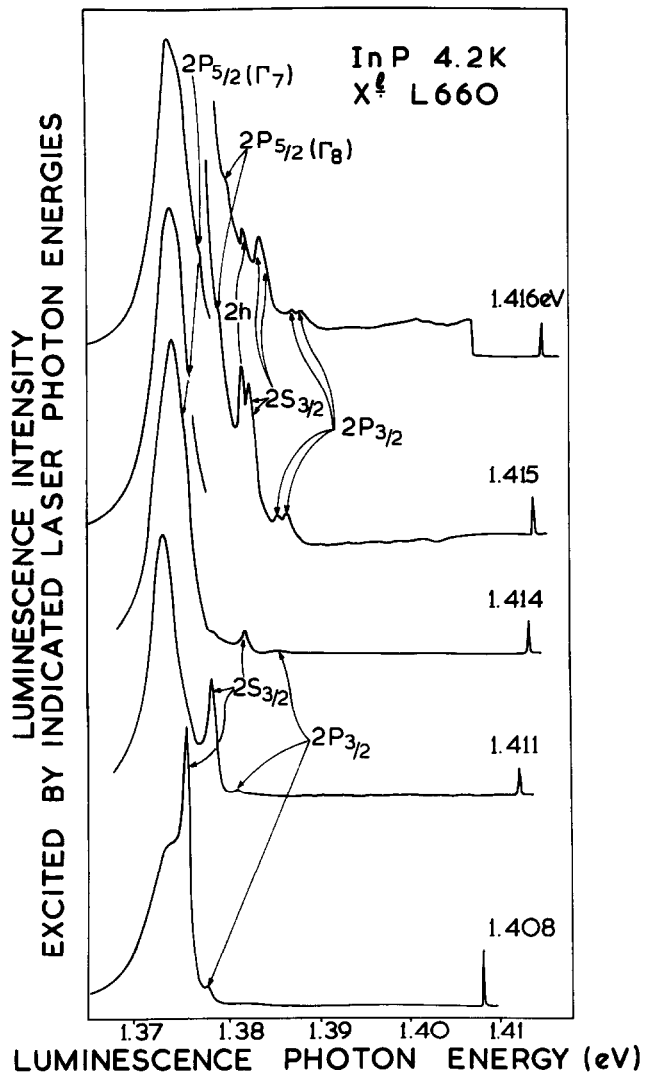


Fig. 25. Selectively excited DAP photoluminescence spectra in a refined InP crystal grown by the LEC technique. The attenuated line of the tuneable dye laser excitation source is shown at the right. The broad band at the left is caused by recombinations at non selectively-excited distant DAPs, while the structure on its high energy tail represents luminescence from DAP selectively excited to the indicated excited states of the shallow Zn acceptor.⁹⁴

phonon components can be achieved with kinetic methods, as exemplified for the featureless photoluminescence spectra in ZnS related to the 1.25 eV Cu acceptor.⁶⁴ Shionoya and co-workers⁶⁴ demonstrated that this luminescence has non-exponential, relatively slow time decay with a small spectral downshift for long delay times,

characteristic of DAP transitions.⁷⁰ They also showed that the photo-induced infra-red absorption associated with the Cu acceptor and Al donor were quenched with a similar time decay.⁹⁹ Fair *et al.*¹⁰⁰ attributed optically-induced electron spin resonance (ESR) to selectively photo-excited D-A associates in ZnS:Cu, Ga. The green DAP luminescence of ZnS:Cu, Al shows complex behaviour of stimulation and quenching under simultaneous illumination by infra-red light which is probably typical for this type of system with deep acceptor (~ 1.25 eV) and shallow donor (~ 0.1 eV). The stimulation observed at low temperatures is attributed to migration of trapped holes between the 2E excited states of the Cu acceptors, some 0.4 eV above the valence band, whereas the photo-induced quenching at 300 K results from the release of the holes to the valence band and their subsequent recombination at other non-radiative centres.¹⁷⁵ Resonance transfer of the excitation energy can also occur at low temperatures from these DAP to certain transition metals, notably Mn²⁺. Others, such as Fe²⁺, Co²⁺ and Ni²⁺ may act mainly through their competition for the primary excitation, and can only produce infra-red light from their lowest energy intra *d*-shell excitations.¹⁷⁶

(vii) Optically Detected Magnetic Resonance of DAP Photoluminescence

Relatively recently, the technique of optically detected magnetic resonance (ODMR) has found very fruitful application in this type of problem (Fig. 26). This technique offers a direct connection between the ESR signal and a particular luminescence band,¹⁰¹ although this straightforward view can be misleading in certain complicated situations as recently found for O in GaP.¹⁰² The great advantage is that ODMR offers most of the detailed characterisation familiar for the ESR technique, including the chance of observing the hyperfine interactions between the electronic and nuclear magnetic moments which can contribute very specific information on the nature of the atomic species local to the centre and hence its overall structure. Smaller hyperfine splittings may still be resolved even when the luminescence spectrum is very broad, for example that corresponding to the hyperfine constant $A \sim 9.6$ GHz for the very deep In_{Zn}¹¹⁵ donor in ZnS.¹⁰³ The ODMR technique applied to the Ti_{Si} BE spectrum in SiC has even shown up local crystal field splitting parameters which vary significantly with the isotopic mass of the Ti.¹⁰⁴ This example illustrates the applicability of the ODMR technique to the analysis of general luminescence spectra, not just those related to distant DAP transitions. Another example is GaP:O, where it appears that the triplet state resonance detected in ODMR may involve transitions of the second electron in the O_p⁻ charge state¹⁰⁵ rather than internal relaxations of the single electron in the neutral O_p⁰ charge state through which the resonance is detected.¹⁰² Transitions of the O⁻ ground state are apparently entirely non-radiative, so this illustrates the ability of ODMR to provide information on non-radiative processes

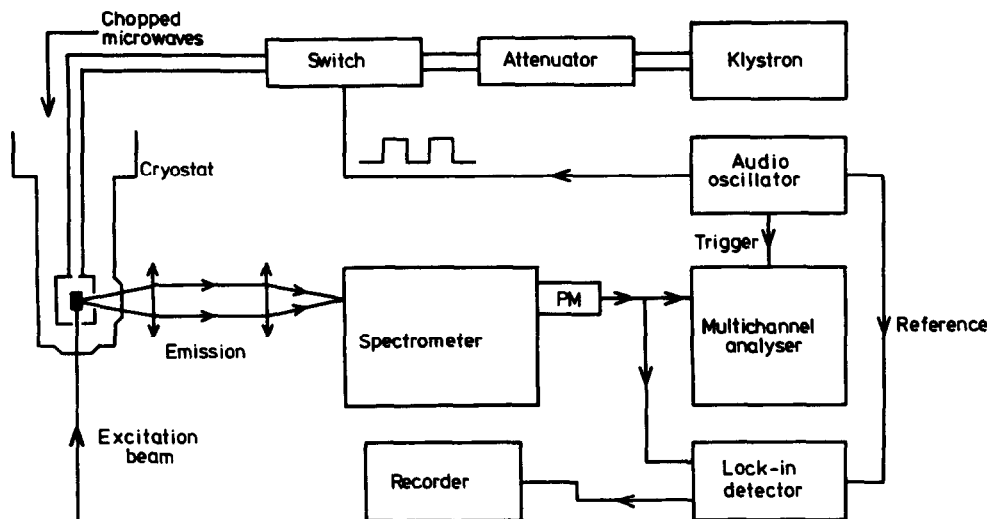


Fig. 26. Schematic apparatus for ODMR. The sample in the cryostat at the left is held in a magnetic field, which is slowly swept to obtain the ODMR spectrum through measurement of the changes in total intensity or polarization of the luminescence in a given spectral region using lock-in detection. The spectral response of a given ODMR signal can also be measured if the magnetic field is held at an appropriate value and the luminescence changes measured as the spectrometer is scanned through the luminescence spectrum.¹⁰⁶

which can influence the recombination rates for the luminescence transitions which produce the ODMR signal. The ODMR technique is frequently considerably more sensitive than ESR, since efficient luminescence may be detected from a small number of centres more readily than absorption of the overall microwave power. A further advantage, typical of photoluminescence, is the ability of ODMR to probe different regions of a sample by using focussed exciting light, perhaps also with adjustable penetration depth.

The general ESR advantage obtains for ODMR compared with Zeeman spectroscopy, namely that the microwave field induces transitions directly between the magnetic subcomponents. This removes much of the spectral broadening which limits the resolution of the Zeeman technique. However, there is some price to be paid for the specific connection between the ODMR signal and a DAP luminescence spectrum. The ODMR resonance is broadened by the unresolved variation of the DAP exchange interaction energy over the range in separation of the moderately close DAP's dominantly responsible for the signal.¹⁰⁶ Nevertheless, the ODMR signal can still

be obtained even when there is no detectable no-phonon line available for Zeeman study.

The magnetic resonance is detectable optically because the radiative transitions responsible for the luminescence obey spin selection rules. When the electron population amongst the magnetic spin substates of the simple DAP in Fig. 27 is altered by microwave pumping, the polarization and in general also the intensity of

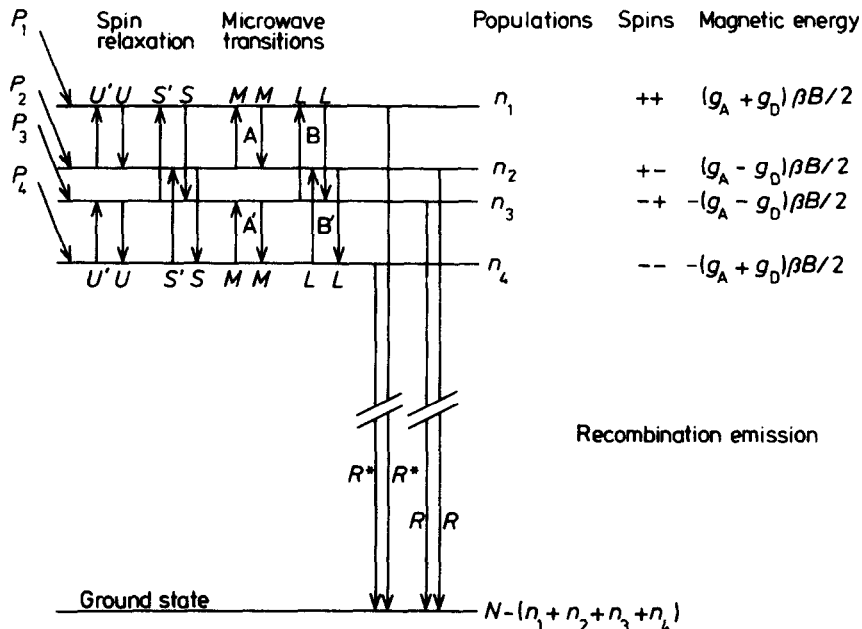


Fig. 27. Energy levels of a DAP in a magnetic field for vanishingly small electron-hole exchange interaction, assuming that the J value of the bound hole is the pure spin value, $J = \frac{1}{2}$, like the electron spin at the donor. Microwave-induced transitions between the spin states are denoted by rate constants M (donors) and L (acceptors), spin-relaxation transitions by U and U' (donors, with $U = U' \exp(g_D\beta H/kT)$) and by S and S' (acceptors, with $S = S' \exp(g_A\beta H/kT)$). The DAP recombination rate constants are R and R^* , with population of excited states from the ground state by rate constants P_1 - P_4 .¹⁰⁶

the luminescence is altered.^{101,106} Typically, the radiative fraction of the DAP recombination rate constants R and R^* will differ, but it can be shown¹⁰⁶ that ODMR-induced changes in equilibrium luminescence intensity will occur at optical saturation. For the opposite extreme of complete thermal equilibrium between the magnetic substates, the equilibrium signal is much larger if R^* is much greater than R , due to non-radiative processes. In either case, the maximum equilibrium luminescence intensity changes at microwave saturation are $\sim 1-2\%$ at X band and $T = 2$ K.¹⁰⁶ Practical signal levels are frequently much less. However, good signal

to noise is still available with lock-in techniques, particularly for efficient luminescence centres excited by powerful laser sources¹⁰⁷ (Fig. 28). The sensitivity is often high enough to allow a check that the form of the spectral

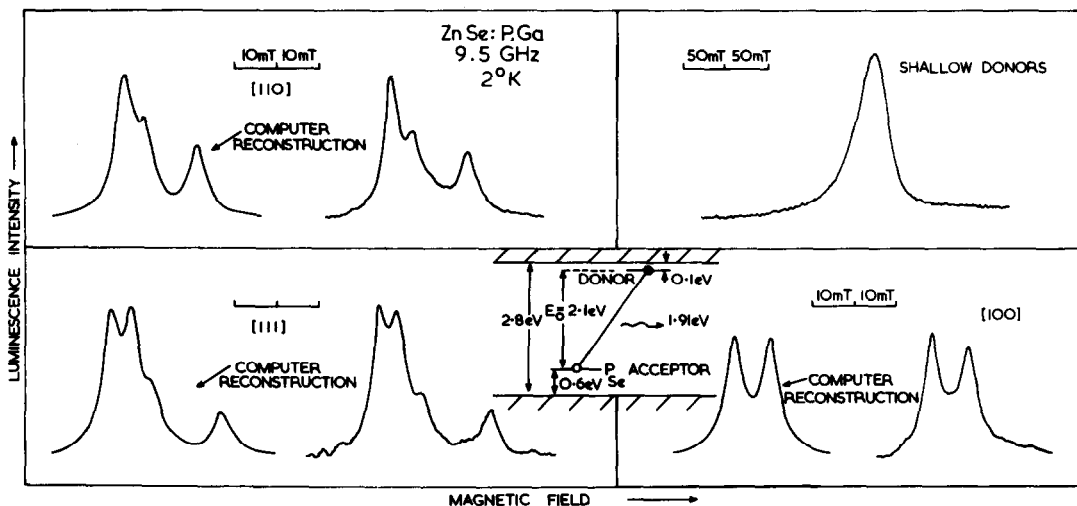


Fig. 28. Increase in red DAP luminescence intensity of ZnSe:P as a magnetic field is swept with 9.5 GHz radiation incident on the sample. The isotropic but asymmetric high-field resonance is due to shallow donors. The complex, anisotropic low-field resonance has spectral form which is well-reproduced by computer simulations using the anisotropic hole g-values of the deep P_{Se} acceptor determined from ESR. The inset shows the energy levels responsible for this red luminescence.¹⁰⁷

dependence of the ODMR signal is identical to the luminescence component of interest. This technique has confirmed the DAP origin for a number of broad luminescence bands in II-VI semiconductors, as well as for the edge luminescence where the phonon structure is fully resolved and other techniques are available to support this identification, including Zeeman spectroscopy.²⁷ Thermalisation is incomplete for many of these spectra. Analysis suggests that recombinations between well-isolated pairs must predominate in most cases, with recombination rate-dependent spin populations, otherwise vanishingly small ODMR signals are predicted.¹⁰⁶ This latter factor also causes large spikes in the ODMR response to transients in the microwave field.¹⁰⁶

C. FREE TO BOUND (FB) SPECTRA

(i) Introduction of Concept

This recombination process, in many ways simpler than the DAP process, has similar virtues of persistence in recognisable form at higher doping levels than the

relatively weakly bound ABE and DBE processes of Section 2 A. It also persists to higher temperatures for a similar reason. With increasing T , the DAP transitions evolve towards the FB process at acceptors for systems where $E_A \gg E_D$, as in the low energy gap, direct semiconductors (Fig. 29). The low energy threshold of

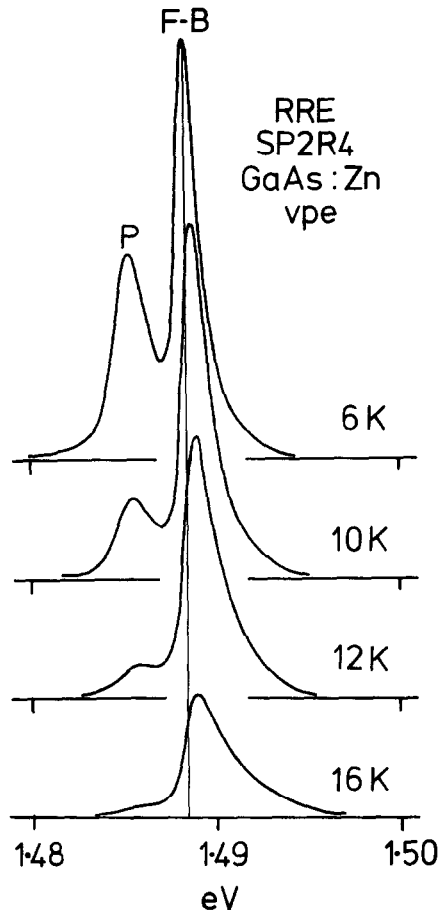


Fig. 29. The evolution of the AFB band (F-B) from the DAP band (P) with increasing temperature in VPE GaAs which contains only one significant shallow acceptor, identified with Zn. These spectra were recorded at very low excitation intensity. Since the donors are energetically indistinguishable, this results in only one pair of bands P and F-B.³¹

this FB band is then simply

$$h\nu = E_g - E_A \quad (9)$$

The FB band is broadened by the kinetic energy of the electron before recombination (Fig. 30). Usually, electron-hole pairs are created at energies appreciably greater

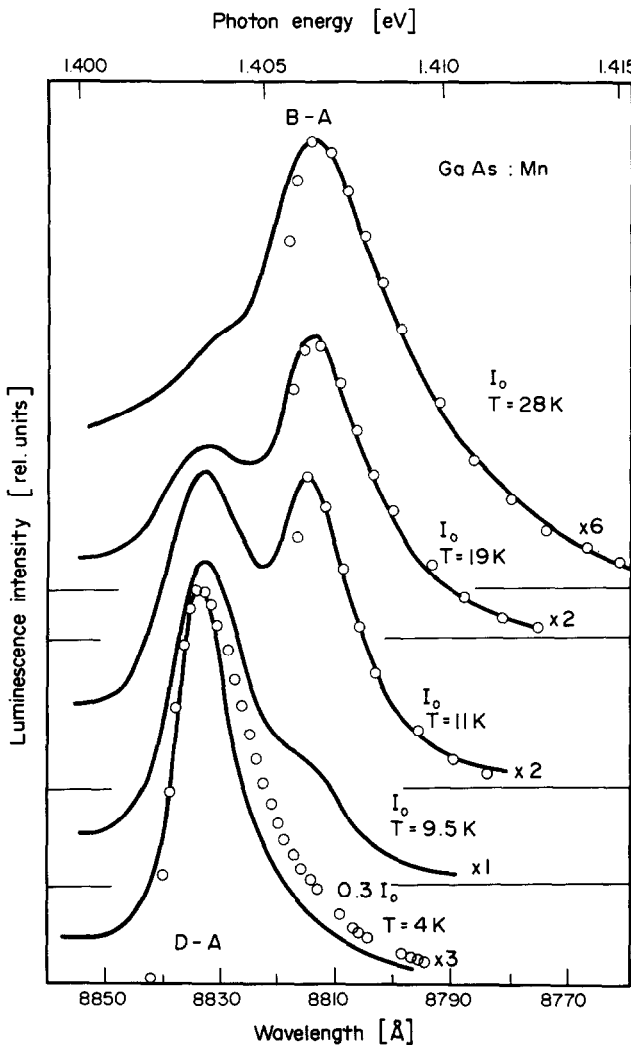


Fig. 30. Analysis of the no-phonon FB (B-A) luminescence bands of GaAs:Mn in terms of simple Maxwell-Boltzmann forms (eqn. 13) indicated by the O points and by the theoretical form for distant DAP luminescence (D-A) (eqn. 11). The DAP mechanism predominates at 4 K and low excitation intensity I_0 for appropriately-doped crystals. Phonon-assisted DAP recombination components which are relatively strong for this deep acceptor occur at lower energies and are not shown.¹⁹⁰

than E_g , particularly for relatively narrow direct gap semiconductors like GaAs, where there is no convenient gas laser with photon energy only just above E_g . When the carrier density is high, readily achieved under these excitation conditions, and the impurity density and lattice temperature are both low enough that electron-electron and hole-hole collisions predominate over the collisions with impurities or phonons which alone dissipate energy from the total photoexcited

carrier system, it is common to find electron and hole temperatures appreciably in excess of the lattice temperature in the fast radiative recombination processes characteristic of direct gap semiconductors at low temperatures. This effect was first studied for band to band (intrinsic) transitions in GaAs¹⁰⁸ and in CdS¹⁰⁹ but has since been demonstrated for FB processes in GaAs by Ulbrich¹¹⁰ using 0.2 n sec excitation pulses. Electron-electron collisions efficiently randomise the electron energies at least within a few tenths n sec, even at very low injected densities. However, the electron temperature does not fully decay to the lattice temperature of 4.2 K even after 10 n sec for a high purity GaAs crystal.¹¹⁰ Recent measurements under p sec optical excitation¹¹¹ have established the form of the much faster energy loss process to L0 phonons. These processes dissipate the majority of the excess energy $\hbar\nu_{\text{exc}} - E_g$, until the residual energy is too low for dissipation other than to acoustic phonons. Similar temperature excesses also appear under steady state excitation, when very accurate Maxwell-Boltzmann forms of the greatly heated electron distribution may be deduced from the FB spectra¹¹⁰ (Fig. 31).

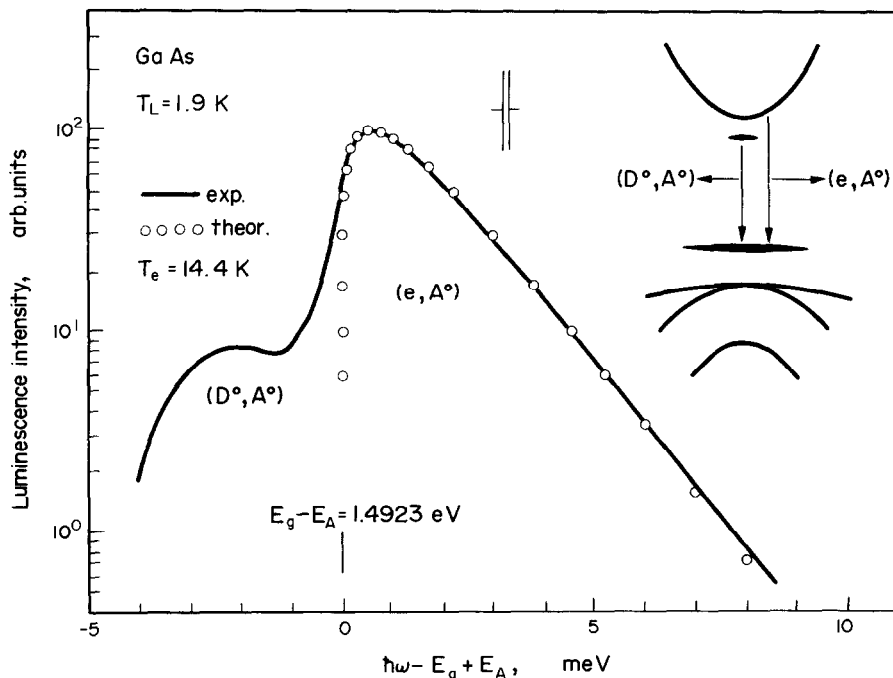


Fig. 31. The low temperature CW photoluminescence of a strongly excited ($\sim 6 \text{ W cm}^{-2}$), lightly doped LPE GaAs single crystal, recorded on a logarithmic intensity scale. Only the $\sim 26.9 \text{ meV}$ C_{As} acceptor is significant. Analysis of the FB spectral component (e, A°) indicates a Maxwell-Boltzmann form (0 points) with electron temperature $T_e \gg$ lattice temperature T_L . The inset shows the origin of the FB and DAP (D°, A°) spectral components.¹¹⁰

Evidence of strong coupling to LO phonons is also obtained from various types of excitation spectroscopy (Fig. 32). The appearance of undulatory structure with period approximately $\hbar\omega_{LO}$, observed in many semiconductors, proves that energy relaxation by LO phonon emission is the fastest of several competing processes. However, it was in GaAs that comparison of the excitation spectra for DAP and FB photoluminescence first showed that the capture of hot conduction band electrons by ionized donors involving cascade emission of LO phonons is an efficient relaxation channel, contributing minima in the FB PLE spectra matching maxima in the DAP PLE spectra.¹¹² The oscillations are observable only because the rate of the direct capture process is comparable with the scattering rate of hot electrons by acoustic phonons. Conservation of energy and momentum requires that oscillatory structure depending upon such hot electron effects obeys the energy series

$$\hbar\nu = E_g + n\hbar\omega_{LO} \left(1 + m_e^*/m_{hh}^*\right) \quad (10)$$

since transitions from the heavy hole valence band, mass m_{hh}^* predominate for density of states reasons. On the other hand, the periodicity of oscillatory effects associated with excitons, which may appear in PLE of both FE and BE luminescence, is just $\hbar\omega_{LO}$. Spectrally sharper features connected with resonant Raman scattering generally also appear in these spectra (Fig. 32).¹¹³

The strong coupling between electronic transitions and phonons may be used to indicate deviations of the phonon energy distribution from thermal equilibrium conditions appropriate to the local lattice temperature. Thus, the cascade emission of LO phonons may be detected specifically from anomalies in the intensity of the anti-Stokes phonon replica in an appropriate BE luminescence. This has been reported for the shallow ABE in CdS, recorded under intense local excitation with energy excess $\hbar\nu_{EXC} - E_g$ appreciably larger than $\hbar\omega_{LO}$.¹⁹⁵ Alternatively, LO phonons might be generated directly by infra-red lattice absorption, for example with an intense pulsed H₂O laser, then detected by enhancements in the intensity of the Stokes phonon replica of an appropriate independently-excited system such as the NBE in GaP. However, no such effects were seen in this work, only photo-dissociation of the BE states by the infra-red photons.¹⁹⁶ LO phonons decay into pairs of acoustic phonons, so the intensities of luminescence sidebands involving these phonons should also be modified.¹⁹⁵ They are generally broader and therefore somewhat less readily used for this purpose. However, heat pulses applied through surface metallisation result only in an increase in the density of low energy acoustic phonons. These may propagate ballistically at low temperatures. Evidence for the existence of such ballistic phonons produced by the absorption of light at one face of a 40 μm plate of CdS was obtained through appropriate intensity

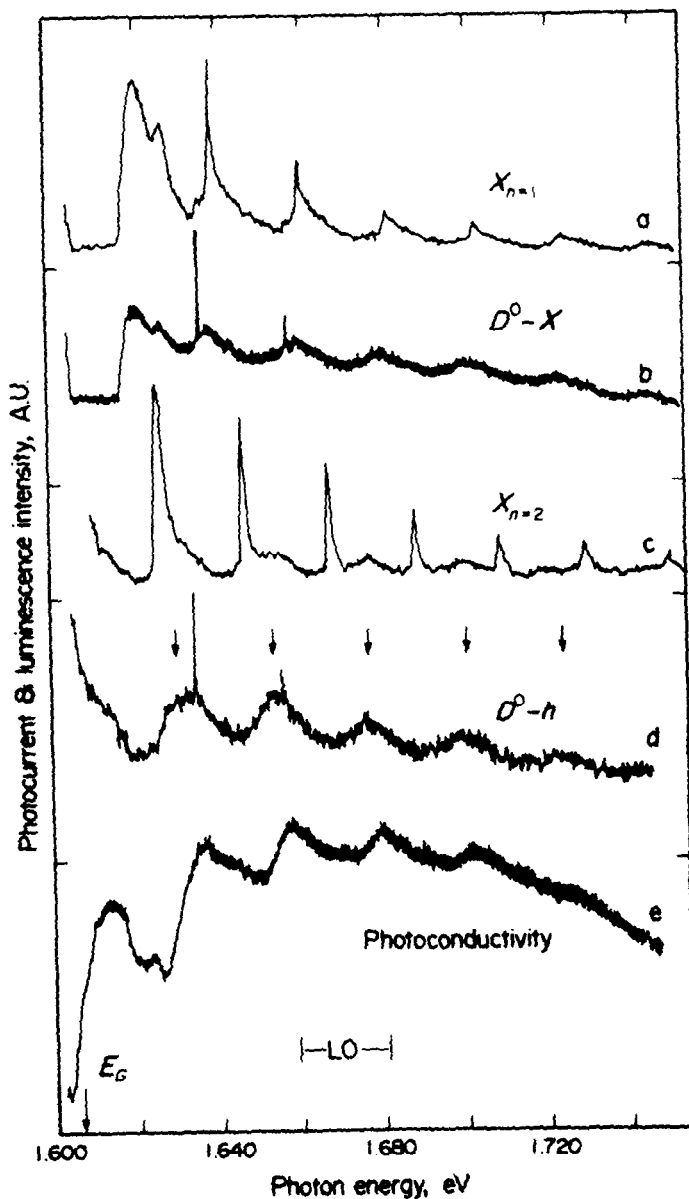


Fig. 32. Photo-excitation spectra of luminescence and electrical conductivity at 1.8 K in refined single crystal CdTe for constant levels of incident optical power. Spectra (a) - (d) involve detection of luminescence from the $n = 1$ FE, DBE, $n = 2$ FE and DFB recombinations while spectrum (e) is the photo-conductivity response. The arrows indicate the energies $E_g + 1.1 \hbar\omega_{LO}$ (eqn. (10)), which describes the periodic structure in (d) and (e) but not in the exciton-related processes of (a) - (c). Note the 180° phase difference between (d) and (e). The sharp peaks in (a) - (c) are attributed to resonant Raman scattering.¹¹³

modulation of the luminescence of the shallow ABE due to its strong coupling with low energy acoustic phonons.¹⁹⁷

(ii) Use of FB Luminescence for Acceptor Discrimination

Study of the transient behaviour of the FB luminescence provides a lot of detailed information on energy relaxation processes for hot electrons. However, from an analytical point of view, we are interested in the fact that these FB bands provide direct spectroscopic evidence on the acceptor species present, through eqn. (9). It is advantageous to record spectra at a temperature where the DAP transition is fully quenched in favour of the FB transition (Fig. 31 inset), so that only a single band appears for each acceptor species. However, the temperature and excitation rate must both be sufficiently low that the FB bands remain as narrow as possible (Fig. 29 and 30). The excess electron temperature mentioned above in fact diminishes much above 10 K, as the lifetime for acoustic phonon scattering decreases with increasing phonon occupation number and the radiative lifetime increases due to thermal quenching of the shallow BE transitions, which have very short radiative lifetimes.⁴² The FB luminescence was used in addition to the ABE 'two-hole' satellite technique (Section 2 A) to distinguish the shallow acceptors in GaAs³¹ in Fig. 33. Different acceptor species were found to be persistently present in crystals grown by different techniques (Fig. 34), whereas similar species are usually found for the same growth technique used in different laboratories. Similar results have now been obtained for a number of semiconductors, including InP⁵⁶ and ZnTe.^{30,92} The FB bands become narrower in a magnetic field. Spin substructure can be resolved for the luminescence transitions from the lowest Landau conduction sub-band.^{115,116} The form of this substructure indicates that negligible exchange interaction exists between the free electron and bound hole at the instant of recombination.

(iii) Extension of FB Concept

Other FB processes are possible, including the radiative recombination of free holes at neutral donors. The low energy threshold of this process, at $E_g - E_D$, occurs very close to the energy of an exciton bound to an ionized donor, stable when $m_e^*/m_h^* \ll 1$ as in GaAs (Section 2 A). These processes are both seen in absorption for ZnTe in Fig. 14 (upper). There has been some controversy over whether this D^+ BE process contributes to the broad band observed in GaAs between the ABE and DBE involving excitons bound at *neutral* species. Recent spectroscopic evidence¹¹⁷ suggests that the n^+ BE process is significant in very pure InP (Fig. 35), particularly at low excitation densities and for excitation energies near E_g . However, neither the D^+ BE nor the DFB luminescence is useful for discrimination between donor species, since the donor chemical shifts are much too small in InP (and GaAs).

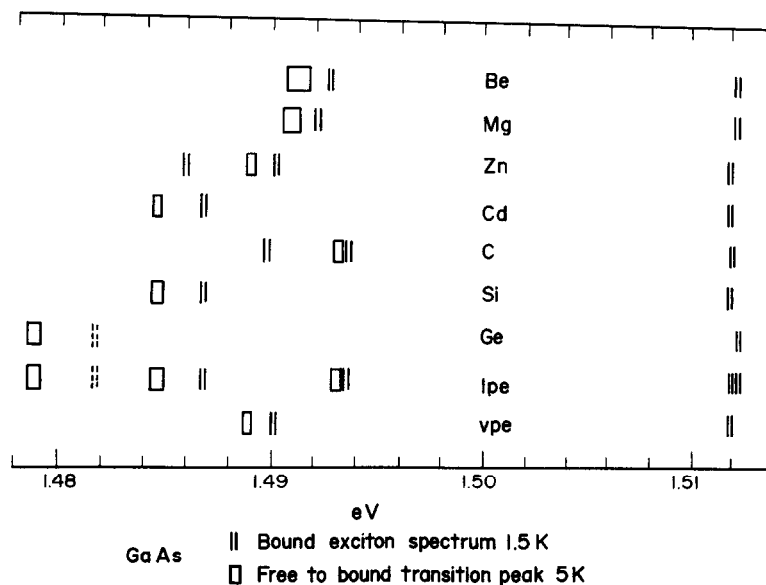


Fig. 33. Schematic representations of the energy positions of the broad AFB and narrow 'two-hole' ABE satellites in the near gap photoluminescence of refined GaAs, lightly back-doped with the indicated shallow acceptors. The principal ABE transitions at the right do not obey eqn. (3). The two lower rows are for undoped LPE and VPE GaAs of state of the art purity. No 'two-hole' satellite was seen for the relatively deep Ge acceptor. Two-hole satellites to the 3s excited hole states have been seen for Zn and C. The exceptionally deep acceptor Sn not listed, has the lowest energy ABE line near 1.5067 eV.^{191,192} Again no two-hole satellites are visible, only AFB and DAP luminescence¹⁹³ has been seen.³¹

Selective excitation might be helpful here, but the best prospect involves the DBE 'two-electron' satellites described in Section 2 A. The relative intensities of D^+ BE and DBE luminescence components can vary markedly with excitation energy, with much greater contributions from the D^+ BE for excitation just above E_g , and vice-versa for excitation at E_{gx}^{59} (Fig. 15).

The FB process has great generality in the recombination luminescence of semiconductors, including Si the most important of all from an applications viewpoint. Evidence has been presented in GaAs,¹¹⁸ Si¹¹⁹ and GaP⁶³ suggesting that the spectrum into which the DAP system evolves with increasing T is caused by recombinations of electrons in excited donor states with holes in acceptor ground states, involving pairs of greater τ than are responsible for the normal DAP recombinations. The evidence for this or any other additional recombination process from the spectral positions in Si and GaP disappears when the revised value

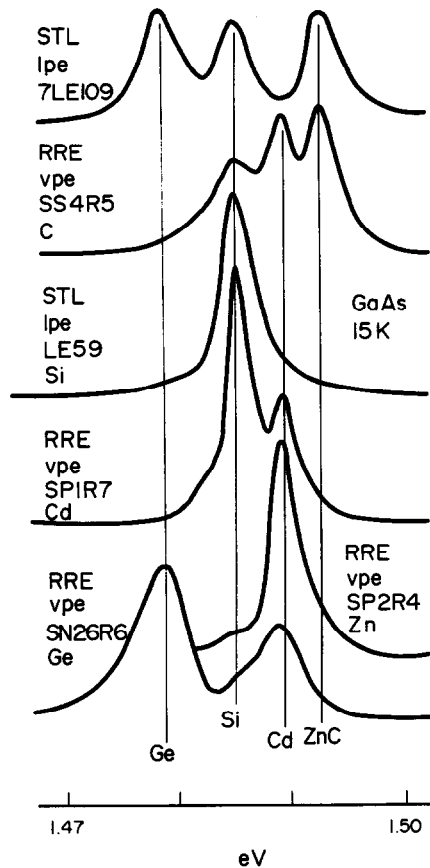


Fig. 34. The near-gap (edge) photoluminescence of a variety of refined back-doped GaAs single crystals, recorded at 15 K to favour AFB over DAP recombinations (Fig. 29). The undoped LPE crystal in the upper spectrum shows residual doping by Ge, Si and C acceptors, impossible to distinguish in the principal ABE components (Fig. 33).³¹

of E_g , E_D and E_A are used, discussed in Section 2 B for GaP and by Shaklee *et al.*¹²⁰ for Si. It is probable that only the simple FB described through eqn. (9) need be considered in general.

(iv) Effects of High Impurity Concentration and Bandgap Variation

The behaviour of the extrinsic near gap luminescence in a semi-conductor doped just below the critical concentration for a semiconductor-metal phase transition, $\sim 3 \times 10^{18} \text{ cm}^{-3}$ for donors in weakly compensated Si, is complex at low temperatures. Two types of luminescence bands can be discerned, a HL type dominant at short decay times $\sim 100 \text{ nsec}$ after intense pulsed excitation, optical density $\sim 100 \text{ W cm}^{-2}$, and an LL system.¹²¹ The HL evolves into the LL after 500 nsec or so, and

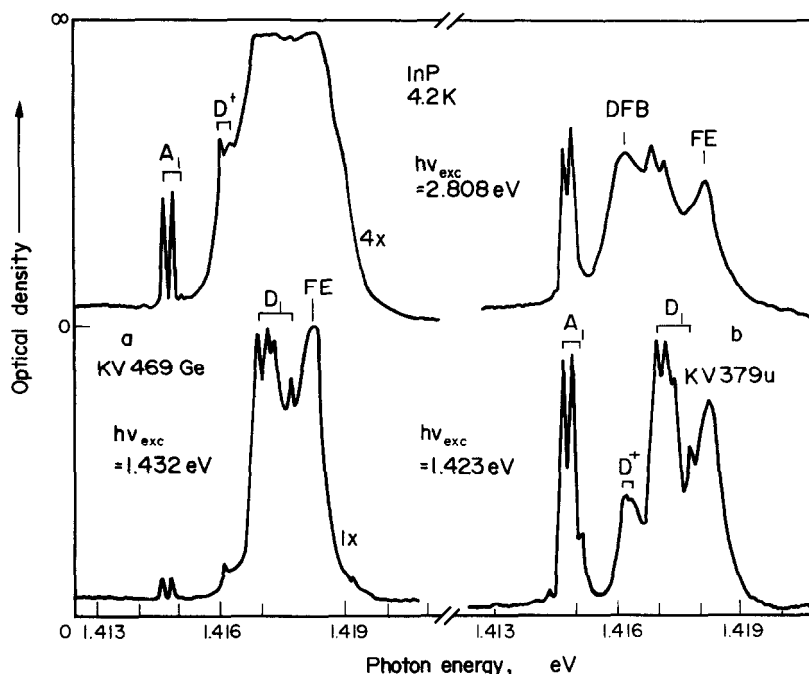


Fig. 35. Small portions of the near gap photoluminescence of refined VPE InP, recorded photographically with the indicated relative exposure times. The sharp line near 1.4160 eV, attributed to D^+ BE luminescence, is seen particularly clearly in the sample with larger low temperature mobility (KV 469 Ge) and for excitation near E_g rather than at much higher energies.¹¹⁷

the LL is also dominant under $< 0.1 \text{ W cm}^{-2}$ continuous excitation, where 0.1 W cm^{-2} is estimated as the threshold for complete photo-neutralisation of the 10^{16} cm^{-3} acceptors in the sample studied by Parsons.¹²¹ The LL system has the attributes of a DAP process involving the donor impurity band (Fig. 36), whereas the HL system, into which the LL evolves at temperatures such that $kT \sim E_A$, is attributed to recombination of free holes with electrons in the donor impurity band. The HL band is bounded by E_g and the optical band gap, measured to the electron Fermi level (Fig. 36). The 'Lifshits tail' in Fig. 36 arises from the scattering of free holes by the donor impurities, and is estimated to be $\sim 3 \text{ meV}$ for $2 \times 10^{18} \text{ cm}^{-3}$ P donors in Si.¹²¹

The near band gap luminescence in GaAs is well known to evolve towards band to band and acceptor free to bound processes at high doping levels or with increase in temperature to $\sim 300 \text{ K}$, the latter in the presence of a sufficient concentration of shallow acceptors.¹²² The influence of doping concentration on the near-gap photoluminescence spectrum of such a semiconductor, doped too heavily for

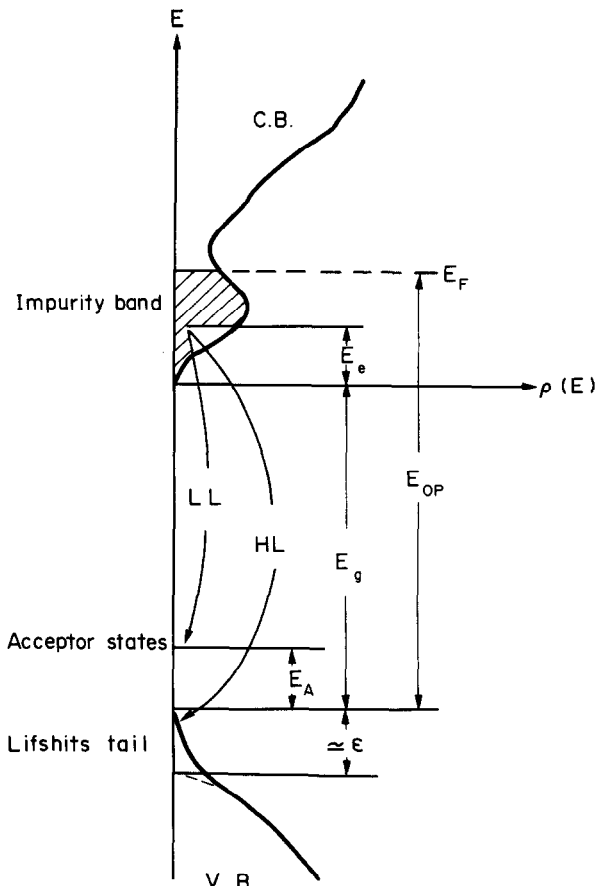


Fig. 36. A schematic representation of the origins of the HL and LL low temperature photoluminescence bands in heavily P donor-doped Si. $\rho(E)$ is the density of electronic states, displayed as a function of electron energy E .¹²¹

observation of transitions associated with isolated impurity centres, can be turned to advantage in an optical technique for the measurement of free carrier concentration. This is usually demonstrated in n -type, direct gap semiconductors, where the criterion in eqn. (4) is violated for donor concentrations relevant for a wide variety of semiconductor devices, $> 2 \times 10^{16} \text{ cm}^{-3}$ for GaAs. The simple band to band luminescence recorded at convenient temperatures $\gtrsim 100 \text{ K}$ involves a degenerate electron distribution, unlike the injected hole distribution. The luminescence spectrum is then skewed to high energies above a low energy cut off near E_g , reflecting the Maxwell-Boltzmann form of the injected hole distribution.²⁰² A feature of particular interest for characterisation is the progressive increase in width (ΔE) of this luminescence spectrum with increase in electron concentration above a critical limit, as the spectral distribution becomes more Gaussian under

the influence of donor-related conduction band tail states (Fig. 36). This effect has been examined for several direct gap semiconductors and advocated for the assessment of the electron concentration. Of course, this presupposes injection levels under the optical or electron beam excitation which are well below those at which conductivity modulation sets in. There is usually no difficult in meeting this prescription, particularly when measurements are made at ~ 100 K rather than ~ 300 K, taking advantage of the generally much higher luminescence efficiency at the lower temperature. For example, a linear increase of ΔE with n was reported for $\text{GaAs}_{0.62}\text{P}_{0.38}$ above $n \sim 10^{17} \text{ cm}^{-3}$.²⁰³ The efficiency of the band to band luminescence is also linearly related to n under these conditions and when the minority hole lifetime is independent of n (eqn. (15) below). Quite different behaviour is observed in such moderately narrow, direct gap semiconductors when p-type at comparable doping levels, since $A\ell \rightarrow B$ transitions predominate at the acceptor states which remain substantially localised. This is like the LL system in Fig. 36, but the very large transition rates characteristic of direct gap semiconductors ensure that this process remains significant to much higher temperatures than in Si.

The fact that these luminescence processes occur very close to the semiconductor energy gap, particularly in direct gap materials, provides a useful technique for evaluating this parameter for alloy semiconductors such as $\text{Al}_x\text{Ga}_{1-x}\text{As}$. Typically, the energy gap is a strong and often nearly linear function of x , so that the average alloy composition is readily derived in this way. Deviations from the virtual crystal approximation, which introduce non-linear terms in the dependence of E_g on x , can also be evaluated if the average composition is measured by X-ray fluorescence. These two measurements can both be performed very conveniently in a single equipment, using a suitably equipped electron beam system.²⁰⁴ Such techniques may have the high spatial resolution typical of the scanning electron microscope. Automatic systems involving wavelength derivative techniques have been reported²⁰⁵ whereby small scale variations in x may be revealed through continuous recordings of peak luminescence wavelength and intensity across a semiconductor slice.

(iv) Determination of Compensation Ratio from Optical Spectra

We have seen in Section 2 A and 2 B that the identification of minority dopant species is certainly best achieved by optical spectroscopy, and that photoluminescence is a very convenient method provided that relevant species give adequate spectral dispersion, as for acceptors in GaAs.³¹ However, the magnitude of the compensation ratio is also of great concern. This is traditionally estimated from the electrical mobility, μ , through the recognition that limitations to μ arising from scattering at the ionized donors and acceptors can be separated

from other scattering processes through their characteristic temperature dependence. This technique works quite well for Si and Ge, but is less sensitive because of much stronger phonon scattering in a III-VI semiconductor such as GaAs. The semi-empirical technique derived for GaAs⁸ involves measurement of the Hall constant and resistivity at 77 K and is sensitive only for $n \gtrsim 10^{15} \text{ cm}^{-3}$, since additional scattering mechanisms obtrude at lower doping concentrations. However, compensation at somewhat lower concentrations can be estimated from electrical measurements in the less-convenient 20-40 K temperature range. It has recently been shown that the 300 K mobility and free carrier absorption near 10 μm can be used to derive the compensation ratio in GaAs, respectively for $n > 10^{15} \text{ cm}^{-3}$ and $n > 10^{16} \text{ cm}^{-3}$, and can lead to concordant values for sufficiently uniformly doped material.¹ However, alternative methods are of interest for GaAs at $n < 10^{15} \text{ cm}^{-3}$, and for other semiconductors where the empirical electrical mobility technique has not yet been established.

The compensation ratio may be estimated from certain intensity ratios in BE photoluminescence spectra recorded under appropriately defined conditions, provided that appropriate pre-calibration is available (Section 2 A). However, an alternative, more independent technique proposed by Kamiya and Wager¹²³ involves an extension of an earlier theory of the DAP lineshape¹²⁴ in which the FB and DAP bands are considered together. This lineshape analysis requires n to be known, from a 300 K measurement of the Hall voltage or the capacitance of a Schottky barrier. Then, N_D , N_A and the non-radiative 'shunt path' recombination rate w_{NR} can be determined from the measured lineshapes under weak photoexcitation rates, provided that E_D , E_A and E_G are accurately known. The envelope of the luminescence band for unresolved transitions at distant DAP is given by

$$I_{DA}(E)dE = P[\tau(E)] \frac{dr}{dE} w_{DA}[\tau(E)] P_A^0[\tau(E)] N_A dE \quad (11)$$

where E is the photon energy hv , $w_{DA}(\tau)$ is the DAP transition rate for separation r , $P(\tau)$ is the probability that a neutral donor will have a nearest-neighbour neutral acceptor at distance r , and $P_A^0(\tau)$ is the occupation probability under steady state conditions such that the total DAP luminescence intensity is proportional to the excitation intensity. Assuming a hydrogenic acceptor, such as C in GaAs,³¹ $w_{DA}(r)$ is given by⁷⁰

$$w_{DA}(r) = w_{DA}(0) \exp(-2r/a_D) \quad (12)$$

where $w_{DA}(0)$ is the maximum volume of the DAP transition rate at $r=0$ and a_D is the Bohr radius of the more diffuse species, the donor in GaAs. The envelope of the FB luminescence is given by

$$I_{eA}(E)dE = c(E-E_g+E_A)^{\frac{1}{2}} \exp[-(E-E_g+E_A)/kT] N_A^0 dE \quad (13)$$

where c is a constant and N_A^0 is the stationary value of the neutral acceptor concentration. The experimental data for the high quality n -type GaAs sample in

Fig. 37 are best fit for $N_A/N_D \sim 0.27$, whereas the standard electrical analysis suggests a much higher value 0.8-0.9. It is believed that this discrepancy arises

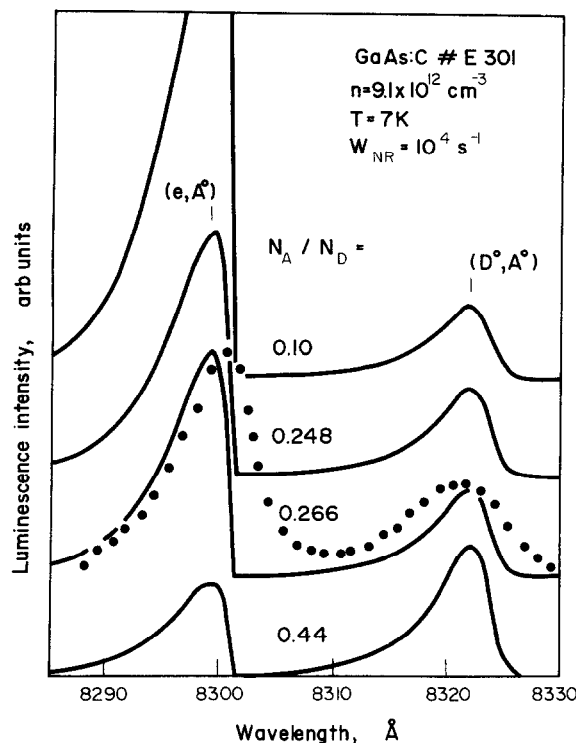


Fig. 37. Photoluminescence spectra containing DAP (D^0, A^0) and AFB (e, A^0) bands of the shallow C acceptor in refined n-type LPE GaAs. The experimental spectrum obtained under weak excitation conditions is dotted. The solid lines are calculated with the aid of eqns. 11 and 13 for the indicated values of compensation ratio.¹²³

from a substantial gradient in the compensation ratio parallel to the growth direction of these liquid phase epitaxial layers. The existence of the discrepancy confirms expectation that the optical technique assesses only the outer $\sim 1 \mu\text{m}$ of the layer, while the electrical data are obtained as an average from the whole layer thickness, typically $\sim 10 \mu\text{m}$. Spatial profiling is clearly important for a realistic comparison of these techniques.

This technique has been applied recently to DAP and FB spectra in p-type ZnTe and yielded credible values of the compensation ratio and its variation for different techniques of diffusion doping.¹²⁵ It should be noted that this method yields estimates of the total compensation, like the electrical data, even though transitions involving only a single acceptor are studied directly and the selected acceptor may not predominate in compensation. Measurements on the DAP and FB bands

associated with different acceptors in a given sample do yield concordant values of the compensation ratio in favourable cases.¹²³

An alternative but related optical technique for the analysis of compensation ratio, which also depends upon knowledge of E_g , E_D , E_A , the electron and hole effective masses and the dielectric constant, is due to Nam *et al.*¹²⁸ These authors show that if the intensity ratios of AFB to DAP and DFB luminescence components can be estimated in the two opposite limits of negligible and infinite excitation intensity, then $N_D - N_A$ and N_D/N_A can be derived. Preliminary tests of this technique for p-type GaAs appear to be encouraging, and gave a compensation ratio of about 0.2 at $N_A - N_D \sim 6.5 \times 10^{14} \text{ cm}^{-3}$.¹²⁸

(v) Carrier Heating by Electric Fields

The form of the FB band has also been used as a probe of perturbations in the energy distribution of conduction band electrons under heating in an electric field at very low temperature.¹²⁶ The FB band becomes favoured relative to the DAP band as a consequence of impact ionization of the donors by the tail of the heated electron distribution. This effect, and the increase in electron temperature, become noticeable above only $\sim 1.0 \text{ V cm}^{-1}$ in a high quality GaAs sample at 2 K, (Fig. 38), much lower than the $\sim 1 \text{ kV cm}^{-1}$ necessary to seriously influence the intrinsic band to band luminescence lineshape at 77 K.¹²⁷ Very high mobilities are derived from these 2 K analyses, more than 10x larger than Hall values, presumably due to photoneutralisation of the charged impurity scattering centres.¹²⁶

3. PHOTOLUMINESCENCE FROM OTHER TYPES OF CENTRE

(i) Isoelectric Traps

We have already noted in Section 1 that the photoluminescence technique can be used to analyse for and estimate the concentration of other types of centre, most obviously for luminescence activators. This application is so obvious for impurity recognition that little need be said here. Many examples exist, and some have been reviewed in a discussion of the operation mechanism of light emitting diodes.¹²⁹ It is perhaps useful to note here that isoelectric traps such as N_p in GaP are a particularly important type of luminescence activator in semiconductors. These centres are of practical interest for the bound exciton recombination they promote (Fig. 39), a dominant mechanism even when the total electron plus hole binding energy barely exceeds the thermal energy kT at 300 K.¹³⁰ The basic properties are derived from the strong electronegativity difference between the isoelectronic substituent and the host atom it replaces. The short range potential created around the isoelectronic impurity tends to produce a bound state for one or other type of electronic particle. The electronic particle of opposite type is

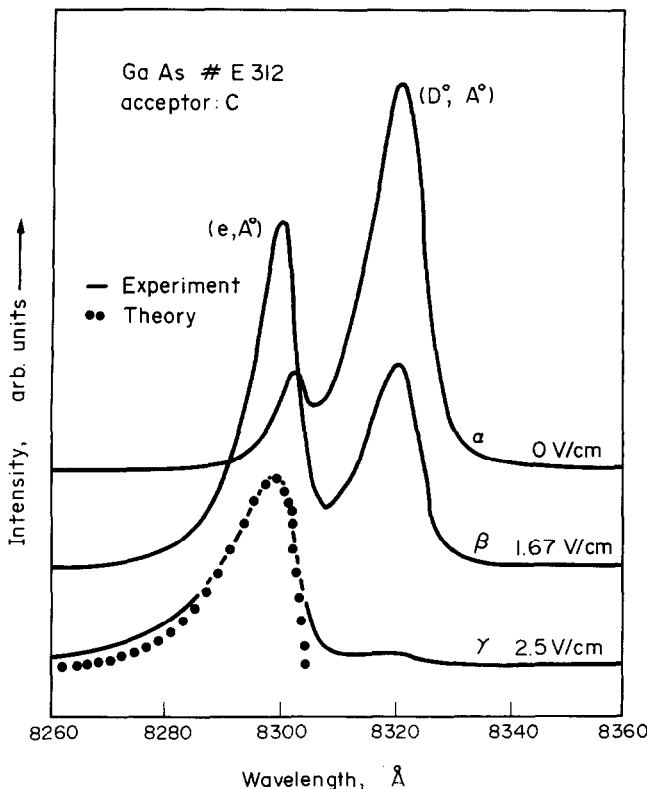


Fig. 38. Photoluminescence spectra containing the DAP (D^0, A^0) and AFB (e, A^0) bands of the shallow C acceptor in refined n-type LPE GaAs, obtained without and with the indicated electric fields. The fields were applied between ohmic contacts shielded from the exciting light.¹²⁶

then captured in the long range Coulomb potential of the first, so creating the BE.¹⁷⁹ This type of centre is best detected by the optical properties of these BE states, since isoelectronic substituents do not introduce excess electronic particles into the crystal by which they may be detected, unlike donors and acceptors. However, isoelectronic traps can also take part in inter-impurity recombination processes, for example, Bi_p^{131} or the 'molecular' isoelectronic trap $\text{Cd}_{\text{Ga}}-\text{O}_p$ in GaP (Fig. 3). Such spectra exhibit many of the generic kinetic properties of recombinations within distant pairs discussed for DAP in Section 2 B, excluding the spectral shift. The term $e^2/\epsilon r$ in eqn. (7), dominantly responsible for this shift in DAP spectra, is absent for these pair spectra. This happens since one member of the pair is neutral in both the initial and final state of the luminescence transition. The no-phonon line is therefore relatively sharp, and its position is given by

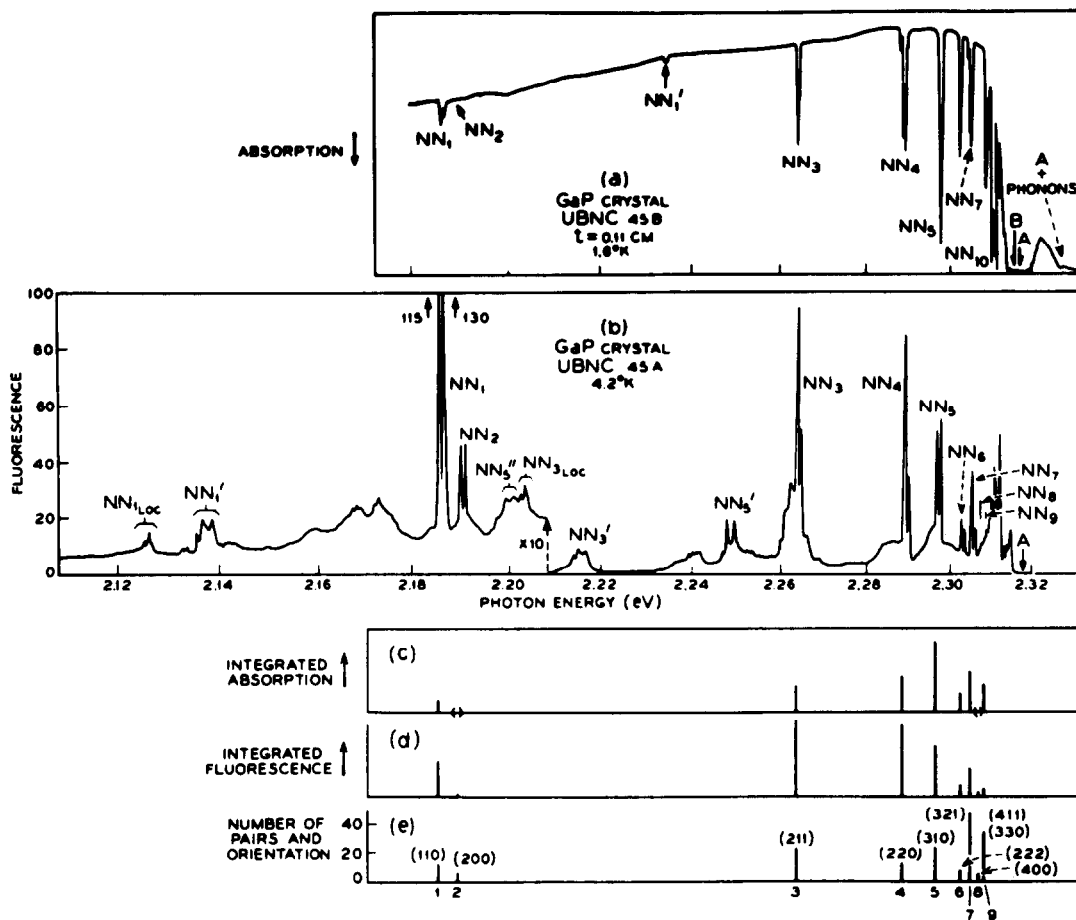


Fig. 39. Bound exciton lines due to Np isoelectronic traps and their associates, observed for a GaP single crystal containing about $2 \times 10^{18} \text{ cm}^{-3}$ N. At this high concentration, the isolated N centres which dominate the absorption spectrum (a) contribute little to the luminescence spectrum (b), since non-resonant excitation tunnelling to the deeper Np-Np pair traps occurs before radiative recombination of the BE. Lattice phonon replicas are designated NN₅', NN₅'' etc, while local modes are labelled NN₁LOC etc. The energies of the local modes shift on isotopic substitution of the N atoms. Spectra (c) and (d) show the relative strengths of the NN no-phonon lines in absorption and fluorescence. Spectrum (e) shows the relative intensities expected if the N atoms are distributed at random on the P sublattice and if the optical intensities are controlled by these site densities. The crystallographic orientations of the NN pairs are indicated.³⁹

$$h\nu = E_g - (E_D + E_h) \quad (14)$$

where E_h is the binding energy of a hole to Bi_p in GaP.¹³¹ We have already noted that E_g and E_D may not be well known. Similar techniques were recently used to obtain the energy $E_g - (E_A + E_e)$ from a distant pair spectrum involving the NN_3 electron binding trap in GaP, where NN_3 represents the third nearest neighbour N_p-N_p pair,¹³² (Fig. 40). Now, $(E_g - E_e)$ was already known from an analysis of

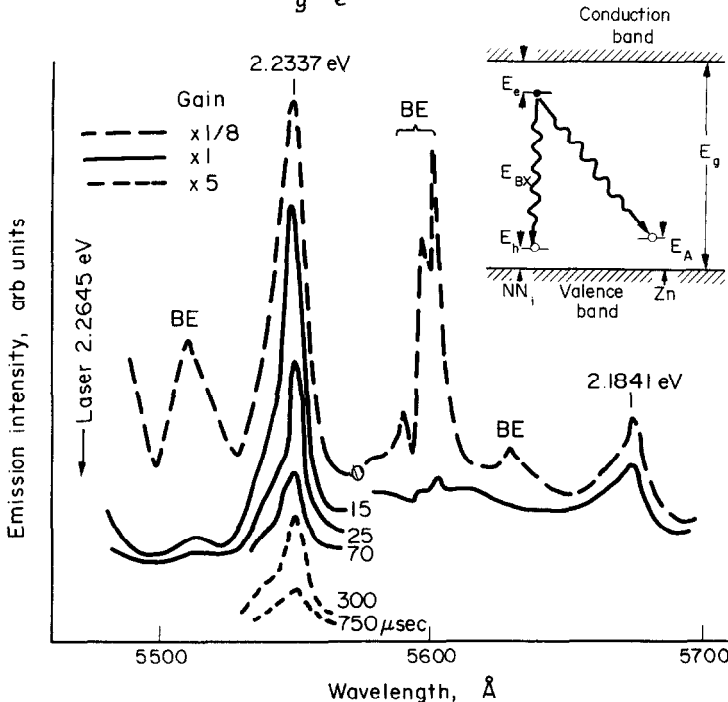


Fig. 40. Time-resolved SPL spectra of a GaP single crystal heavily doped with N and moderately Zn-doped to favour the recombination of electrons bound to NN_3 isoelectronic associates and holes bound to distant Zn acceptors (no-phonon line 2.2337 eV) at low excitation levels on pumping in the NN_3 BE no-phonon line. The average delays in μsec are indicated. Lines marked BE are phonon replicas of the NN_3 BE. The inset contains the BE and distant inter-impurity recombination transitions from which an absolute value of the acceptor ionization energy can be determined.¹³²

excited state structure in the PLE of the NN_3 luminescence, where a quasi-Rydberg series of excited states of the hole in the Coulomb field of the tightly bound electron could be identified.¹³³ Thus, these results yield an absolute estimate of E_A , which helped to confirm the revised values quoted in Section 2 B.

The concentration of such a luminescence centre can be determined from a kinetic analysis under excitation conditions where the luminescence intensity is proportional to the optical excitation rate. This may require low level excitation in some cases, though often the shunt path recombination dominates at all available

excitation levels. A good example is afforded by N_p in GaP, where the shallow electron and hole states in the BE are in thermal equilibrium with the conduction and valence bands at 300 K and the low electroluminescence efficiency η can be represented simply by¹³⁴

$$\eta \propto \tau_{mc}^e [N_p] p \quad (15)$$

where τ_{mc}^e is the electron minority carrier lifetime, p is the hole concentration and $[N_p]$ the N activator concentration on the p side of the pn junction, assumed to dominate in the electroluminescence. The experimental data (Fig. 41) confirm eqn. (15) and are fitted by the calculations at a value of $[N_p]$ which agrees with the independent estimates obtainable from optical absorption.¹³⁴ Measurement of concentration from optical absorption also requires luminescence data if it is made on an absolute basis, connecting the oscillator strength δ with the lifetime τ of the transition using the detailed balance relationship

$$\tau^{-1} = n \delta g_1 / 1.5 \lambda^2 g_2 \quad (16)$$

where n is the refractive index at wavelength λ and g_2 , g_1 are, respectively the degeneracies of the initial and final states of the radiative transition. The observed integrated strength of an optical absorption line $\alpha_{\max} \Gamma$ can then be related to the concentration of absorbing centres N_S by the relationship

$$N_S = 0.97 \times 10^{16} n \alpha_{\max} \Gamma / \delta \quad (17)$$

where $\alpha_{\max} \Gamma$ is measured in cm^{-1} eV. The value of δ derived from eqn. (17) is correct only if the lifetime can be measured under conditions where radiative transitions predominate. This is always possible for isoelectronic traps, provided only that measurements are made at sufficiently low majority carrier concentrations that Auger effects involving additional free electronic particles are insignificant. Such processes are responsible for the deviation of the experimental data from the predicted variation above $N_A - N_D \sim 2 \times 10^{18} \text{ cm}^{-3}$ in Fig. 41. In addition, because of splittings in the BE due to J-J coupling, visible in Fig. 39, care must be taken to extract the luminescence lifetime for the allowed transition, which predominates in absorption.¹³⁵ We have seen in Section 2 A that the transition oscillator strength cannot be obtained in this way for ABE and DBE in indirect gap semiconductors because of the Auger effect inherently always possible for this type of BE complex.¹³⁶ The whole procedure for extraction of a proportionality factor linking optical absorption and species concentration by this absolute technique is quite

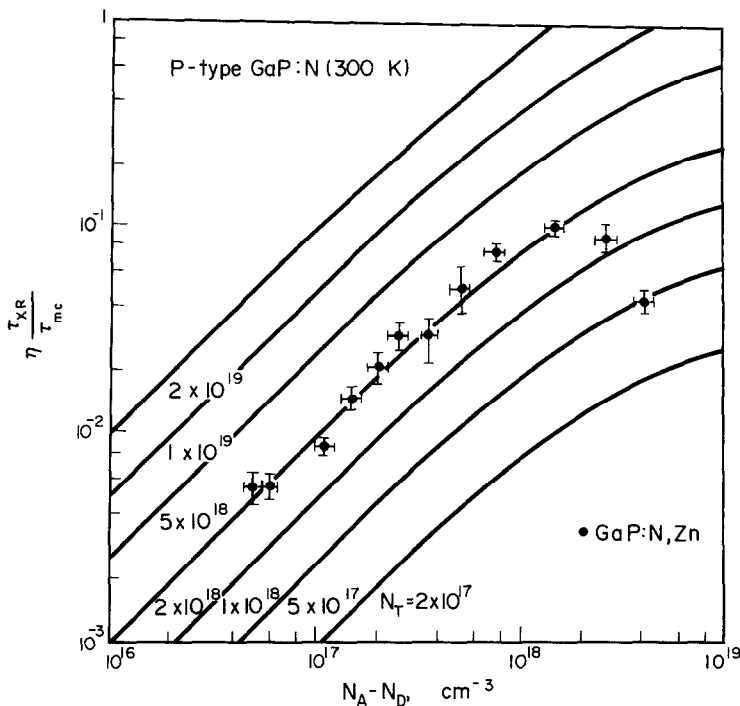


Fig. 41. Increase in the product $n\tau_{XR}/\tau_{mc}$ with hole concentration in p-type LPE GaP:N. The solid lines are estimates from the kinetic model of eqn. 15, calculated on an absolute basis for the indicated concentrations N_T of the N_p isoelectronic trap. The experimental data (points) indicate a value of N_T which agrees with independent estimates. Parallel Auger recombinations become significant above $N_A - N_D \sim 2 \times 10^{18} \text{ cm}^{-3}$, reducing τ_{XR} further.¹³⁴

tricky, and it is usually advisable to check by some independent technique. This was done for N in GaP using charged particle activation analysis. This is also an elaborate procedure if accurate results are to be obtained.¹³⁷ It is subject to the potential drawbacks of all such analytical procedures in being destructive, and it is also necessary to assume that all the detected species is in a single site in the crystal. However, the activation analysis provided a reliable calibration for the non-destructive optical techniques, initially derived partly from measurements of the relative strengths of features involving isolated N and NN pairs in GaP.³⁹

We have seen that the localised recombination involving isoelectronic traps are essentially free of the Auger processes which can always contribute to the recombination rate for the D or ABE discussed in Section 2 A, where three weakly localised and strongly interacting electronic particles are available. The absence of a long-range Coulomb potential at these traps is responsible for their ability

to be incorporated in crystal at much higher concentrations compared with donors and acceptors before very severe broadening occurs for the bound states they produce for electronic particles. This emphasises the general importance of Stark electrostatic field contributions to these broadening processes,¹⁷⁸ as well as electrostatic screening due to the additional electronic particles contributed by the donors and acceptors¹¹ which leads to the phase transition described by eqn. (4). However, Auger processes can occur from inter-centre interactions, even for iso-electronic traps, as observed for B_{1p} in *n*-type GaP.¹⁸⁰ Other examples are the case of N_p in heavily *p*-type GaP already discussed (Fig. 41) and similar inter-centre processes such as observed through the effect of increases in *p*-type doping on the capture luminescence of the deep donor O_p in GaP.¹⁷ In each case, information about these essentially non-radiative microscopic processes may be obtained from a study of a radiative channel to which the non-radiative channel is intimately linked. The information is provided though the influence of the non-radiative process on the intensity or decay time of the radiative one. The latter effect introduces a substantial deviation from the relationship between τ and δ (eqn. (16)) which is an inherent property of DBE and ABE in indirect gap semiconductors. This does not occur in direct gap semiconductors at least for the shallowest species,⁴² although Auger-like processes similar to those considered for the impurity-band-Auger process in GaP¹⁸⁰ have been invoked to account for broadening of DBE in CdS.¹⁸¹ There is a very simple relationship between the non-radiative (Auger) transition rate $1/\tau_{NR}$ and the binding energy of the centre at which the exciton is localised, first noticed for ABE in GaP.³⁸

$$1/\tau_{NR} \propto E_A^4 \quad (18)$$

Auger processes produce a particularly dramatic effect in *p*-type GaP:O.¹⁷ The capture luminescence at the O_p donor can be strongly quenched by transitions in which the donor de-excitation energy is transferred non-radiatively to the hole bound to a typically distant neighbouring acceptor. The arrival of the electron in the donor ground state is proved through the observation of distant DAP luminescence involving the same pairs (Fig. 42), no Auger process being possible for this two-particle transition (Section 2 B). We shall see in Section 4 that effects of non-radiative transitions also appear in topographic studies, again rendered visible through their quenching effects on radiative processes.

Isoelectronic (neutral) centres can also produce BE states when in the form of a complex, such as nearest-neighbour DAP associates (Fig. 3). This provides a connection with the luminescence processes discussed in Section 2 B. However, this extreme form of DAP recombination is more naturally discussed in terms of BE

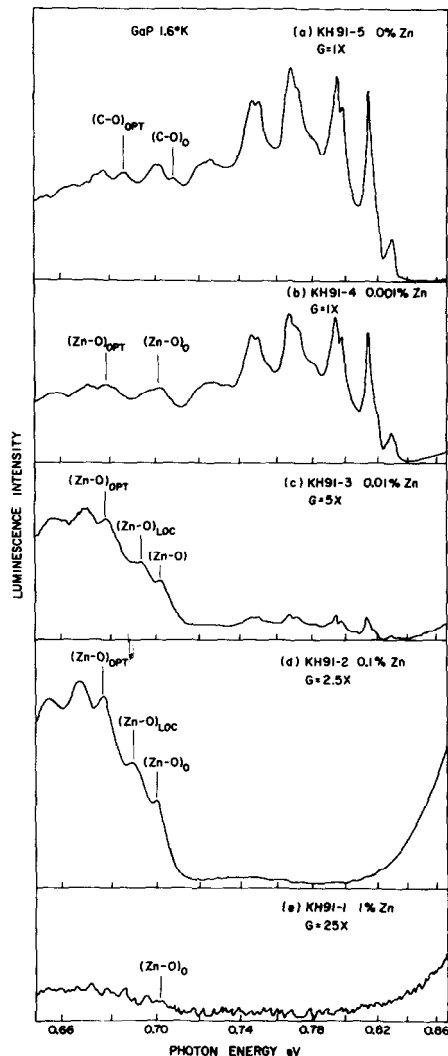


Fig. 42. Photoluminescence spectra of p-type GaP:O grown from Ga solution and co-doped with an increasing concentration of shallow Zn acceptors in the sequence (a) - (e). The relative gain of the recording system is indicated by G. All luminescence processes become inefficient at the highest Zn concentration, $\sim 5 \times 10^{18} \text{ cm}^{-3}$ in spectrum (e). The Zn concentrations in spectra (b) + (d) are, respectively 1.5 , 5 , and $15 \times 10^{17} \text{ cm}^{-3}$. The structured band peaking near 0.79 eV, due to radiative electron capture at ionized O_p donors, becomes quenched at the higher Zn concentrations. However, these donors are still being photoneutralised, since the distant O_p-Zn_{Ga} DAP band still persists, shown here in second order. Electron capture at O_p is presumed to occur via an Auger process involving the moderately distant neutral Zn acceptors which also promote the DAP luminescence.¹⁷

processes, since only a single centre is involved with a well-defined exponential decay time. The electronic states are usually subject to significant J-J coupling, perturbed weakly or strongly by the local axial field of the associate, depending upon the centre.³ One of the best known examples of this 'molecular' type of isoelectronic trap is the Zn_{1-x}Ga_x-O_p A-D associate in GaP.¹²⁹ The absolute concentrations of this trap initially determined from an analysis using eqns. (16) and (17)¹³⁸ are over-estimated by a factor of 9, due to a numerical error in the analysis. This has been confirmed from subsequent measurements of photoluminescence saturation,¹⁴¹ nuclear activation analysis¹³⁹ and deep level transient capacitance spectroscopy.¹⁴⁰

(ii) Transition Metals and Rare Earths

Photoluminescence can also be used to detect and recognise the presence of impurities other than main-group chemical substituents, for example transition metals or rare earths. Transition metals are particularly significant for group IV, III-V and II-VI semiconductors, in that they are frequently present as contaminants and can also be added in high concentrations as luminescence activators, for example Mn in ZnS.¹⁴² They are also frequently used to produce the deep states which induce the high electrical resistivity required for some device applications. The final step in de-excitation between the substates of the free ion, split in the tetrahedral crystal field for most of the binary semiconductor types mentioned above, is frequently radiative. The energy and form of the luminescence spectrum and comparison with optical or photoluminescence excitation spectra frequently yields enough information to distinguish the nature and charge state of the transition metal. Initial suspicion that a transition metal may be responsible for a particular spectrum is usually aroused by the weak phonon coupling (Fig. 43) characteristic of intra-d shell transitions involving states relatively well-shielded from the host lattice. This shielding is even stronger for rare earths, resulting in sharp line spectra even at 300 K whose energies are readily predicted since they are rather insensitive to the nature of the host crystal.¹⁴³ Transition metal luminescence usually occurs in the near infra-red, well below the energy gap of the semiconductor and in a spectral region where recombinations involving main group species typically involve strong phonon coupling. This arises from the greater sensitivity of the impurity-host bonding to the charge state of the impurity for the unscreened states available for these species.

Mis-identifications sometimes occur when the main information available is luminescence, as recently discovered for GaP:Ni where rather detailed studies involving magneto-optics,¹⁴⁴ uniaxial stress¹⁴⁵ and PLE spectra¹⁴⁶ (Fig. 43) were

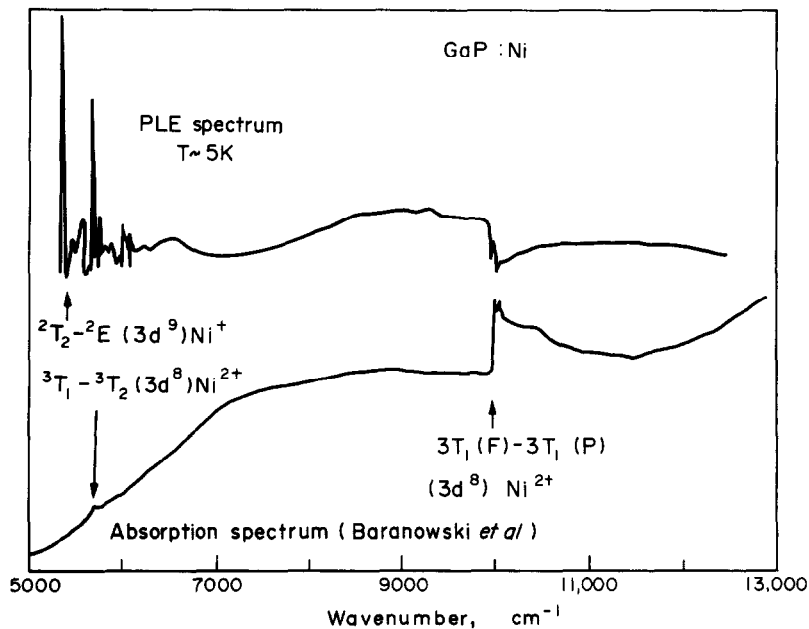


Fig. 43. The PLE spectrum (upper) of the indicated transition within Ni^+ ($3d^9$) for an n-type GaP crystal co-doped with Ni. Some of the Ni is also present as Ni^{2+} ($3d^8$), which has a series of excited states widely spaced towards the energy of the GaP bandgap, unlike Ni^+ . These excitations within Ni^{2+} , shown in the lower absorption spectrum, occur as negative features in the PLE of luminescence within Ni^+ . The relatively weak phonon coupling shown for the low energy transition within Ni^+ is typical for transition metals in semiconductors.¹⁴⁶

required to establish the totally unanticipated result that the luminescence originates from Ni_{Ga}^+ , $3d^9$. The dominant luminescent state of the isolated transition metal is usually the divalent M^{2+} , as is true for Ni in many other binary semiconductors and for other transition metals in GaP, such as Fe^{2+} and Co^{2+} .¹⁴⁷ Such an identification may be confirmed by correlation between optical absorption and ESR using crystals with different Fermi levels to alter the dominant charge state of the Ni.¹⁴⁸ The strength of the ESR response can be used to calibrate the optical absorption spectra for transition metal concentrations.

The optical and ESR behaviour of transition metals in a number of III-V semiconductors has been reviewed recently.¹⁴⁹ The solubilities of these species are usually appreciably higher in II-VI semiconductors. Other types of optical transition involving hybrid transition metal-semiconductor host states have been reported for the wider gap hosts. One example is the 'charge-transfer' spectrum, significantly luminescent only for Cu in ZnO ,¹⁵⁰ which involves excitations to

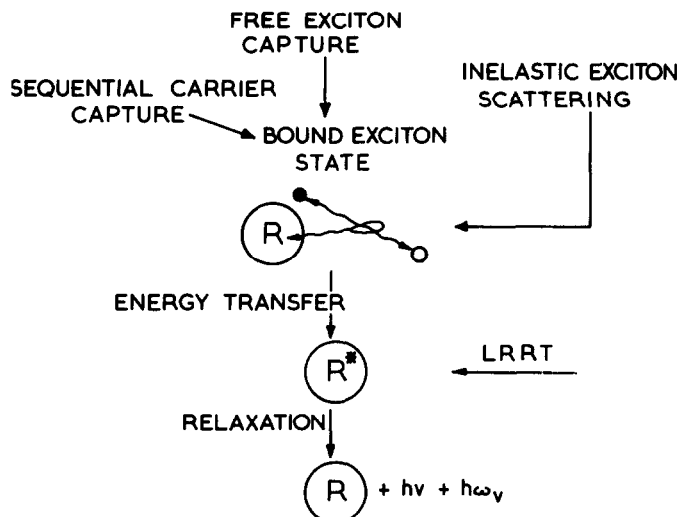
extended hole states. Careful study of ZnSe:Co has recently revealed many inter-linked luminescence bands caused by weakly radiative transitions between excited states of Co^{2+} , $3d^7$ and possibly Co^{3+} , $3d^6$, as well as the usual strong luminescence between the lowest crystal field-split states.¹⁵¹ Thus, luminescence spectra provide a great deal of information about these species. Examination of their kinetic behaviour and PLE spectra yield still further properties, particularly information on the mechanism by which the observed luminescence is excited. This may involve charge exchange with the bands of the semiconductor^{146,152} or, possibly the formation of intermediate states which may be associated with a BE¹⁵³ (Fig. 44). The recently reported BE in GaAs:Co¹⁵⁴ could be an example of this situation.

4. LUMINESCENCE TOPOGRAPHY AND RELATED PHENOMENA

(i) Examples of use in a Variety of Semiconductor Devices

Measurements of the spatial variation of luminescence intensity can provide a variety of 'positive' and 'negative' information about a semiconductor, and may also be applicable directly to a semiconductor device structure. An example of the latter is provided by Si high power rectifiers, where it has been found very instructive to look for defects in the manufacturing process by a topographic study of the recombination luminescence observed under forward bias using an infra-red vidicon camera.¹⁵⁵ Such analytical techniques can provide a much more revealing test of the integrity of the manufacturing process than is possible simply from analysis of the overall current-voltage characteristic, since the local electroluminescence intensity is closely related to the local current density in the device. Similar techniques have been used to provide much valuable information about initial performance limitations and particularly the degradation of GaAlAs-GaAs double hetero-structure lasers, where attention is centred upon the active region defined by a stripe of area only $\sim 10\mu \times 200\mu$ perpendicular to the junction plane. In one such study,¹⁵⁶ a differential screw translator permitted a resolution of $\sim 2 \mu\text{m}$ across this area for a window structure DH laser made with a special capping layer only $\sim 1 \mu\text{m}$ thick. The resolution in the topography of the spontaneous luminescence intensity L_S was adequate to show the presence of dark line defects DLD associated with rapid degradation. The DLD are caused by tangled networks of interstitial-type dislocation loops, which grow by a climb mechanism and which introduce strong local non-radiative recombination. Other types of defect were also seen, for example those associated with holes in the thin epitaxial layers due to defective LPE growth (Fig. 45). Allowance must be made for re-radiation from the GaAs substrate for DH lasers with some Al in the active region.¹⁵⁶ Such measurements also provide evidence for saturation in L_S at

(a) Excitation of transition series impurity



(b) Potential at transition series impurity

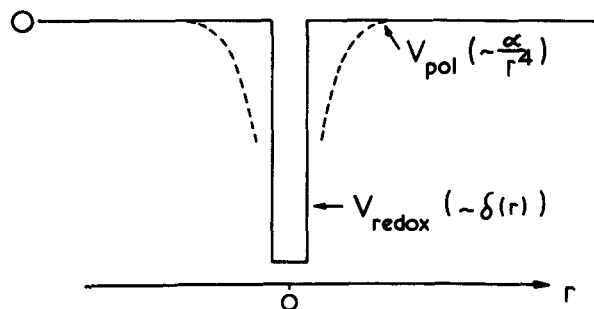


Fig. 44a. Schematic indication of the energy pathways by which an 'internal' transition within a transition series impurity such as a transition metal (M) may result from an ionization process in the host lattice, caused by absorption of a high energy photon or other means. The two main routes are by direct interaction of the impurity with electrons and holes in the host lattice, possibly with the intermediary of a localised exciton state, and long range resonant transfer (LRRT) from some other defects which may have large capture cross-sections for the host energy and relatively low recombination probabilities, such as distant DAP.

Fig. 44b. Two possible contributions to the effective lattice potential of an open-shell isoelectronic impurity, such as M^{2+} in a II-VI or M^{3+} in a III-V compound semiconductor. V_{redox} results from preferential electron or hole capture into the open shell, and can be strong though short ranged. V_{pol} represents a van der Waals-type polarisation interaction which is probably more important for the capture cross-section.¹⁹⁴

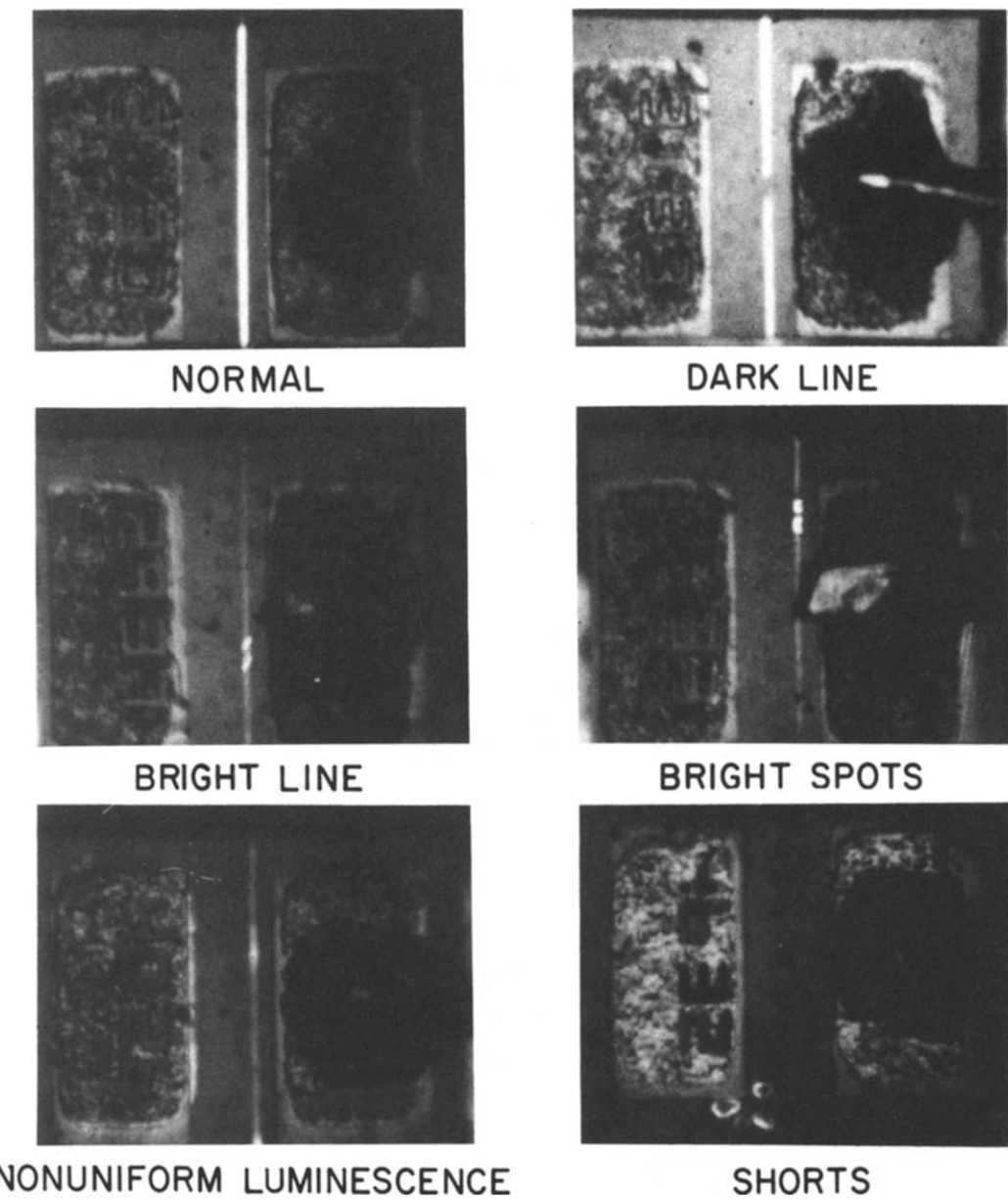


Fig. 45. Infrared photomicrographs of window-geometry LPE ($\text{Al},\text{Ga}\text{As}$) injection lasers with aluminium in the active region and in the last-grown epitaxial layer. Double exposures were taken, first focussing on the spontaneous luminescence L_S emitted perpendicular to the plane of the pn junction, then using reflected light and focussing on the upper n metallisation. The top left photomicrograph was obtained for a typical good laser, with a uniform intensity for L_S emerging through the substrate window. The others show various defects, as indicated.¹⁵⁶

threshold for laser action, and spatial changes in L_S when movement of lasing filaments (pulsations) occurred. Spatial scans through a DLD, using the analytical technique describe below, suggest that the local diffusion length is significantly reduced for aged material.

Similar effects may be observed in photoluminescence if the window in the stripe involves a high Al-content alloy and a laser beam is chosen, for example the deep red Kr⁺, which can pass through this window material but is still strongly absorbed in the active layer of low Al content and therefore lower E_g . In this way, effects of deliberate damage at the outer surface of the confinement layer of a DH device have been shown to propagate $\sim 100\mu$ to the active layer, causing localised non-radiative recombination there, visible in an IR vidicon topograph.¹⁵⁷ Related effects were studied by Johnson,¹⁵⁸ who reported large dark spots LDS of dimension $\sim 100 \mu\text{m}$ in the pn junction plane. Henry and Logan¹⁵⁹ showed that the large extent of these LDS is due to long range minority carrier transport, which is an inherent feature of the electrical properties of forward biassed pn junctions containing localised regions of intense non-radiative recombination. Such regions frequently occur at the outer edge of the pn junction when present inadvertently. Photoluminescence topographs made with a laser mirror-scanned system showed that scribed lines given much more intense non-radiative recombination than etched grooves.¹⁵⁹

(ii) Photo-degradation at Semiconductor Surfaces

Decreases in photoluminescence intensity for strongly absorbed excitation can be stimulated by surface oxidation processes which may be enhanced in turn by the recombination processes themselves.¹⁶⁰ Probably, such effects can be described by an increase in band bending caused by the build up of charge in surface states associated with the oxide. The strong electric field of the depletion layer so formed reduces the probability of all types of electron-hole recombination processes, particularly radiative recombination through shallow states.¹⁶¹ Strong localized photoexcitation in DH laser material can cause catastrophic damage at a perfect cleaved crystal facet or an internal defect. This results from transient melting due to intense local non-radiative recombination in such a region, leaving recrystallised material containing high concentrations of non-radiative point defects and dislocation loops.¹⁶² The general uniform decrease in L_S characteristic of long term degradation of DH lasers¹⁵⁶ may be related to the increase in the active region of the density of the E3 electron trap. This trap has been associated with V_{Ga} from capacitance spectroscopy.¹⁶³ The E3 trap does not appear to correlate with 1.0 eV luminescence which apparently predominates outside the active region of the laser structure.¹⁶⁴ More recently, increases in concentration of a 0.24 eV hole trap have been reported to correlate with slow degradation of

GaAlAs lasers.²⁰⁶ However, the non-radiative rate through this trap seems to be only $\sim 10\%$ of that required to account for the slow degradation, like the 'A' hole trap in GaAs, whose concentration has also been observed to increase with degradation.²⁰⁷ Clouds of small dislocation loops, of interstitial type like those responsible for the rapid degradation, but size $< 1000 \text{ \AA}$ and densities $10^7 \text{ to } 10^9 \text{ cm}^{-2}$ apparently always accompany the slow degradation.²⁰⁶ These ' μ -loops' are also of interstitial character and grow slowly by climb, probably involving condensation of interstitial Ga. A key distinguishing feature of the rapid climb responsible for the DLD may be the requirement of a threshold length of nucleating dislocation required to produce a mechanical wedge action²¹⁰ which is postulated to be an inherent feature of the mechanism of climb by vacancy emission,²⁰⁸ stimulated by the combined effects of the high local temperature and the even more localised effects of recombination enhanced defect reactions (REDR) produced by the intense non-radiative recombination at the dislocation edge. The fast process is not a feature of InP-based semiconductor systems such as InGaAsP, of great current practical interest for injection lasers with longer emission wavelength ($\sim 1.3 \mu\text{m}$) compared with GaAlAs (0.8-0.9 μm). The reason for this is partly due to the lesser significance of the REDR process in semiconductors with much lower E_g than GaAlAs.²⁰⁹ However, the probable absence in InP-based semiconductors of electronic states in the band gap associated with the dangling bonds inherently present in the core regions of fresh dislocations will also be very significant. These matters, of great device importance, are subjects of intense research interest at present.²¹⁰ However, it still seems true that energy levels of the relevant electronic states at the dislocation cores remain undetected by any of the standard spectroscopic techniques discussed in this article, including those depending on thermal release of trapped charge carriers.

(iii) Topographic Study of Non-Radiative Recombination at Dislocations

The examples given above relate to the 'negative' information provided from luminescence topographs. The defects are revealed through the quenching they induce in their vicinity for luminescence associated with different species, particularly for the near band gap processes which are usually of greatest interest in devices. Thus, information is obtained on such extended defects as dislocations, which usually promote intense local electron-hole recombination without introducing any characteristic luminescence. The dislocation is viewed through the quenching it induces in luminescence which may originate from any one of the processes described in earlier sections of this review. The transverse dimension of the dislocation core is of order the size of the crystal unit cell, and cannot be imaged directly, not even in the transmission electron microscope (TEM). The photoluminescence or even the scanning electron microscope (SEM) used for many of

the broader-area topographical studies have far lower resolution than the TEM. The dislocations are imaged through the dark spots or lines they induce, whose dimensions are frequently attributed to the diffusion of minority carriers to the dislocation cores, where the recombination velocity is usually assumed infinitely high. Recent topographical measurements of¹ deny this for GaAs, however.²¹⁶

Dissociated dislocations appear to cause particularly intense non-radiative recombination.¹⁶⁵ Strongly non-radiative dislocations in GaAs are found to be of 60° type, dissociated into two Shockley partials separated by a stacking fault region $\sim 60 \text{ \AA}$ wide.²¹⁵ The edge sessile dislocation is undissociated and electrically neutral, probably the result of a core reconstruction which leaves no dangling bonds. The cathodoluminescence intensity contours observed around dislocations in GaP:N can be described in this way. The diffusion model accounts quantitatively for the minority carrier lifetime and therefore luminescence efficiency (eqn. (15)) for dislocation densities $> 10^5 \text{ cm}^{-2}$, where dislocation-induced recombination predominates.¹⁶⁶ By contrast, photoluminescence topographs in GaAs and InP, taken with a resolution of $\sim 3 \mu\text{m}$,¹⁶⁷ suggest that the half-width of luminescence intensity reduction around dislocations at 300 K can be much greater than the diffusion length and does not exhibit the reduction with T anticipated on the diffusion model. As-grown and fresh, deformation-induced dislocations show similar properties, and no evidence of special dislocation-induced electronic energy levels was found through DLTS, optical absorption or photoluminescence spectra.¹⁶⁷ It is suggested that the luminescence quenching near dislocations arises from locally-enhanced bulk non-radiative recombination.

One-to-one correlations between dark spots in luminescence topographs,¹⁶⁸ or electron beam induced current topographs¹⁶⁹ which can be taken when the SEM is used on a sample with a barrier close to the excited surface, and the dislocation density as revealed by careful etching techniques have been reported in many studies (Fig. 46). The detailed connection between such regions of reduced luminescence and dislocations has been proven still more directly through the comparison between SEM and TEM topographs,¹⁶⁸ where the dislocations are imaged through the effect on the electron diffraction of the local strain they induce (Fig. 47). Additional information is revealed in the relatively new technique of transmission cathodoluminescence, whereby high resolution topographs are obtained with good sensitivity using a Si diode photodetector mounted close behind the sample, which may be a suitably prepared device structure.¹⁷⁰ The cathodoluminescence probes the sample volume beyond the luminescent region, and can thereby reveal structural imperfections such as stacking faults and dislocation lines which lie beyond the range of the incident electron beam. This technique has the advantage of minimal sample preparation for the imaging of such defects deep within

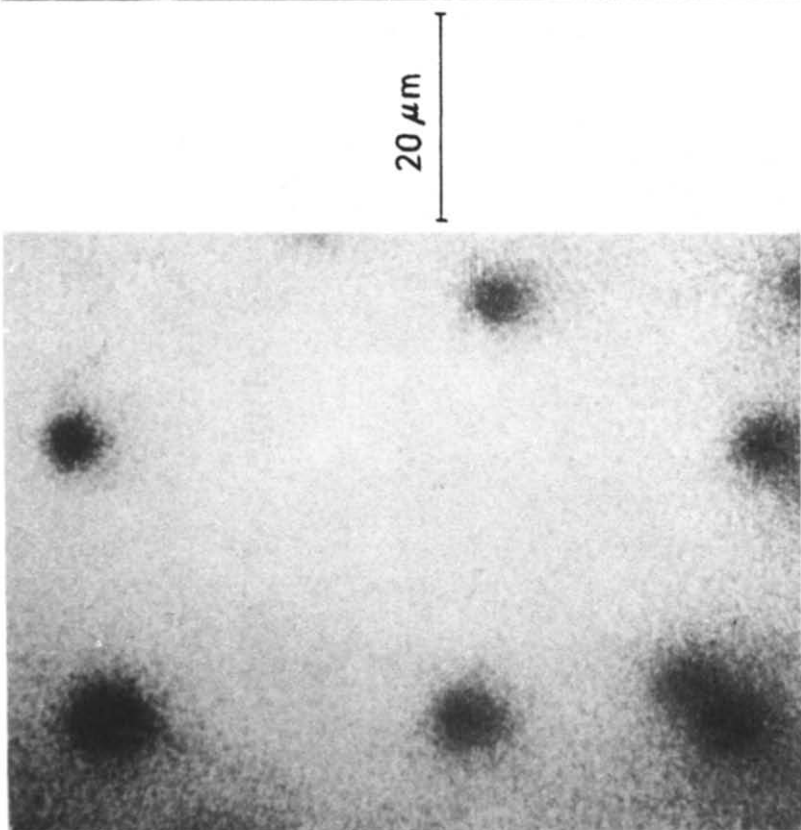
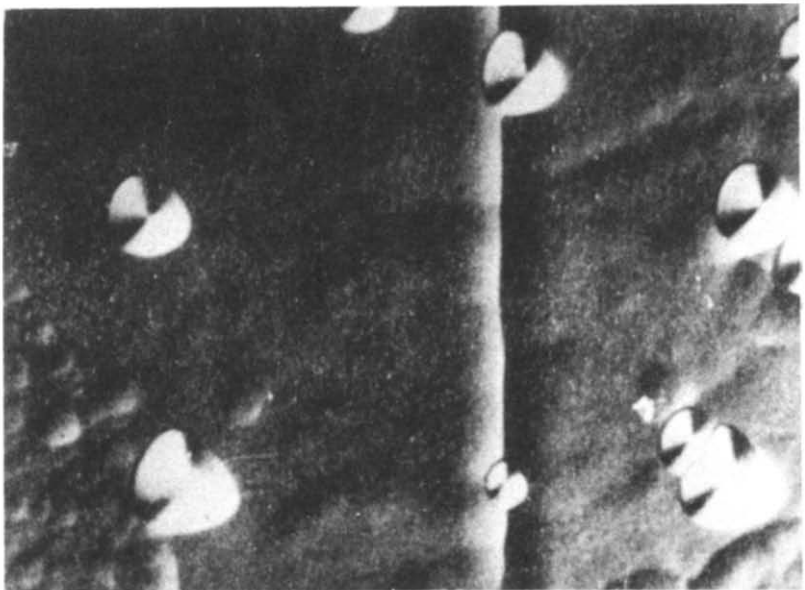


Fig. 46. One-to-one correspondence between dark spots in a SEM cathodoluminescence image (left panel) and an array of dislocation etch-pits observed by optical microscopy of a <111> P-rich surface of an LPE GaP layer.

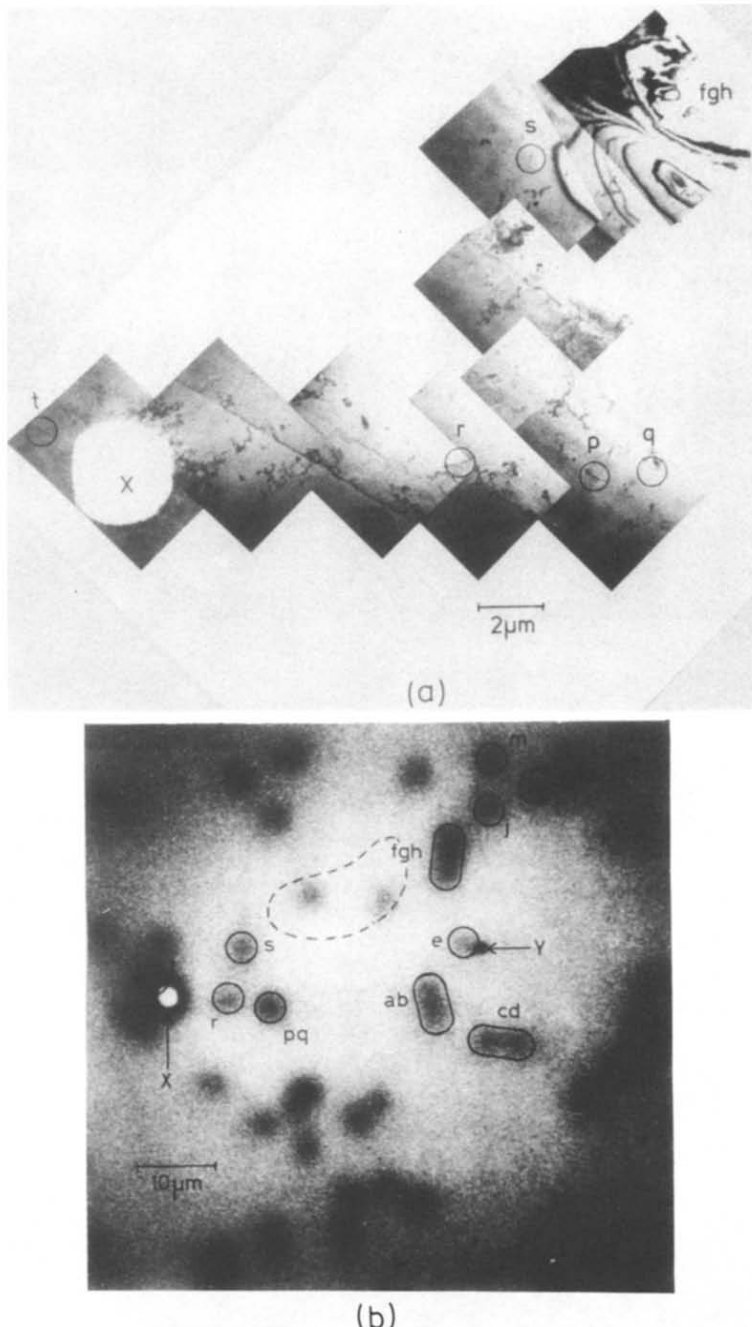


Fig. 47. (a) Shows a montage of TEM topographs from a region of an LPE single crystal of GaP used for the cathodoluminescence (SEM) topograph in (b). Dislocations are revealed in (a) through the effect on electron diffraction of the local strain they induce and in (b) through the local excess non-radiative recombination they cause. Every linear dislocation line image labelled $p \rightarrow t$ in (a) is matched by a dark spot in (b). The white spot at X is a hole in the epitaxial layer, while region fgh is a larger hole produced during thinning for the TEM.¹⁶⁸

the interior of a semiconductor. It forms a valuable diagnostic technique for semiconductors like InP, where reliable etchants are not yet available.¹⁷¹

(iv) Topographic Study of Luminescence Activator Distributions

The 'positive' use of luminescence topography may be exemplified by a recent study of bulk-grown ZnTe using the SEM. Moderate heat treatments were found to produce strong cathodoluminescence haloes around defects which were identified with entrained metallic Te. These Te inclusions are active sources of Li and Cu, which are dominant shallow acceptors in bulk ZnTe.^{33,34} Spatially resolved cathodoluminescence spectra have proved that the green luminescence in the haloes was due to enhanced recombinations through these acceptor centres.¹⁷² Photo- and cathodoluminescence topographic studies have also revealed enhanced incorporation of shallow donor and acceptor species in GaAs, at the risers of both minor and major terrace structures which are a common feature of LPE growth of III-V semiconductors.²¹⁴

ACKNOWLEDGEMENTS

The author is grateful to several colleagues for helpful comments on a number of points in this review. Particular thanks are due to Dr G. Rees of Plessey Research Laboratory and to Drs C. Pickering, M. S. Skolnick, P. Tapster and A. M. White of RSRE.

REFERENCES

1. W. Walukiewicz, J. Lagowski, L. Jastrzebski, M. Lichtensteiger and H.C. Gatos, *J. Appl. Phys.* 50, 899 (1979).
2. W. Walukiewicz, J. Lagowski, L. Jastrzebski, P. Rava, M. Lichtensteiger, C.H. Gatos and H.C. Gatos, *J. Appl. Phys.* 51, 2659 (1980).
3. P.J. Dean and D.C. Herbert 'Bound Excitons' in 'Excitons' Edited by K. Cho, Topics in Current Physics (Springer, Berlin, 1979), 14, Chapter 3.
4. M.D. Sturge, E. Cohen and K.F. Rodgers, *Phys. Rev. B* 15, 3169 (1977).
5. A. Halperin and A.A. Branner, *Phys. Rev.* 117, 408, (1960).
6. C.O. Almbladh and G.J. Rees, *Phys. Rev.* To be published.
7. R.A. Smith, Semiconductors (Cambridge University Press, 1959), p. 28 et seq.
8. For GaAs, C.M. Wolfe, G.E. Stillman and J.O. Dimmock, *J. Appl. Phys.* 11, 504, (1970).
9. J.D. Cuthbert, C.H. Henry and P.J. Dean, *Phys. Rev.* 170, 739 (1968).
10. M.G. Clark, *J. Phys. C: Solid State Phys.* 13, 2311, (1980).
11. H.C. Casey Jr, F. Ermanis and K.B. Wolfstirn, *J. Appl. Phys.* 40, 2945, (1969); see also G.F. Neumark, *Phys. Rev. B* 5, 408, (1972).
12. J.J. Hopfield, *J. Phys. Chem. Sol.* 10, 110, (1958).
13. R.L. Hartman and L.A. Koszi, *J. Appl. Phys.* 49, 5731, (1979).
14. C.H. Henry and D.V. Lang, *Phys. Rev. B* 15, 989, (1977).
15. A.M. White, P.J. Dean and P. Porteous, *J. Appl. Phys.* 47, 323, (1976).
16. D.V. Lang, *J. Appl. Phys.* 45, 3014, (1974); D.S. Day, M.Y. Tsai, B.G. Streetman and D.V. Lang, *J. Appl. Phys.* 50, 5093, (1979).
17. P.J. Dean, C.H. Henry and C.J. Frosch, *Phys. Rev.* 168, 812, (1968); P.J. Dean and C.H. Henry, *Phys. Rev.* 176, 928, (1968).

18. C.H. Henry, H. Kukimoto, G.L. Miller and F.R. Merritt, *Phys. Rev.* B.7, 2499, (1973).
19. L.C. Kimerling, Radiation effects in semiconductors, Dubrovnik, 1976 (*Inst. Phys. Conf. Ser.* 31, 1977) p. 221; L.C. Kimerling, P. Blood and W.M. Gibson, *ibid*, Nice 1978 (*Inst. Phys. Conf. Ser.* 46, 1979), p. 273.
20. D.V. Lang, 'Radiation effect in semiconductors', Dubrovnik, (*Inst. Phys. Conf. Ser.* 31, 1977), p. 70; also A. Mircea and D. Bois, *ibid*, Nice, 1978 (*Inst. Phys. Conf. Ser.* 46, 1979), p. 82.
21. D.V. Lang, *Proc. Int. Conf. Phys. Semicond.* Kyoto, (1980). *J. Phys. Soc. Japan* 49A, 215 1980.
22. D.V. Lang, R.A. Logan and M. Jaros, *Phys. Rev.* B.19, 1015, (1979).
23. G.A. Baraff, *Proc. Int. Conf. Phys. Semicond.* Kyoto (1980). *J. Phys. Soc. Japan* 49A, 231 1980.
24. J.R. Haynes, *Phys. Rev. Lett.* 4, 361, (1960).
25. D.G. Thomas and J.J. Hopfield, *Phys. Rev.* 128, 2135 (1962).
26. K. Nassau, C.H. Henry and J.W. Shiever, *Proc. Intern. Conf. Phys. Semicond.* Cambridge 1970, Edited by J.C. Hensel and S.P. Keller (USAEC, Oak Ridge, Tenn., 1970), p. 629.
27. C.H. Henry, K. Nassau and J.W. Shiever, *Phys. Rev.* B.4, 2453 (1971).
28. J.J. Hopfield, *Proc. Intern. Conf. Phys. Semicond.* Paris, 1964, (Dunod, Paris, 1964), p. 725.
29. P.J. Dean, Luminescence of Crystals, Molecules and Solutions, Edited by F.E. Williams (Plenum Press, New York, 1973), p. 538.
30. P.J. Dean, H. Venghaus, J.C. Pfister, B. Schaub and J. Marine, *J. Luminesc.* 16, 363 (1978).
31. D.J. Ashen, P.J. Dean, D.T.J. Hurle, J.B. Mullin, A.M. White and P.D. Greene, *J. Phys. Chem. Sol.* 36, 1041, (1975).
32. D.C. Herbert, P.J. Dean, H. Venghaus and J.C. Pfister, *J. Phys. C.*, 11, 3641 (1978).
33. P.J. Dean, *J. Luminesc.* 21, 75 (1979).
34. N. Magnea, D. Bensahel, J.L. Pautrat and J.C. Pfister, *Phys. Stat. Sol. b* 94, 627 (1979).
35. N.F. Mott, *Rev. Mod. Phys.* 40, 677 (1968).
36. J.G. Gay, *Phys. Rev.* B.4, 2567 (1971).
37. T.N. Morgan, *Phys. Rev. Letters* 21, 819 (1968).
38. P.J. Dean, R.A. Faulkner, S. Kimura and M. Ilegems, *Phys. Rev.* B.4, 1926 (1971).
39. D.C. Thomas and J.J. Hopfield, *Phys. Rev.* 150, 680 (1966).
40. M. Tajima, *Appl. Phys. Lett.* 32, 719 (1978).
41. Sh. M. Kogan and T.M. Lifshits, *Phys. Stat. So. a* 39, 11 (1977).
42. C.H. Henry and K. Nassau, *Phys. Rev.* B.1, 1628 (1970).
43. C.M. Wolfe and C.E. Stillman, *Proc IIIrd Symp. on GaAs*, Aachen, 1970, Edited by K. Paulus (*Inst. Phys. Conf. Ser.* 9), p. 3.
44. P.J. Dean and A.M. White, *Solid State Electron* 21, 1351 (1978).
45. Y. Shiraki and H. Nakashima, *Solid State Commun.* 29, 295 (1979).
46. R.A. Street and P.J. Wiesner, *Phys. Rev.* B.14, 632 (1976).
47. H.B. de Vore, *Phys. Rev.* 102, 86 (1956).
48. M. Tajima and A. Yusa, *NTD Silicon* (Plenum, New York, 1981), p.
49. H. Nakayama, T. Nishino and Y. Hamakawa, *Japan, J. Appl. Phys.* 19, 501, (1980).
50. J.C. Irvin, *Bell Syst. Tech. J.* 41, 387 (1962).
51. M. Tajima, A. Yusa and T. Abe, *Japan, J. Appl. Phys. Suppl.* 19-1, (1980).
52. M. Tajima, A. Kanamori and T. Iizuka, *Japan J. Appl. Phys.* 18, 1401 (1979); H. Nakayama, J. Katsura, T. Nishino and Y. Hamakawa, *Japan, J. Appl. Phys.* 19, 945 (1980).
53. C.G. Kirkpatrick, J.R. Noonan and B.G. Streetman, *Radiation Effects* 30, 97 (1976).
54. M.S. Skolnick, A.G. Cullis, H.C. Webber, *Appl. Phys. Lett.* 6, 464 (1981).
55. P.J. Dean, unpublished data.
56. A.M. White, P.J. Dean, W. Bardsley, E.W. Williams and B. Day, *Solid State Commun.* 11, 1099 (1972).

57. N. Apsley, M. Skoknick and P.J. Dean, unpublished data.
58. P.J. Dean, D.C. Herbert and A.M. Lahee, *J. Phys. C.* 13, 5071 (1980).
59. P.J. Dean, R.N. Bhargava, B.J. Fitzpatrick, D.C. Herbert and C.J. Werkhoven, *Phys. Rev. B*, 23 May (1981).
60. H. Venghaus and P.J. Dean, *Phys. Rev. B*.21, 1596 (1980).
61. C. Weisbuch, Proc. Int. Conf. Phys. Semicond. Edinburgh, 1978 (*Inst. Phys. Conf. Ser.* 43, 1979), p. 93.; D. Munz and M. H. Pilkuhn, *Solid State Commun.* 36, 205 (1980)
62. H. Tews and H. Venghaus, *Solid State Commun.* 30, 219 (1979).
63. P.J. Dean, Progress in Solid State Chemistry, Edited by J.O. McCaldin and G. Somorjai (Pergamon Press, Oxford 1973) 8, p. 1.
64. K. Era, S. Shionoya and Y. Washizawa, *J. Phys. Chem. Solids* 29, 1827, 1968; K. Era, S. Shionoya, Y. Washizawa and H. Ohmatsu, *J. Phys. Chem. Solids* 29, 1843 (1968).
65. R.C. Enck and A. Honig, *Phys. Rev.* 177, 1182 (1969).
66. U.O. Ziemelis, R.R. Parsons and M. Voos, *Solid State Commun.* 32, 445, 1979 and private communication (1980).
67. J.J. Hopfield, D.G. Thomas and M. Gershenson, *Phys. Rev. Lett.* 10, 162 (1963).
68. J.S. Prener and F.E. Williams, *Phys. Rev.* 101, 1427 (1956).
69. P.J. Dean, C.J. Frosch and C.H. Henry, *J. Appl. Phys.* 39, 5631 (1968).
70. D.G. Thomas, J.J. Hopfield and W.M. Augustyniak, *Phys. Rev.* 140, A202 (1965).
71. P.J. Dean and Lyle Patrick, *Phys. Rev. B*.2, 1888 (1970).
72. Lyle Patrick, *Phys. Rev.* 180, 794 (1969).
73. A. Hutson, *Phys. Rev. B*.12, 1404 (1975).
74. T.N. Morgan and H. Maier, *Phys. Rev. Lett.* 27, 1200 (1971).
75. P.J. Dean, R.A. Faulkner and E.G. Schonherr, Proc. Intern. Conf. Phys. Semicond. Cambridge 1970, Edited by J.C. Hensel and S.P. Keller (USAEC, Oak Ridge, Tenn, 1970), p. 286.
76. C.H. Henry, R.A. Faulkner and K. Nassau, *Phys. Rev.* 183, 798 (1969).
77. A.T. Vink, R.L.A. van der Heijden and J.W.A. van der Does de Bye, *J. Luminesc.* 8, 105 (1973).
78. P.J. Dean and D.G. Thomas, *Phys. Rev.* 150, 690 (1966).
79. D.R. Wight, *J. Phys. C.*, 1 1759 1968; C.D. Mobsby, E.C. Lightowers and G. Davies, *J. Luminesc.* 4, 29 (1971).
80. F.A. Trumbore and D.G. Thomas, *Phys. Rev.* 137, A1030 (1965).
81. P.J. Dean, J.D. Cuthbert, D.G. Thomas and R.T. Lynch, *Phys. Rev. Lett.* 18, 122 (1967).
82. A. Onton, *Phys. Rev. B*.4, 4449 (1971).
83. P.J. Dean and C.H. Henry, *Phys. Rev.* 176, 928 (1968).
84. P. Lawaetz, *Solid State Commun.* 16, 65 (1975).
85. A.C. Carter, P.J. Dean, M.S. Skolnick and R.A. Stradling, *J. Phys. C*:10, 5111 (1977).
86. A.A. Kopylov and A.N. Pikhtin, *Fiz. Tekh. Poluprovodn.* 11, 867 (1977), [Engl. Transl. Sov. Phys. Semicond. 11, 510 (1977)].
87. A.A. Kopylov and A.N. Pikhtin, *Solid State Commun.* 26, 735 (1978).
88. G.F. Glinski, A.A. Kopylov, and A.N. Pikhtin, *Solid State Commun.*, 30, 631 (1979).
89. P.J. Dean, *Czech. J. Phys. B*.30, 272 (1980).
90. R.A. Street and W. Senske, *Phys. Rev. Lett.* 37, 1292 (1976).
91. H. Tews and H. Venghaus, *Solid State Commun.* 30, 219 (1979).
92. H. Venghaus, P.J. Dean, P.E. Simmonds and J.C. Pfister, *Z. Physik*, B.30, 125 (1978).
93. A.T. Vink, R.L.A. Van der Heijden and A.C. Van Amstel, *J. Luminesc.*, 9, 180 (1974).
94. P.J. Dean, D.J. Robbins and S.G. Bishop, *Solid State Commun.* 32, 379 (1979).
95. W. Senske, M. Sondergeld and H.J. Quiesser, *Phys. Stat. Sol. b*, 89, 467 (1978).
96. S. Nakashima and Y. Yamaguchi, *J. Appl. Phys.* 50, 4958 (1979).
97. H. Tews, H. Venghaus, and P.J. Dean, *Phys. Rev. B*.19, 5178 (1979).

98. G. Neu, Y. Marfaing, R. Legros, R. Triboulet and L. Svob, *J. Luminesc.* To be published.
99. A. Suzuki and S. Shionoya, *J. Luminesc.* 3, 74 (1970).
100. H.D. Fair Jr, R.D. Ewing and F.E. Williams, *Phys. Rev. Lett.* 15, 355 (1965).
101. B.C. Cavenett, 'Luminescence Spectroscopy', Edited by M.D. Lumb (Academic Press, London 1978), Ch. 6, p. 299.
102. M. Gal, B.C. Cavenett and P. Smith, *Phys. Rev. Lett.* 43, 1611 (1979).
103. J.E. Nicholls and J.J. Davies, *J. Phys. C.* 13, 2393 (1980).
104. K.M. Lee, Li Si Dang, G.D. Watkins and W.J. Choyke, *Solid State Commun.* 35, 527 (1980).
105. M. Gal, B.C. Cavenett and P.J. Dean, *J. Phys. C.* 14, 1507 (1981).
106. D.J. Dunstan and J.J. Davies, *J. Phys. C* 12, 2927 (1979).
107. J.E. Nicholls and J.J. Davies, *J. Phys. C* 12, 1917 (1979).
108. J. Shah and R.C.C. Leite, *Phys. Rev. Lett.* 22, 1304 (1969).
109. U. Heim and P. Wiesner, *Phys. Rev. Lett.* 30, 1205 (1973).
110. R. Ulbrich, *Phys. Rev. B* 8, 5719 (1973).
111. D. von der Linde and R. Lambrich, *Phys. Rev. Lett.* 42, 1090 (1979); R.F. Leheny, J. Shah, R.L. Fork, C.V. Shank and A. Migus, *Solid State Commun.* 31, 809 (1979).
112. R. Ulbrich, *Phys. Rev. Letters* 27, 1512 (1971).
113. A. Nakamura and C. Weisbuch, *Solid State Electronics* 21, 1331 (1978).
114. P.J. Dean, Defects and Radiation Effects in Semiconductors, Nice, 1978, Edited by J.H. Albany (Inst. Phys. Conf. Ser. 46, 1979), p. 100.
115. W. Ruhle and E. Gobel, *Phys. Status Solidus B* 78, 311 (1976); D. Bimberg, *Phys. Rev. B* 18, 1974 (1978).
116. P.J. Dean, H. Venghaus and P.E. Simmonds, *Phys. Rev. B* 18, 6813 (1978).
117. P.J. Dean, *Phys. Stat. Sol. b* 98, 439 (1980).
118. J. Shah, R.C.C. Leite and J.P. Gordon, *Phys. Rev.* 176, 938 (1968).
119. P.J. Dean, J.R. Haynes and W.F. Flood, *Phys. Rev.* 161, 711 (1967).
120. K.L. Shaklee and R.E. Nahory, *Phys. Rev. Lett.* 24, 942 (1970).
121. R.R. Parsons, *Solid State Commun.* 29, 763 (1979).
122. W.P. Dumke, *Phys. Rev.* 132, 1998 (1963).
123. T. Kamiya and E. Wagner, *J. Appl. Phys.* 48, 1928 (1977).
124. M.R. Lorenz, T.N. Morgan and G.D. Pettit, Proc. Intern. Conf. Phys. Semicond. Moscow 1968, Edited by S.M. Ryvkin (Nauka, Leningrad 1968), p. 495.
125. E. Molva, N. Magnea, J.L. Pautrat, D. Bensahel and J.C. Pfister to be published.
126. W. Bludau, E. Wagner and H.J. Queisser, *Solid State Commun.* 18, 861 (1976).
127. N. Takenaka, M. Inoue, J. Shirafuji and Y. Inuishi, *J. Phys. Soc. Japan* 45, 1630 (1978).
128. S.B. Nam, D.W. Langer, D.L. Kingston and M.J. Luciano, *Appl. Phys. Lett.* 31, 652 (1977).
129. A.A. Bergh and P.J. Dean, 'Light Emitting Diodes' Clarendon Press, Oxford, 1976) Ch. 3.
130. R.Z. Bachrach and O.G. Lorimer, *Phys. Rev. B* 7, 700 (1973).
131. P.J. Dean, J.D. Cuthbert and R.T. Lynch, *Phys. Rev.* 179, 754 (1969).
132. M.D. Sturge, A.T. Vink and F.P.J. Kuijpers, *Appl. Phys. Lett.* 32, 49 (1978).
133. E. Cohen and M.D. Sturge, *Phys. Rev. B* 15, 1039 (1977).
134. P.D. Dapkus, W.H. Hackett Jr, O.G. Lorimer and R.Z. Bachrach, *J. Appl. Phys.* 45, 4920 (1974).
135. J.D. Cuthbert and D.G. Thomas, *Phys. Rev.* 154, 763 (1967).
136. D.F. Nelson, J.D. Cuthbert, P.J. Dean and D.G. Thomas, *Phys. Rev. Lett.* 17, 1262 (1962).
137. E.C. Lightowers, J.C. North and O.G. Lorimer, *J. Appl. Phys.* 45, 2191 (1974).
138. J.D. Cuthbert, C.H. Henry and P.J. Dean, *Phys. Rev.* 170, 739 (1968).
139. E.C. Lightowers, J.C. North, A.S. Jordan, L. Derick and J.L. Merz, *J. Appl. Phys.* 44, 4758 (1973).
140. D.V. Lang, *J. Appl. Phys.* 45, 3014 (1974).
141. J.S. Jayson, R.Z. Bachrach, P.D. Dapkus and N.E. Schumaker, *Phys. Rev. B* 6, 2357 (1972).
142. W. Busse, H.E. Gumlich, B. Meissner and D. Theis, *J. Luminesc.* 12,13, 693 (1976).

143. G. Dieke, 'Spectra and energy level of rare-earth ions in crystals' Edited by H.M. Crosswhite and H. Crosswhite, (Interscience, New York, 1968).
144. U. Kaufmann, W.H. Koschel, J. Schneider and J. Weber, *Phys. Rev. B* 19, 3343 (1979).
145. W. Hayes, J.F. Ryan, C.L. West and P.J. Dean, *J. Phys. C* 13, L149 (1980).
146. S.G. Bishop, P.J. Dean, P. Porteous and D.J. Robbins, *J. Phys. C* 13, 1331, (1980).
147. M.J. Clark, and P.J. Dean, *Proc. Int. Conf. Phys. Semicond.*, Edinburgh 1980, (*Inst. Phys. Conf. Ser.* 43), p. 291.
148. H. Ennen and U. Kaufmann, *J. Appl. Phys.* 51, 1615 (1980).
149. U. Kaufmann and J. Schneider, 'Optical and ESR spectroscopy of deep defects in III-V semiconductors', Festkorperprobleme (Advances in solid state physics) XX, p. 87, Edited by J. Treusch (Verlag, Braunschweig, 1980).
150. R. Dingle, *Phys. Rev. Lett.* 23, 579 (1969).
151. D.J. Robbins, P.J. Dean, J.L. Glasper and S.G. Bishop, *Solid State Commun.* 36, 61 (1980).
152. S.G. Bishop, P.B. Klein, R.L. Henry and B.D. McCombe, *Proc. Semi-Insulating III-V Materials Conference*, Edited by G.J. Rees (Shiva, Orpington, UK, 1980), p.161.
153. D.J. Robbins and P.J. Dean, *Adv. in Phys.* 27, 499 (1978).
154. M. Ozeki, A. Shibatomi and S. Ohkawa, *J. Appl. Phys.* 50, 4823 (1979).
155. H. Kressel, private communication, 1973, see also E.A. Panyutin and I.G. Chashnikov, *Inst. Exp. Tech. (Engl. Transl)* 18, 941 (1975).
156. R.L. Hartman and L.A. Koszi, *J. Appl. Phys.* 49, 5731 (1979).
157. O. Nakada, R. Ito, H. Nakashima and N. Chinone, *J. Appl. Phys. Japan, Suppl.* 43, 43 (1973).
158. W.D. Johnston Jr, *Appl. Phys. Lett.* 24, 494 (1974).
159. C.H. Henry and R.A. Logan, *J. Appl. Phys.* 48, 3962 (1977).
160. T. Suzuki and M. Ogawa, *Appl. Phys. Lett.* 31, 473 (1977).
161. R.A. Street, R.H. Williams and R.S. Bauer, *J. Vac. Sci. Tech.* 17, 1001 (1980).
162. C.H. Henry, P.M. Petroff, R.A. Logan and F.R. Merritt, *J. Appl. Phys.* 50, 3721 (1979).
163. D.V. Lang, R.L. Hartman and N.E. Schumaker, *J. Appl. Phys.* 47, 4986 (1976).
164. J.P. van der Ziel and R.L. Hartman, *Appl. Phys. Lett.* 34, 520 (1979).
165. For Si, A. Ourmazd, D.B. Darby and G.R. Booker, *Inst. Phys. Conf. Ser.* 36, 251 (1977).
166. D.R. Wight, *J. Phys. D* 10, 431 (1977).
167. K. Bohm and B. Fischer, *J. Appl. Phys.* 50, 5453 (1979).
168. J.M. Titchmarsh, G.R. Booker, W. Harding and D.R. Wight, *J. Mat. Sci.* 12, 341 (1977).
169. G.B. Stringfellow, P.F. Lindquist, T.R. Cass and R.A. Burmeister, *J. Elect. Mat.* 3, 497 (1974).
170. A.K. Chin, H. Temkin and R.J. Roedel, *Appl. Phys. Lett.* 37, 637 (1979).
171. A.K. Chin, S. Mahajan and A.A. Ballman, *Appl. Phys. Lett.* 35, 784 (1979).
172. D. Bensahel and M. Dupuy, *Phys. Stat. Sol. (a)* 55, 203 (1979).
173. P.J. Dean, *Phys. Rev.* 168, 889 (1968).
174. T. Fukushima and S. Shionoya, *J. Phys. Soc. Japan*, 38, 797 (1975).
175. M. Tabei and S. Shionoya, *J. Luminesc.* 15, 201 (1977).
176. M. Tabei, S. Shionoya and H. Ohmatsu, *Japanese J. Appl. Phys.* 14, 240 (1975).
177. A.M. White, P.J. Dean, L.L. Taylor and R.C. Clarke, *J. Phys. C* 5, L110 (1972).
178. D.M. Larsen, *Phys. Rev. B* 13, 1681 (1976).
179. D.G. Thomas, J.J. Hopfield and R.T. Lynch, *Phys. Rev. Lett.* 17, 312 (1966).
180. J.C. Tsang, P.J. Dean and P.T. Landsberg, *Phys. Rev.* 173, 814 (1968).
181. E.F. Gross, S.A. Permagorov, A.N. Reznitskii and E.N. Usarov, *Fiz. Tekh. Poluprov.* 7, 1255, 1973 [Engl. Transl. Sov. Phys. Semicond. 7, 844, 1974].
182. D.S. Pan, D.L. Smith and T.C. McGill, *Phys. Rev. B* 21, 3581 (1980).
183. T. Hoshina and H. Kawai, *Japan. J. Appl. Phys.* 19, 267 (1980).
184. T. Hoshina and H. Kawai, *ibid*, 19, 279 (1980).

185. U. Kaufmann and J. Schneider, *Appl. Phys. Lett.* 36, 747 (1980).
 186. G.H. Stauss, J.J. Krebs, S.H. Lee and E.M. Swiggard, *Phys. Rev. B* 22, 3141 (1980).
 187. N. Magnea, E. Molva, D. Bensahel and R. Romestain, *Phys. Rev. B* 22, 2983 (1980).
 188. C.H. Henry, private communication, (1975).
 189. P.J. Dean, *J. Luminesc.* 18,19, 755 (1978).
 190. W. Schairer and M. Schmidt, *Phys. Rev. B* 10, 2501 (1974).
 191. D. Bimberg, W. Schairer, M. Sondergeld and T.O. Yep, *J. Luminesc.* 3, 175 (1970).
 192. A.M. White, I. Hinchliffe, P.J. Dean and P.D. Greene, *Solid State Commun.*, 10, 497 (1972).
 193. W. Schairer and E. Grobe, *Solid State Commun.* 8, 2017 (1970).
 194. D.J. Robbins, B. Cockayne, J.L. Glasper and B. Lent, *J. Electrochem. Soc.*, 126, 1221 (1979).
 195. J. Shah, R.F. Leheny and W.F. Brinkman, *Phys. Rev. B* 10, 659 (1974).
 196. M. Gunderson and W.L. Faust, *Phys. Rev. B* 7, 3681 (1973).
 197. J. Shah, R.F. Leheny and A.H. Dayem, *Phys. Rev. Lett.* 33, 818 (1974).
 198. P.J. Dean, *Phys. Rev.* 157, 655 (1967).
 199. K.R. Elliott and T.C. McGill, *Phys. Rev. B* 21, 2426 (1980).
 200. Y.C. Chang and T.C. McGill, *Solid State Commun.* 33, 1035 (1980).
 201. D.G. Thomas, J.J. Hopfield and K. Colbow, *Symposium on Radiative Recombination in Semiconductors*, Paris, 1964 (Dunod, Paris, 1965), p. 67.
 202. A. Mooradian and H.Y. Fan, *Phys. Rev.* 148, 873 (1966).
 203. M.R. Lorenz and A.E. Blakeslee, *Int. Symp. on GaAs*, 1972 (Inst. of Phys. London 1972), p. 106.
 204. M.R. Lorenz and A. Onton, *Proc. 10th Int. Conf. Phys. Semicond.* Edited by S.P. Keller et al. (USAEC, Oak Ridge, 1970), p. 444.
 205. A. Onton and R.E. Fern, *Appl. Spectr.* 28, 558 (1974).
 206. T. Uji, T. Suzuki and T. Kamejima, *Appl. Phys. Lett.* 36, 655 (1980).
 207. K. Kondo, S. Yamanoshi, S. Isozumi and T. Yamaoka, Japan, *J. Appl. Phys.* 19, Supp. 19-1, 437 (1980).
 208. P.W. Hutchinson, P.S. Dobson, B. Wakefield and S. O'Hara, *Solid State Electron.* 21, 1413 (1978).
 209. P.J. Dean and W.J. Choyke, *Adv. in Phys.* 26, 1 (1977).
 210. I. Hayashi, *J. Phys. Soc. Japan* 49, Supp. A 57 (1980).
 211. E. Ohta and M. Sakata Japan, *J. Appl. Phys.* 17, 1795 (1978).
 212. R.G. Humphreys, private communication (1981).
 213. R.M. Gibb, G.J. Rees, B.W. Thomas, B.L.H. Wilson, B. Hamilton, D.R. Wight and N.F. Mott, *Phil. Mag.* 36, 1021 (1977), see also C.H. Henry, H. Kukimoto, G.L. Miller and F.R. Merritt, *Phys. Rev. B* 7, 2499 (1973).
 214. B. Fischer, E. Bauser, P.A. Sullivan and D.L. Rode, *Appl. Phys. Lett.* 33, 78 (1978).
 215. P.M. Petrott, R.A. Logan and A. Savage, *Phys. Rev. Lett.* 44, 287 (1980).
 216. A. Steckenborn, H. Müntzel and D. Bimberg,

NOTE ADDED IN PROOF

Equation (11) should also include the term $P_D^0 r(E)$, which is the donor occupation probability, equal to $(N_D - N_A) / N_D$ for small $n = (N_D - N_A)$. The constant c in Eqn. (13) contains the Boltzmann factor n/N_c , which includes the term $\exp(E_F/kT)$. Here N_c is the density of conduction band states and E_F is the Fermi level. The Boltzmann factor contains a term $\exp(E_D/kT)$. It is important to include the dependence of E_D on the donor concentration in the numerical analysis of the DAP and A FB lineshape. This dependence becomes important in GaAs for donor concentrations $\geq 10^{14} \text{ cm}^{-3}$ (Fig 5b). When this dependence is accounted for, a significant proportion of the under-estimate of the compensation ratio by the optical technique described in Section II Civ is removed for samples doped in this range.